

THE AQUEOUS PROCESSING OF BARIUM TITANATE:  
PASSIVATION, DISPERSION, AND BINDER FORMULATIONS  
FOR MULTILAYER CAPACITORS

By

ROBERT E. CHODELKA

A DISSERTATION PRESENTED TO THE GRADUATE SCHOOL  
OF THE UNIVERSITY OF FLORIDA IN PARTIAL FULFILLMENT  
OF THE REQUIREMENTS FOR THE DEGREE OF DOCTOR OF PHILOSOPHY

UNIVERSITY OF FLORIDA

1996

Dedicated to:

my mother and father  
Eleanor and Edward Chodelka

and

my sister and niece, brothers, and dog  
Theresa and Erica Rogers, David Chodelka and Timothy Chodelka, and Zor  
in appreciation of their endless support, guidance, patience, and belief in me.

## ACKNOWLEDGMENTS

I would like to take this opportunity to thank all of the people who made this research project not only possible, but successful. Sincere thanks is extended to Dr. James H. Adair, my committee chair and advisor, for his scientific guidance in academic affairs and fatherly advice in personal matters. My relationship with him has made me not only a better scientist, but a better human being. I would like to thank the other members of my committee, Drs. Robert T. DeHoff, Brij M. Moudgil, and Michael D. Sacks, from the Department of Materials Science and Engineering, Russell S. Drago from the Department of Chemistry, and Stephen A. Costantino from the sponsor of the current research, Cabot Performance Materials (CPM), Boyertown, PA. Without their advice and the monetary support from CPM, this research would not have been a success.

I would like to acknowledge Dr. Stanley Bates and the staff at the Major Analytical Instrumentation Center (MAIC) at the University of Florida for their analytical support and technical advice, specifically, the high resolution transmission electron microscopy conducted by Dr. Augusto Morrone.

I am grateful to all my friends, both past and present colleagues in Dr. Adair's research group and in the Department of Materials Science and Engineering, for their technical advice and support. Special thanks goes out to Dr. Sridhar Venigalla, Dr. Melanie Carasso, and soon to be Drs. Craig Habeger and Jeff Kerchner for proof-reading my dissertation, as well as Pam Howell for her support and assistance during my enrollment in the Ph.D. program at the University of Florida. In the times of need, I felt that I could always rely on my friends. I will never forget the competitive Hearts card games, the departmental I.M. sports teams, and the social functions that made my years at the University of Florida quite enjoyable.

In closing, I would like to thank my mother, father, sister, niece, and two brothers for the continuous support, guidance, and patience. Their belief in me enabled my perseverance.

## TABLE OF CONTENTS

ACKNOWLEDGMENTS.....	iii
LIST OF TABLES .....	viii
LIST OF FIGURES .....	ix
ABSTRACT .....	xvi
CHAPTERS	
1. INTRODUCTION.....	1
1.1. Introduction.....	1
1.2. Literature Review .....	2
1.3. Chemical Passivation of the Barium Titanate Particle Surface via Oxalic Acid.....	4
1.4. Dispersion of Aqueous Barium Titanate Suspensions.....	5
1.5. Binder Formulations.....	6
1.6. Conclusions and Future Work .....	7
2. LITERATURE REVIEW .....	8
2.1. Introduction.....	8
2.2. Processing of Multilayer Capacitors.....	8
2.3. Aqueous Environment.....	15
2.3.1.Solubility of Barium Titanate and Titanium Dioxide in Water.....	15
2.3.2.Passivation of Thermodynamically Unstable Metals and Glasses .....	20
2.3.3.Feasibility of Passivating Barium Titanate.....	24
2.4. Dispersion .....	28
2.4.1.Electrostatic Surface Charge Formation and Stabilization.....	28
2.4.2.Polymeric Dispersion.....	36
2.4.3.Electrophoretic Behavior of Titanium Dioxide and Barium Titanate.....	38
2.4.4.Electrophoretic Behavior of Calcium Oxalate Monohydrate .....	45
2.5. Binders.....	47
2.6. Variations in the Ba:Ti Ratio on Sintering of Barium Titanate.....	47
2.7. Characterization Techniques.....	50
2.7.1. Solution Chemistry .....	50
2.7.2. Surface Charge Analysis.....	51
2.7.2.1. Light Scattering Techniques.....	53
2.7.2.2. Electroacoustic Analysis.....	53
2.7.2.3. Sedimentation analysis.....	54

2.7.3. Particle Observation.....	54
2.7.3.1. Scanning Electron Microscopy .....	54
2.7.3.2. Transmission Electron Microscopy .....	56
2.7.4. Viscosity .....	56
2.8. Chapter Summary.....	59
 3. CHEMICAL PASSIVATION OF THE BaTiO <sub>3</sub> PARTICLE SURFACE VIA OXALIC ACID ADDITIONS.....	 62
3.1. Introduction.....	62
3.2. Approach.....	68
3.3. Materials and Methods .....	70
3.3.1. General .....	70
3.3.2. Barium Titanate Powder Characterization .....	71
3.3.3. Preparation of Aqueous Barium Titanate Suspensions .....	74
3.3.4. Preparation and Characterization of the Various Barium Titanate Powders for High Resolution Transmission Electron Microscopy .....	75
3.4. Results and Discussion.....	76
3.4.1. Solution Chemistry Analysis .....	76
3.4.2. High Resolution Transmission Electron Microscopy Analysis.....	81
3.4.3. Electrophoretic Behavior of Barium Titanate Suspensions at Various Solids Loading .....	88
3.4.4. Electrophoretic Behavior of Barium Oxalate Monohydrate and Barium Titanate Suspensions at Various Oxalic Acid Concentrations ....	92
3.4.5. Electroacoustic Analysis of High Solids Loading Barium Titanate Suspensions .....	95
3.5. Conclusions .....	98
 4. DISPERSION OF AQUEOUS BaTiO <sub>3</sub> SUSPENSIONS .....	 101
4.1. Introduction.....	101
4.2. Approach.....	106
4.3. Materials and Methods .....	107
4.3.1. Preparation of Low Solids Loading Barium Titanate Suspensions .....	107
4.3.2. High Solids Loading Barium Titanate Slurries .....	109
4.3.2.1. Preparation of Barium Titanate Slurries .....	109
4.3.2.2. Characterization of the Barium Titanate Slurries.....	112
4.4. Results and Discussion.....	113
4.4.1. Preliminary Studies at Low Solids Loading .....	113
4.4.1.1. Solution Chemistry.....	113
4.4.1.2. Sedimentation Results .....	116
4.4.1.3. Electrophoretic Behavior .....	123
4.4.2. High solids loading Barium Titanate Slurries.....	125
4.5. Conclusions .....	135
 5. BINDER FORMULATIONS FOR THE OXALATE/POLYETHYLENE IMINE-TREATED BaTiO <sub>3</sub> SUSPENSIONS FOR MULTILAYER CAPACITORS.....	 139
5.1. Introduction.....	139

5.2.	Approach.....	143
5.3.	Materials and Methods .....	145
5.3.1.	General .....	145
5.3.2.	Preliminary Studies Low Solids Loading .....	146
5.3.2.1.	Electrophoretic and Sedimentation Studies.....	146
5.3.2.2.	Polymer Interactions .....	147
5.3.3.	High Solids Loading Barium Titanate Slurries .....	148
5.3.3.1.	Preparation of BaTiO <sub>3</sub> Slurries with Binder Present .....	148
5.3.3.2.	Characterization of the Barium Titanate Slurries.....	148
5.4.	Results and Discussion.....	149
5.4.1.	Preliminary Studies at Low Solids Loading .....	149
5.4.1.1.	Electrophoretic and Sedimentation Studies.....	149
5.4.1.2.	Polymer Interactions .....	151
5.4.1.3.	Titration Curves .....	155
5.4.2.	High solids loading BaTiO <sub>3</sub> Slurries.....	163
5.5.	Conclusions .....	171
CONCLUSIONS AND SUGGESTIONS FOR FUTURE WORK .....		175
6.1.	Conclusions .....	175
6.2.	Suggestions for Future Work .....	178
APPENDIX A .....		180
LIST OF REFERENCES .....		186
BIOGRAPHICAL SKETCH .....		195

## LIST OF TABLES

<u>Table</u>	<u>page</u>
3.1. Summary of the chemical constituents and pH ranges used for analyzing 1% BaTiO <sub>3</sub> suspensions via electroacoustic analysis.....	75
5.1. Summary of the sample designation, weight percent BaTiO <sub>3</sub> , binder composition, and rheological properties (apparent viscosity and Bingham yield point) for the oxalate/polyethylene imine-treated BaTiO <sub>3</sub> slurry formulations.....	165
A.1. Summary of the chemical constituents and physical characteristics for BaTiO <sub>3</sub> slurries prepared with 0.5% oxalic acid, and varying amounts of polyethyleneimine (PEI) without binder present.....	181
A.2. Summary of the chemical constituents and physical characteristics for BaTiO <sub>3</sub> slurries prepared with 1.0% oxalic acid, and varying amounts of polyethyleneimine (PEI) without binder present.....	182
A.3. Summary of the chemical constituents and physical characteristics for BaTiO <sub>3</sub> slurries prepared with 2.0% oxalic acid, and varying amounts of polyethyleneimine (PEI) without binder present.....	183
A.4. Summary of the chemical constituents and physical characteristics for BaTiO <sub>3</sub> slurries prepared with 3.0% oxalic acid, and varying amounts of polyethyleneimine (PEI) without binder present.....	184
A.5. Summary of the chemical constituents and physical characteristics for BaTiO <sub>3</sub> slurries prepared with 5.0% oxalic acid, and varying amounts of polyethyleneimine (PEI) without binder present.....	185

## LIST OF FIGURES

Figure	page
2.1. Production flowchart for the fabrication of the multilayer capacitor. <sup>(5)</sup>	9
2.2. Schematic showing both the 3-dimensional view and the side-view of the laminated polycrystalline ceramic and metal structure of the multilayer capacitor. <sup>(5,22)</sup>	10
2.3. Different types of rheological behavior characteristics for various suspensions. <sup>(34)</sup>	13
2.4. Theoretical phase stability diagram for the Ba-Ti-CO <sub>2</sub> -H <sub>2</sub> O system. <sup>(14,15)</sup>	17
2.5. The theoretical stability diagram for aqueous TiO <sub>2</sub> suspensions. <sup>(54,55)</sup>	18
2.6. Schematic summarizing the problems associated with aqueous processing of barium titanate, specifically the incongruent dissolution of Ba <sup>2+</sup> and the formation of the Ti-rich and Ba-rich surface layer depicted in the corresponding particle diagram. <sup>(14,35)</sup>	19
2.7. Schematic showing two different views of the BaTiO <sub>3</sub> perovskite structure. <sup>(1,2,21)</sup>	21
2.8. A schematic of the various techniques with corresponding reactions to passivate metals where (a) an oxide surface layer forms in the presence of O <sub>2</sub> , (b) cathodic protection which involves a sacrificial magnesium anode to assure that the galvanic cell makes the pipeline the cathode, (c) anodic protection which passivates through exposure of the metal to a highly concentrated oxidizing solution, and (d) inhibitor ions associate with the surface to protect the underlying metal from corrosion. <sup>(58)</sup>	23
2.9. Five different types of glass surfaces produced during corrosion. <sup>(59)</sup>	25
2.10. Speciation diagrams for (a) the Ba-C <sub>2</sub> O <sub>4</sub> -H <sub>2</sub> O system <sup>(33,58)</sup> and (b) the Ca-C <sub>2</sub> O <sub>4</sub> -H <sub>2</sub> O system. <sup>(63,64)</sup>	27
2.11 The separation distance, d, between the two pairs of particles is determined at the initial interaction of the surrounding ionic clouds. The effective thickness of the surrounding ionic cloud (diffuse layer) is the reciprocal of the Debye-Hückel parameter where the k value in (a) is smaller than (b).	31
2.12. The potential distribution near the surface of a particle for different ionic strength values for a simple Gouy-Chapman model of the double layer. <sup>(70)</sup>	32

2.13. The electrical double layer structure showing the strongly adsorbed ions within the Stern plane and the diffuse surrounding cloud of counter ions that decreases in concentration with distance from the particle surface. <sup>(68)</sup>	34
2.14. (a.) A schematic showing the attractive, repulsive and total electrostatic interaction energy curves for a specific solution conditions, and (b.) the total electrostatic interaction energy curves for a poorly dispersed system, a moderately dispersed system, and a well dispersed system. <sup>(68,70)</sup>	35
2.15. Schematic showing a possible interaction between aqueous species, specifically a PVA-Ba <sup>2+</sup> interaction. <sup>(44,45)</sup>	37
2.16. Schematic showing two different polymeric dispersing mechanisms for suspensions, (a) depletion dispersion where the polymer remains in solution and prevents particle collisions and (b) adhesion of the cationic polyelectrolyte to the particle surface preventing particle-particle contact by both polymeric and electrostatic repulsion. <sup>(38)</sup>	39
2.17. (a) Summary of the mobility vs. pH curves for the rutile at different alkaline earth cations at 0.33 x 10 <sup>-3</sup> M concentration. (b) Electrophoretic mobility vs. pH curves for rutile in the presence of different concentrations of Ba(NO <sub>3</sub> ) <sub>2</sub> . <sup>(72,84)</sup>	41
2.18. Particle electrophoresis data for various lots of commercial BaTiO <sub>3</sub> powder that shows variation in lot to lot behavior as well as the powder supplier. <sup>(49)</sup>	43
2.19. Electrophoretic behavior for three BaTiO <sub>3</sub> suspensions at different solids loading. <sup>(49)</sup>	44
2.20. Both the theoretical and experimental electrophoretic behavior of COM are illustrated and a relatively constant charge is depicted over the pH range from pH 4 to pH 10. <sup>(64)</sup>	46
2.21. (a.) Schematic representing the particle movement in an applied electric field to determine the electrophoretic mobility. (b.) The electrophoretic mobility can be plotted as a function of pH or used to calculate the zeta potential and plotted as a function of pH.	52
2.22. Schematic showing variations in the sedimentation of the suspensions and the sediment height recorded in the sedimentation analysis. Finger shows variations in the transparency of the suspensions.	55
2.23. Scanning electron micrographs of the particle packing within the hand cast pseudo-tapes showing the difference between (a.) good dispersion and (b.) bad dispersion.	57
2.24. Schematic showing the various components and mathematical variables for the cone/plate viscometer and the corresponding mathematical expressions to determine the shear stress, shear rate, and viscosity. <sup>(105)</sup>	58
2.25. A summary of various interactions that can take place between the BaTiO <sub>3</sub> particles, water, and polymeric additives.	60

3.1. (a) Schematic summarizing the problems associated with aqueous processing of barium titanate and (b) a schematic representing the incongruent dissolution of barium from the surface of the barium titanate particle with the formation of an amorphous Ti-rich and Ba-rich layers during fabrication. <sup>(14,35)</sup>	64
3.2. Schematic diagram of the proposed additive, oxalate ions, to minimize the dissolution of $\text{Ba}^{2+}$ , and corresponding particles depicting the passivation layer with unknown solubility effects, surface charge formation, and dispersion characteristics.	67
3.3. (a) X-ray diffraction patterns for the as-received $\text{BaTiO}_3$ powders with JCPDS X-ray diffraction standards for tetragonal and cubic $\text{BaTiO}_3$ , respectively, and (b) scanning electron micrographs of the as-received $\text{BaTiO}_3$ powder.	72
3.4. (a) Cumulative particle size distribution and (b) log normal probability distribution for the as-received $\text{BaTiO}_3$ powder from Cabot Corporation, Boyertown, PA.	73
3.5. ICP data for the $\text{Ba}^{2+}(\text{aq})$ concentration in solution from three different $\text{BaTiO}_3$ suspensions (10 g of $\text{BaTiO}_3$ powder/l oxalic acid or 0.15%) as a function of oxalic acid ( $10^{-2}\text{M}$ , $10^{-3}\text{M}$ , and $10^{-4}\text{M}$ ) concentration.	78
3.6. Stability diagram for the $\text{Ba-TiO}_2\text{-CO}_2\text{-H}_2\text{O}$ system. <sup>(14)</sup> Data lines entitled "Virgin $\text{BaTiO}_3$ " and " $\text{BaTiO}_3$ with Oxalate Present" show the concentration of dissolved $\text{Ba}^{2+}$ from the supernatants of 10 g $\text{BaTiO}_3$ /l $\text{H}_2\text{O}$ (0.15%) and 10 g $\text{BaTiO}_3$ /l $10^{-4}\text{M}$ oxalic acid (0.15%) respectively.	79
3.7. (a) Speciation diagram for the $\text{Ba-C}_2\text{O}_4\text{-H}_2\text{O}$ system <sup>(17,63)</sup> and (b) the $\text{TiO}_2$ stability diagram. <sup>(34,55)</sup>	80
3.8. Transmission electron micrograph of the acetic acid-washed $\text{BaTiO}_3$ particles.	83
3.9. Transmission electron micrograph of the water-washed $\text{BaTiO}_3$ particles.	84
3.10. Transmission electron micrograph of the ammoniated water-washed $\text{BaTiO}_3$ particles.	85
3.11. Transmission electron micrograph of the oxalate-treated $\text{BaTiO}_3$ particles.	86
3.12. Zeta potential measurements as a function of suspension pH for the hydrothermally derived $\text{BaTiO}_3$ powder as a function of solids loading.	89
3.13. ICP analysis for the hydrothermally derived $\text{BaTiO}_3$ powder as a function of solids loading.	91
3.14. Electrophoretic behavior for $\text{BaC}_2\text{O}_4\text{-H}_2\text{O}$ and $\text{BaTiO}_3$ in deionized water and $\text{BaTiO}_3$ suspensions (10 g/l or 0.15%) in various concentrations of $\text{H}_2\text{C}_2\text{O}_4\cdot 2\text{H}_2\text{O}$ ( $10^{-2}$ , $10^{-3}$ , $10^{-4}\text{M}$ ).	94
3.15. $\text{BaTiO}_3$ suspensions (1%) with various amounts of oxalic acid incorporated as a weight percent of the solids ( $\text{BaTiO}_3$ powder).	96

3.16. Electroacoustic behavior for two different 1% BaTiO <sub>3</sub> suspensions with 0.0 and 3.0% oxalic acid present in comparison with electrophoretic behavior of similar suspensions where the zeta potential determined is determined using a light scattering technique (suspensions 1 through 4 respectively). For additional information about the electroacoustic suspensions see Table 3.1.....	97
3.17. (a) Schematic showing the incongruent dissolution of Ba <sup>2+</sup> in deionized water and the formation of Ti-rich and Ba-rich layers which circumvent the stoichiometric BaTiO <sub>3</sub> core, and (b) the passivation treatment for minimizing the dissolution of Ba <sup>2+</sup> from the BaTiO <sub>3</sub> particle surface via oxalic acid provides uncertain colloidal stability.....	99
4.1. (a) Schematic showing the incongruent dissolution of Ba <sup>2+</sup> in deionized water and the formation of Ti-rich and Ba-rich layers which circumvent the stoichiometric BaTiO <sub>3</sub> core, and (b) the passivation treatment for minimizing the dissolution of Ba <sup>2+</sup> from the BaTiO <sub>3</sub> particle surface via oxalic acid provides uncertain colloidal stability. <sup>(14,35,108)</sup> .....	102
4.2. A summary of various interactions that can take place between the BaTiO <sub>3</sub> particles, water, and polymeric additives. <sup>(108)</sup> .....	103
4.3. Schematic showing two different polymeric dispersion mechanisms for suspensions, (a) depletion dispersion where the polymer remains in solution and prevents particle collisions and (b) adhesion of the cationic polyelectrolyte to the particle surface preventing particle-particle contact by both polymeric and electrostatic repulsion. <sup>(38)</sup> .....	105
4.4. (a) Flow diagram for preparing slurries using a stainless steel mixer or polished zirconia mixing media. (b) Revised mixing order use to passivate and disperse the BaTiO <sub>3</sub> particles simultaneously.....	110
4.5. The solubility of BaC <sub>2</sub> O <sub>4</sub> ·H <sub>2</sub> O (theoretical as well as experimental) and BaC <sub>2</sub> O <sub>4</sub> ·H <sub>2</sub> O with various polymeric additives as a function of suspension pH. <sup>(17,45,63,108)</sup> .....	114
4.6. Schematic showing a possible interaction between aqueous species, specifically a PVA-Ba <sup>2+</sup> interaction. <sup>(44)</sup> .....	115
4.7. (a) Sedimentation results for 3% BaTiO <sub>3</sub> powder as a function of suspension pH and time. (b) Sedimentation rate for the same suspensions calculated at the one hour time period.....	117
4.8. (a) Sedimentation results for 3% BaTiO <sub>3</sub> and 5% oxalic acid (where the oxalic acid is added as a % of the solids) suspensions as a function of pH and time. (b) Sedimentation rate for the same suspension calculated for the one hour time period.....	119
4.9. (a) Sedimentation results for 3% BaTiO <sub>3</sub> and 1% PEI (where the PEI is added as a % of the solids) suspensions as a function of pH and time. (b) Sedimentation rate for the same suspensions calculated at the one hour time period.....	120

4.10. (a) Sedimentation results for 3% BaTiO <sub>3</sub> , 5% oxalic acid, and 1% PEI (where both the oxalic acid and PEI are added as a % of BaTiO <sub>3</sub> ) suspensions as a function of pH and time. (b) Sedimentation rate for the same suspensions calculated at the one hour time period.....	122
4.11. Electrophoretic behavior for 3% hydrothermally derived BaTiO <sub>3</sub> (Cabot Corporation) suspensions with 5% oxalic acid (% of BaTiO <sub>3</sub> ) as a function of PEI and suspension pH. ....	124
4.12. Schematic of the PEI molecular structure and its conformation on the negatively charged oxalate-treated BaTiO <sub>3</sub> surface. <sup>(116)</sup> .....	126
4.13. Rheological curves for a typical slurry to demonstrate how the viscosity and Bingham yield point were ascertained. ....	128
4.14. A summary of the rheological properties (viscosity and Bingham yield point), weight percent of the BaTiO <sub>3</sub> powder (wt.%), and passivation/dispersion dosages for possible and rejected (shaded regions) formulations. Criteria for rejected formulations are viscosity (h) off-scale, or agglomerates noted in the microstructure of hand-cast tapes. Viscosity and Bingham yield point are given in centiPoise and dynes/cm <sup>2</sup> respectively....	129
4.15. Scanning electron micrographs of a smeared sample from slurry 0.5:1 (68% BaTiO <sub>3</sub> , 0.5% oxalic acid, and 1.0% PEI) at four different magnifications (50kX, 25 kX, 10 kX, and 1 kX). Oxalic acid and PEI are added as weight percent of the BaTiO <sub>3</sub> . ....	130
4.16. Scanning electron micrographs of a smeared sample from an aqueous BaTiO <sub>3</sub> (Cabot hydrothermally derived powder) slurry prepared with a conventional tape casting formulation at four different magnifications (50 kX, 25 kX, 10 kX, and 1 kX).....	132
4.17. Rheological behavior (viscosity and shear stress vs. shear rate) for slurries with ~65% BaTiO <sub>3</sub> , 3% oxalic acid and 1%, 2%, 3%, and 5% PEI (slurry 3:1, 3:2, 3:3, and 3:5 respectively) where oxalic acid and PEI are added as weight percent of BaTiO <sub>3</sub> .....	133
4.18. Scanning electron micrographs of a smeared sample from slurry 2:1 (67% BaTiO <sub>3</sub> , 2.0% oxalic acid, and 1.0% PEI) at four different magnifications (50kX, 25 kX, 10 kX, and 1 kX). Oxalic acid and PEI are added as weight percent of the BaTiO <sub>3</sub> . ....	134
4.19. Scanning electron micrographs of a smeared sample from slurry 3:1 (67% BaTiO <sub>3</sub> , 3.0% oxalic acid, and 1.0% PEI) at four different magnifications (50kX, 25 kX, 10 kX, and 1 kX). Oxalic acid and PEI are added as weight percent of the BaTiO <sub>3</sub> . ....	136
4.20. (a) Schematic showing the incongruent dissolution of Ba <sup>2+</sup> and the formation of the Ti-rich and Ba-rich layers which circumvent the stoichiometric BaTiO <sub>3</sub> core. (b) Schematic showing the passivation treatment for minimizing the dissolution of barium from the particle surface and dispersion of the oxalate treated particles with a cationic polyelectrolyte. <sup>(14,35,108)</sup> .....	137

5.1. Different types of rheological behavior characteristics for various suspensions. <sup>(34)</sup> .....	142
5.2. Electrophoretic behavior (zeta potential vs. pH) of 1% BaTiO <sub>3</sub> , 5% oxalic acid, and 1% PEI suspension as a function of PEO concentration. All additives are incorporated as a weight percent of BaTiO <sub>3</sub> .....	150
5.3. Sedimentation results for 1% BaTiO <sub>3</sub> , 5% oxalic acid, 1% PEI, and (a.) 0% PEO or (b.) 12% PEO where all additives are incorporated as a weight percent of BaTiO <sub>3</sub> .....	152
5.4. Sedimentation results for 1% BaTiO <sub>3</sub> , 5% oxalic acid, 2% PEI, and (a.) 0% PEO or (b.) 12% PEO where all additives are incorporated as a weight percent of BaTiO <sub>3</sub> .....	153
5.5. Rheological behavior (shear stress and viscosity vs. shear rate) for the following three solutions, 10% PEO solution, 1% PEI solution, and 0.1M oxalic acid. ....	154
5.6. Rheological behavior for a mixture of equal amounts of 1.0% PEI solution and 0.1M oxalic acid at three different pH conditions (acidic, neutral, and alkaline).....	156
5.7. Rheological behavior for a mixture of equal amounts of 10% PEO solution and 0.1M oxalic acid at three different pH conditions (acidic, neutral, and alkaline).....	157
5.8. Rheological behavior for a mixture of equal amounts of 10% PEO solution and 1% PEI solution at three different pH conditions (acidic, neutral, and alkaline).....	158
5.9. Rheological behavior for a mixture of equal amounts of 10% PEO solution, 0.1M oxalic acid, and 1% PEI solution at three different pH conditions (acidic, neutral, and alkaline). ....	159
5.10. Titration curve for 1% PEI solution where 0.1M HNO <sub>3</sub> was used as the titrant.....	160
5.11. Titration curve for 10% 600L PEO solution where 0.01M HNO <sub>3</sub> and 0.01M TEAOH were used as the titrants. ....	161
5.12. Titration curve for 10% 8000 PEO solution where 0.01M HNO <sub>3</sub> and 0.01M TEAOH were used as the titrants. ....	162
5.13. Scanning electron micrographs of a smeared sample from an aqueous BaTiO <sub>3</sub> (Cabot hydrothermally derived powder) slurry prepared with a conventional tape casting formulation (57.5% BaTiO <sub>3</sub> and 12% binder) at four different magnifications (50 kX, 25 kX, 10 kX, and 1 kX). ....	164
5.14. Scanning electron micrographs of a smeared sample from slurry 9E-8000P (70% BaTiO <sub>3</sub> , 3.0% oxalic acid, 1.0% PEI, and 3.0% PEO-powder form) at four different magnifications (50 kX, 25 kX, 10 kX, and 1 kX). Oxalic acid, PEI, and PEO are added as a weight percent of the BaTiO <sub>3</sub> .....	167

- 5.15. Scanning electron micrographs of a smeared sample from slurry 9F-8000P (68% BaTiO<sub>3</sub>, 3.0% oxalic acid, 1.0% PEI, and 6.0% PEO-powder form) at four different magnifications (50 kX, 25 kX, 10 kX, and 1 kX). Oxalic acid, PEI, and PEO are added as a weight percent of the BaTiO<sub>3</sub>..... 168
- 5.16. Scanning electron micrographs of a smeared sample from slurry 9G-8000P (66% BaTiO<sub>3</sub>, 3.0% oxalic acid, 1.0% PEI, and 12.0% PEO-powder form) at four different magnifications (50 kX, 25 kX, 10 kX, and 1 kX). Oxalic acid, PEI, and PEO are added as a weight percent of the BaTiO<sub>3</sub>..... 169
- 5.17. Scanning electron micrographs of a smeared sample from slurry 9G-PVP (60% BaTiO<sub>3</sub>, 3.0% oxalic acid, 1.0% PEI, and 12.0% PVP) at four different magnifications (50 kX, 25 kX, 10 kX, and 1 kX). Oxalic acid, PEI, and PVP (40k MW) are added as a weight percent of the BaTiO<sub>3</sub>, ..... 170
- 5.18. Scanning electron micrographs of a smeared sample from slurry I-6A (65% BaTiO<sub>3</sub>, 3.0% oxalic acid, 1.0% PEI, and 12.0% PVP) at four different magnifications (50 kX, 25 kX, 10 kX, and 1 kX). Oxalic acid, PEI, and PVP (50/50 mixture of 10k and 49k MW) are added as a weight percent of the BaTiO<sub>3</sub>, ..... 172
- 5.19. Scanning electron micrographs of a smeared sample from slurry 3-1-10 PVP (65% BaTiO<sub>3</sub>, 3.0% oxalic acid, 1.0% PEI, and 10.0% PVP) at three different magnifications (25 kX, 10 kX, and 1 kX). Oxalic acid, PEI, and PVP (50/50 mixture of 10k and 49k MW) are added as weight percent of the BaTiO<sub>3</sub>..... 173

Abstract of Dissertation Presented to the Graduate School  
of the University of Florida in Partial Fulfillment of the  
Requirements for the Degree of Doctor of Philosophy

THE AQUEOUS PROCESSING OF BARIUM TITANATE:  
PASSIVATION, DISPERSION, AND BINDER FORMULATIONS  
FOR MULTILAYER CAPACITORS

By

ROBERT E. CHODELKA

December, 1996

Chairman: Dr. James H. Adair  
Major Department: Materials Science and Engineering

The current work confirms the incongruent dissolution associated with the aqueous processing of submicron  $\text{BaTiO}_3$  in multilayer capacitor (MLC) production, and offers a potential solution, via the use of an organic molecule to passivate the  $\text{BaTiO}_3$  surface. It has been shown that oxalate ion additions generate a nanometer thick surface passivation layer of  $\text{BaC}_2\text{O}_4 \cdot n\text{H}_2\text{O}$  at the surfaces of  $\text{BaTiO}_3$  particles in water. The oxalate-treated aqueous  $\text{BaTiO}_3$  suspensions exhibit a relatively uniform, negative surface charge over most of the pH range when a sufficient oxalate concentration is present relative to the total  $\text{BaTiO}_3$  surface area presented to the solution.

Sedimentation studies demonstrated the modest surface charge imparted by the oxalate-treated  $\text{BaTiO}_3$  particles was inadequate for dispersion. However, the addition of polyethylene imine to the oxalate-treated  $\text{BaTiO}_3$  suspensions provides a relatively constant, positive surface charge, and thus a stable, well dispersed suspension necessary for the fabrication of MLCs. The oxalate:PEI passivation:dispersion scheme is successful when

the suspension pH is above pH 5 and below pH 10, where oxalic acid is fully dissociated and present as  $\text{C}_2\text{O}_4^{2-}$  and PEI remains positively charged, respectively. In addition, these experiments suggest that steric hindrance, in combination with electrostatic forces, is responsible for the colloidal stability of the oxalic acid/PEI-treated  $\text{BaTiO}_3$  suspensions. For higher solids loading suspensions similar to possible MLC slurry formulations, it has been shown that the best passivation:dispersion dosage is 3:1 (i.e., 3.0% oxalic acid and 1.0% PEI) based on the rheological properties and the microstructure (particle packing) of the green "pseudo" tape.

Ceramic slurries incorporate organic binders that are dissolved and dispersed in the solution phase (aqueous or nonaqueous) to provide flexibility and mechanical integrity to the dried green structure. The addition of a 50/50 blend of PVP (10,000MW and 40,000MW) proved to be the most compatible binder system from the various binders analyzed in the current work. The 50/50 blend of PVP as a binder allowed 65%  $\text{BaTiO}_3$  solids loading with permissible tape casting rheological properties and far better particle densities in contrast to conventional tape casting formulations.

## CHAPTER 1 INTRODUCTION

### 1.1. Introduction

Perovskite materials are one of the most widely utilized ceramics in the production of electronic devices. The unique properties inherent to the perovskite structure are a result of the crystal structure, phase transitions as a function of temperature, and the size of the ions present in the unit cell.<sup>(1,2)</sup> Barium titanate ( $\text{BaTiO}_3$ ), in particular, because of a high dielectric constant, is used in the multi-billion dollar multilayer capacitor (MLC) and multilayer actuator industry.<sup>(3)</sup> Although the majority of MLC manufacturers use a doped- $\text{BaTiO}_3$  composition in the production of the MLC, the major or base constituent is  $\text{BaTiO}_3$ . Capacitor applications in electronic equipment include discharge of stored energy, blockage of direct current, coupling of circuit components, by-passing of an AC signal, frequency discrimination, transient voltage, and arc suppression.<sup>(4)</sup>

Demands by the electronic industries for capacitor miniaturization provide the incentive for MLC manufacturers to produce smaller capacitors with greater volume capacitance. In an effort to meet the demands of the electronics market, MLC manufacturers have to reduce the thickness of the ceramic layer within the multilayer polycrystalline ceramic and metal composite.<sup>(5)</sup> A reduction in the thickness of the ceramic layers can be accomplished by decreasing the particle size. A decrease in the particle size one order of magnitude accommodates much larger variations in the particle stacking that determines the thickness of the ceramic layer. In doing so, the importance of colloidal dispersion, solution chemistry, and the significance of flaws becomes much more critical. Thus, the success of MLC production critically relies on the preparation of well dispersed suspensions or slurries.<sup>(5-7)</sup> Slurries used in the wet forming techniques which produce the

ceramic layers of a MLC contain ceramic powder, an aqueous or nonaqueous solvent, an organic binder, and other organic additives such as plasticizers, dispersants, and defoaming agents.<sup>(5)</sup>

The manufacturing of MLCs been well documented.<sup>(5,8-12)</sup> Most commercial processing schemes to produce BaTiO<sub>3</sub> MLCs utilize nonaqueous suspending media such as methyl ethyl ketone and/or various alcohols to provide uniform dispersion of the slip.<sup>(7)</sup> With growing environmental awareness and increasing safety standards for hazardous materials, MLC manufacturers are forced to develop cheaper yet less toxic processing schemes to produce ceramic components with the same reliability and standards of nonaqueous processed devices. BaTiO<sub>3</sub> capacitors are difficult to produce reliably from aqueous suspension because of capricious dispersion and rheology of the slips. The disadvantages of aqueous processing include aggressive chemical attack of the BaTiO<sub>3</sub> particle surface by the aqueous solution and phase separation of the polymer additives via association with the dissolved surface species.<sup>(13-20)</sup> However, the major advantages of aqueous processing are the availability, the low toxicity, and the low cost of water.

Industry has relatively ignored the solution chemistry that is taking place during aqueous processing, including slurry preparation and drying of the BaTiO<sub>3</sub> green tapes. The main purpose of the current work is to improve the aqueous processing of BaTiO<sub>3</sub> tapes for MLC production.

## 1.2 Literature Review

Chapter 2 reviews the pertinent literature for the aqueous processing of ceramics in the production of thin layers for MLC fabrication with an emphasis on the processing steps that are affected by the current research. In an aqueous environment a large concentration of Ba<sup>2+</sup>(aq) may incongruently dissolve from the BaTiO<sub>3</sub> particle surface which can cross-link necessary polymeric additives and effect the sintering of the ceramic. Thermodynamic stability diagrams for both BaTiO<sub>3</sub> and TiO<sub>2</sub> in water are reviewed to provide an understanding of the stability problem associated with the aqueous processing of BaTiO<sub>3</sub>.

The incongruent dissolution problem associated with  $\text{BaTiO}_3$  may be overcome through a better understanding of the well documented passivation of metals and glasses. Therefore, the passivation of metals and glasses is discussed in reference to minimizing the capricious dissolution associated with aqueous  $\text{BaTiO}_3$  suspensions. Considering one of the techniques used to passivate metals, the feasibility to passivate the  $\text{BaTiO}_3$  particle is discussed with respect to possible additives.

Colloidal stability and rheological properties of the aqueous  $\text{BaTiO}_3$  suspensions are dependent on the charge formation associated with the particle surface and the polymeric additives which are both affected by the incongruent dissolution of the  $\text{Ba}^{2+}$  ion from the particle surface. The general electrostatic charge formation on a particle surface is discussed, followed by the presentation of polymeric dispersion mechanisms. The electrophoretic behavior for both aqueous  $\text{BaTiO}_3$  suspensions and aqueous  $\text{TiO}_2$  suspensions is presented. Adsorption studies of alkaline-earth cations onto the  $\text{TiO}_2$  particle surface are reviewed to provide insight to the charge formation of  $\text{BaTiO}_3$  in water. The predominant adsorption mechanism for  $\text{Ba}^{2+}$  absorbing onto the  $\text{TiO}_2$  surface was quantitatively assessed. The electrophoretic behavior of calcium oxalate monohydrate is reviewed to show the possible charge imparted by one of the suggested passivating agents. The location of the binder molecule and its interaction with the particles present in solution is briefly mentioned because there is no literature addressing these binder issues.

In addition, the non-stoichiometric particle surface caused by incongruent dissolution is reported to cause liquid phase sintering and abnormal grain growth in the microstructure of the fired component, which adversely affects the dielectric properties. Sintering of  $\text{BaTiO}_3$  is reviewed to show the optimum grain size and the importance of the Ba:Ti ratio at the surface of the particles. Although several of these studies provide vital information for improving the electronic properties of the MLC, most of the powders used in these studies were naively exposed to an aqueous environment, either through wet milling or atmospheric conditions. Thus the particles employed in the various studies may

exhibit surface layers and Ba:Ti ratios which are different in composition from the reported stoichiometry. However, one researcher accounted for the water effect on the  $\text{BaTiO}_3$  surface and reported its effects on grain size and microstructural uniformity of the sintered  $\text{BaTiO}_3$ .

The literature review strongly demonstrates the need to better understand the solution chemistry at the  $\text{BaTiO}_3$  particle/ $\text{H}_2\text{O}$  interface and its affect on the colloidal properties (i.e., dispersion and rheological behavior) of  $\text{BaTiO}_3$  wet forming suspensions for the MLC.

### 1.3. Chemical Passivation of the Barium Titanate Particle Surface via Oxalic Acid

Chapter 3 examines the feasibility to chemically passivate the unstable  $\text{BaTiO}_3$  particle surface and minimize the incongruent dissolution under aqueous conditions. As-received  $\text{BaTiO}_3$  powders were characterized using X-ray diffractometry (XRD) for phase crystallinity; scanning electron microscopy (SEM) for morphology, topography, and a general particle size; gas adsorption for specific surface area; and a centrifugal sedimentation technique for particle size distribution. The relatively low solubility and the electrophoretic behavior of  $\text{BaC}_2\text{O}_4 \cdot \text{H}_2\text{O}$  provided the basis for the theory that a  $\text{BaC}_2\text{O}_4$  layer on the surface of the  $\text{BaTiO}_3$  particle could (1) minimize the  $\text{Ba}^{2+}$  concentrations in solution, and (2) increase suspension stability by imparting a uniform, relatively constant charge over a wide pH range. Direct current plasma spectroscopy (DCP) and inductively coupled plasma spectroscopy (ICP) were used to demonstrate a reduction in the concentration of  $\text{Ba}^{2+}(\text{aq})$  in aqueous  $\text{BaTiO}_3$  suspensions containing oxalate ions as opposed to aqueous  $\text{BaTiO}_3$  suspensions without oxalate ions present. High resolution transmission electron microscopy (HRTEM) was used to visually confirm the presence of a layer on the oxalate-treated  $\text{BaTiO}_3$  particles. Electrophoretic behavior study of aqueous  $\text{BaTiO}_3$  suspensions as a function of solids loading was used to determine changes in the behavior with increased surface area exposure. Electrophoretic behavior studies of both aqueous BOM suspensions and  $\text{BaTiO}_3$  suspensions as a function of oxalate concentration

were used to confirm the relatively constant charge of the BOM particles with respect to pH and to determine the effectiveness of manipulating the charge of  $\text{BaTiO}_3$  particles by the addition of oxalic acid. Electroacoustic analysis was used to analyze higher solids loading suspensions to provide insight to the charge formation of increased  $\text{BaTiO}_3$  concentrations.

Chapter 3 confirms one of the major problems associated with the aqueous processing of  $\text{BaTiO}_3$  and offers the following potential solution: add the  $\text{BaTiO}_3$  to oxalic acid solution to provide oxalate ions that can react with dissolving  $\text{Ba}^{2+}$  leaving the  $\text{BaTiO}_3$  surface to form a  $\text{BaC}_2\text{O}_4$  passivation layer on the surface of the  $\text{BaTiO}_3$  particles.

#### 1.4. Dispersion of the Aqueous Barium Titanate Suspensions

Chapter 4 investigates the dispersion of aqueous  $\text{BaTiO}_3$  suspensions by the addition of various polymers (cationic, neutral, and anionic). Low solids loading solution chemistry analysis via ICP, sedimentation, and electrophoretic behavior were used as preliminary studies to screen and eliminate dispersants that increased the concentration of  $\text{Ba}^{2+}(\text{aq})$  concentration, increased the sedimentation rate, or reduced the zeta potential when added to the oxalate-treated  $\text{BaTiO}_3$  suspensions. Dispersants that did not increase the  $\text{Ba}^{2+}(\text{aq})$ , compromise the stability, or reduce the zeta potential were characterized at higher solids loading where stability is more apparent due to the increased number of inter-particle collisions. Higher solids loading slurries, similar to industrial tape casting formulations, were investigated by analysis of the rheological behavior (apparent viscosity and Bingham yield point) of each slurry, by visual assessment of hand cast pseudo tapes for agglomerates, and with the SEM to determine the particle packing within the microstructure of the green, pseudo tapes. The particle packing within the pseudo tape corresponds to the dispersion of the oxalate-treated  $\text{BaTiO}_3$  suspension with polymeric dispersants present.

Chapter 4 corroborates the need to add a cationic polyelectrolyte to disperse the oxalate-treated  $\text{BaTiO}_3$  particles without compromising the solubility of the  $\text{BaC}_2\text{O}_4$  passivation layer.

### 1.5. Binder Formulations for Aqueous Barium Titanate System

The experiments in Chapter 5 were specifically designed to determine the colloidal stability of various binder systems with the aqueous passivation-dispersion scheme for  $\text{BaTiO}_3$ . The incongruent dissolution of  $\text{BaTiO}_3$  is inhibited by forming a relatively insoluble salt, barium oxalate, on the particle surface which imparts a relatively constant, negative surface charge over a wide pH range. The addition of PEI to the oxalate-treated  $\text{BaTiO}_3$  imparts a positive surface charge and colloidal stability. Three types of polyelectrolytes (anionic, neutral, and cationic) were evaluated as possible binders for the oxalate/PEI-treated  $\text{BaTiO}_3$ . Polyacrylic acid which readily takes on negative charge, polyvinyl alcohol and polyethylene oxide which are neutral polymers, and polyethylene imine and polyvinyl pyrrolidone which are two cationic polymers were analyzed for compatibility with the chemically modified and dispersed  $\text{BaTiO}_3$ . Preliminary studies at low solids loading include electrophoresis and sedimentation for oxalate/PEI-treated  $\text{BaTiO}_3$  suspension with binder present, and rheological characterization of solutions containing various combinations of the three additives (oxalate, PEI, and binder) without  $\text{BaTiO}_3$  present to determine possible interactions between any two of the three additives without  $\text{BaTiO}_3$  present. High solids loading samples were prepared to analyze samples at a concentration similar to tape casting formulations where colloidal stability is more critical. Instability or interactions within the suspension will be more obvious at the higher solids loading. Binder compatibility will be assessed at the larger solids content via rheological behavior of the slurry, visual inspection for inconsistencies or imperfections within the tape, and scanning electron microscopy of the particle packing within the cast pseudo-tapes.

Chapter 5 shows that the slightly positively charged polyvinyl pyrrolidone when added to the passivated/dispersed  $\text{BaTiO}_3$  as a binder system comprised of a two different molecular weights mixture, is the most effective binder from polymers investigated for the oxalate/PEI-treated  $\text{BaTiO}_3$  particles.

### 1.6. Conclusions and Future Research

Chapter 6 summarizes the conclusions for each topic discussed in the current research and presents suggestions for possible future research topics.

## CHAPTER 2 LITERATURE REVIEW

### 2.1. Introduction

The discovery of the electronic properties exhibited by barium titanate ( $\text{BaTiO}_3$ ) led to a thorough investigation of the solid state properties of this perovskite-structured material.<sup>(1,2,21)</sup> These unique properties make  $\text{BaTiO}_3$  the most prolific polycrystalline ceramic used in the fabrication of multilayer capacitors (MLC).<sup>(8)</sup> With an emphasis to produce higher capacitance from smaller MLCs, knowledge (a fundamental understanding) and control the colloidal properties of proprietary slurries is necessary if increased volume efficiency is accomplished via thinner ceramic layers.<sup>(5-7)</sup> With a general movement by the MLC industry toward tape aqueous production, the first part of this chapter will review multilayer capacitor fabrication emphasizing the processing steps that are most affected by the current research. In later sections, a review of the literature on the stability of aqueous  $\text{BaTiO}_3$  suspensions, the passivation of materials, the formation of electrostatic charge, and mechanisms of polymeric dispersion is provided. More detail is given to the surface charge development of  $\text{BaTiO}_3$ , rutile, and calcium oxalate monohydrate (COM) in water. Sintering behavior of  $\text{BaTiO}_3$  is discussed to show the effect of the Ba:Ti ratio on the grain size, final microstructure, and dielectric properties to emphasize the importance of addressing the instability of  $\text{BaTiO}_3$  in an aqueous environment. This chapter concludes with a discussion of the characterization techniques used to discern the desired information and provide insight to improve the aqueous processing of  $\text{BaTiO}_3$ .

### 2.2. Processing of Multilayer Capacitors

The MLC fabrication has been well documented by many authors.<sup>(5-12)</sup> A general processing flowchart of the MLC is shown in Figure 2.1.<sup>(5)</sup> Figure 2.2 provides a

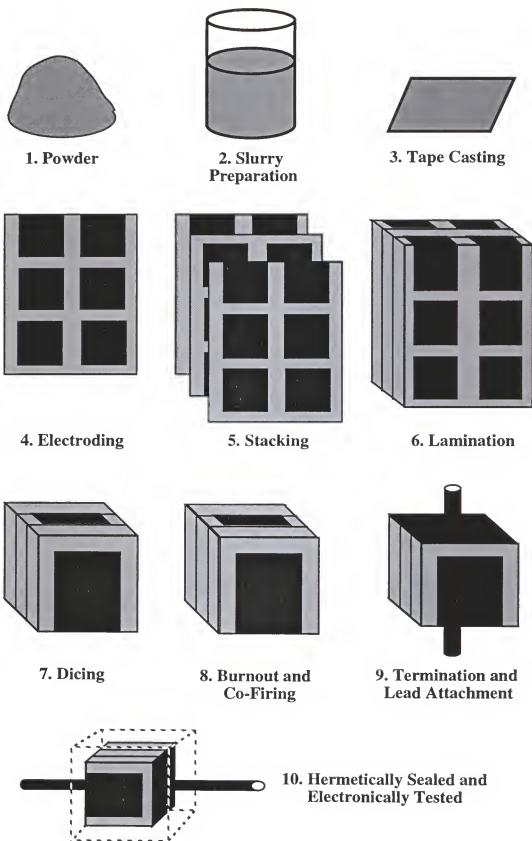


Figure 2.1. Production flowchart for the fabrication of the multilayer capacitor.<sup>(5)</sup>

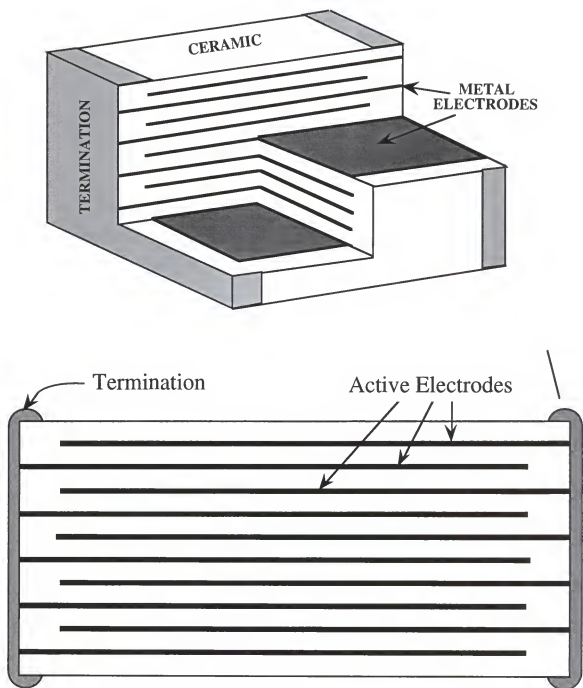


Figure 2.2. Schematic showing both the 3-dimensional view and the side-view of the laminated polycrystalline ceramic and metal structure of the multilayer capacitor.<sup>(5,22)</sup>

schematic representation of the laminated polycrystalline ceramic and metal layers.<sup>(22)</sup> The manufacturing procedure for the MLC will be discussed below starting with a description of the various forms of synthesized powder for use in MLC fabrication up to and including the final testing of the electronic package.

Several different synthesis techniques are used to produce BaTiO<sub>3</sub> powder. BaTiO<sub>3</sub> powder may be synthesized by reaction/calcination, coprecipitation, hydrothermal synthesis, metal organic decomposition, or carbothermic reduction.<sup>(23-27)</sup> The production of Ceramic disk and tube capacitor production does not demand as-received powder with the strict specifications needed for the production of thin ceramic layers for MLCs. The stoichiometry (Ba:Ti ratio), presence of impurities, specific surface area, particle size, and particle size distribution are critical characteristics of the as-received BaTiO<sub>3</sub> powder used in the fabrication of uniform, thin ceramic layers for MLCs.<sup>(28,29)</sup> Ideally, to produce fired ceramic layers less than 5 μm thick the particle size should be less than 0.5 μm with a narrow particle size distribution.<sup>(30,31)</sup> The motivation for reducing the thickness of the ceramic layers is to increase the capacitance of the MLC. The capacitance (C) of each ceramic layer is directly related to the thickness (t) according to the following equation:

$$C = \frac{k\epsilon_o A}{t} \quad [2.1]$$

where  $k$  is the dielectric constant of the material,  $\epsilon_o$  is the permittivity of free space ( $8.85 \times 10^{-12}$  F/m), and  $A$  is the unit area of each layer.<sup>(32)</sup> The total capacitance of the MLC is equal to the summation of the individual layers.

$$C_{MLC} = \frac{nk\epsilon_o A}{t} \quad \text{where} \quad \frac{C}{\text{unit volume}} \propto \frac{1}{t^2} \quad [2.2]$$

An increase in the number of ceramic layers (n) increases the capacitance of the MLC and the capacitance/unit volume is inversely proportionate to the thickness squared emphasizing the importance of reducing the thickness of the ceramic layers. Therefore, the ceramic layer thickness and grain size in the fired microstructure must be tailored to maximize the dielectric properties of the MLC.

The slurry for tape casting thin films for the MLC industry is highly specialized and generally proprietary.<sup>(12)</sup> A slip is composed of ceramic particles, a suspending medium (either water or a nonaqueous medium such as toluene or polymethyl butanol), and several polymeric additives to control dispersion, plasticity, foaming, and viscosity.<sup>(9-12)</sup> The synthesis of submicron-sized particles results in relatively large surface areas. Therefore, surface chemistry interactions at the solid/solution interface that largely govern the quality of dispersion need to be monitored more closely.<sup>(33,34)</sup> These interactions include the dissolution or adsorption of simple ions, surfactants, and polymers at the particle surface. Dispersion of BaTiO<sub>3</sub> powder involves breaking agglomerates and aggregates formed during synthesis and storage, then stabilizing the particles to minimize agglomeration prior to solidification of the slurry into tape form.<sup>(34)</sup> The aggressive chemical attack on the multicomponent ceramic by water may lead to the formation of depleted surface layers, deposition of other metastable phases from saturated solution or via crystallization of surface films, readsorption of the dissolved species, and diffusion of the species through these layers.<sup>(14,20,35,36)</sup> When ceramic particles are placed in water, a charge is formed at the particle/solution interface. When this charge is too small in magnitude to provide electrostatic stability of the suspension, a polymer may be added to the suspension to improve the colloidal properties. Dispersion of the particles with polymer occurs primarily by chemical and physical interactions of the surfactant at the surface of the ceramic particles.<sup>(34,38)</sup> Variation in dispersion of the ceramic powder sacrifices the reproducibility of the multilayer capacitor fabrication from batch to batch. Surface reactions at the BaTiO<sub>3</sub> particle/H<sub>2</sub>O interface, specifically the theoretical stability and the charge formation, are discussed in later sections.

The rheological properties of the slurry are highly dependent on the quality of dispersion of the powder and interactions between the powder, solution, and polymeric additives. Figure 2.3 summarizes the different rheological behavior encountered in the characterization of suspensions.<sup>(34)</sup> Ideally, the rheological behavior of the ceramic slurry

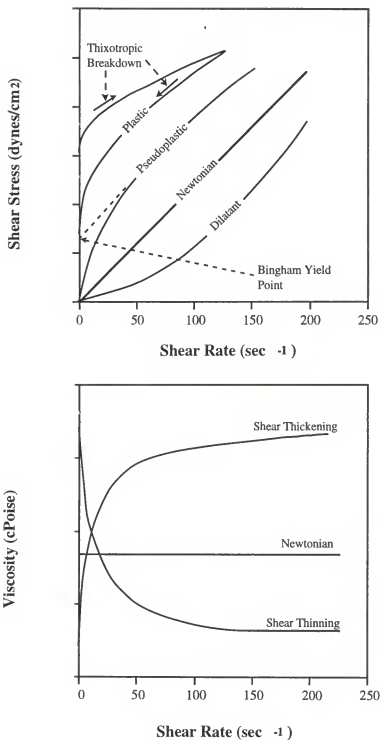


Figure 2.3. Different types of rheological behavior characteristics for various suspensions.<sup>(34)</sup>

should be pseudoplastic with a moderate Bingham yield point (BYP).<sup>(39)</sup> The pseudoplastic (shear thinning) behavior describes a decrease in the viscosity with an increase in the shear rate and the BYP is the force per unit area required to cause the slurry to flow. These two rheological properties dictate the uniformity of the film thickness after the shear of the doctor blade is removed.<sup>(12)</sup>

The slips are generally milled mechanically for extended periods of time ranging from several hours to days in an effort to crush any agglomerates and aggregates present.<sup>(40)</sup> Although the aqueous milling process is generally considered to be effective by MLC manufacturers, this process step continually generates new BaTiO<sub>3</sub> surface that has not reacted with the surrounding water.<sup>(14,15,17-20,35,41-43)</sup> The increase in surface area increases the concentration of Ba<sup>2+</sup> in solution, which promotes the deleterious solution reactions that compromise the aqueous tape fabrication.<sup>(44,45)</sup> After milling, a negative pressure is used to remove trapped gas from within the slurry and to minimize the amount of bubbles in the cast tapes. Gas removal is important because bubbles lead to the formation of holes in the green tapes and allow metal contact between two electrodes, causing shorts in the electronic component.

The most common way to fabricate polycrystalline BaTiO<sub>3</sub> layers is by tape casting, often via a doctor blade or waterfall technique.<sup>(12)</sup> After degassing, the slurry is transferred to a sealed hopper and spread approximately 10 μm to 50 μm thick across a moving stainless steel belt or polymer film. The thickness of the wet tape is controlled by the height setting of the doctor blade, the speed of the moving carrier film, and the rheological behavior of the slurry.<sup>(11)</sup> The waterfall technique relies on the rheological properties of the slurry and the speed of the substrate to control ceramic layer thickness. Variations in the thickness across the tape are directly influenced by the rheological behavior of the slurry and the drying rate of the wet tape. The edges of the dried ceramic tape are cut and removed to reduce variations in the tape thickness before collection on a reel.

The reels of ceramic tape are cut into uniform sizes and printed with an alternating metallic base pattern for the electrode of the capacitor. Up to one hundred sheets are stacked and laminated together by the application of heat and pressure (60°C to 80°C, and up to 30 MPa respectively).<sup>(5)</sup> The number of ceramic layers influences the electrical properties of the final capacitor. The laminated sheets are then diced into individual capacitors and cofired through a continuous furnace. The furnace has specific temperature zones for removal of all fabrication additives that compromise the final electronic properties of the component. The removal of the additives must be completed before the onset of sintering, otherwise gaseous products will be trapped within the structure and destroy the component. Termination and leads are attached to the fired metal/ceramic composite and the MLC package is hermetically sealed to minimize environmental degradation. Finally, selected samples are tested for electronic properties to provide quality control.

The chemical aspects of the MLC aqueous processing are neither trivial nor fully understood by the MLC industry. The solution chemistry (surface reactions) that takes place during processing, including slurry preparation and drying of the BaTiO<sub>3</sub> green tapes, is not normally taken into account. Unfortunately, aqueous-based processing of BaTiO<sub>3</sub> is difficult due to the incongruent dissolution of the particles, which supplies large concentrations of Ba<sup>2+</sup>(aq). If not properly understood and controlled, aqueous processing of BaTiO<sub>3</sub> alters the stoichiometry at the particle surface, reduces the effectiveness of the polymeric additives, and affects the sintering of the ceramic layers, compromising the electrical properties of the MLC.

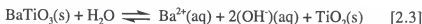
### 2.3. Aqueous Environment

#### 2.3.1. Solubility of Barium Titanate and Titanium Dioxide in Water

In the late seventies and early eighties, nuclear waste management was investigating the perovskite structure, specifically calcium titanate (CaTiO<sub>3</sub>), as a solid solution storage structure for contaminated nuclear by-products. The solid solution nuclear waste/perovskite was named SYNROC in expectation of its success because the perovskite

mineral was thought to be highly resistant to chemical attack.<sup>(46)</sup> However, the chemical stability of the perovskite was quickly refuted when  $\text{CaTiO}_3$  was determined to be unstable in natural ground waters.<sup>(47)</sup>  $\text{CaTiO}_3$  incongruently dissolves in water, leaving behind a  $\text{Ca}^{2+}$ -depleted or Ti-rich region at the solid  $\text{CaTiO}_3$ /solution interface.<sup>(48)</sup> The depth of the Ti-rich layer was found to be dependent upon solution pH, being more profound under acidic conditions. The investigations showed that  $\text{CaTiO}_3$  decomposes to  $\text{CaCO}_3$  and  $\text{TiO}_2$  in the presence of  $\text{CO}_2$ -contaminated water.<sup>(47,48)</sup> The determination that the perovskite structure is unstable in an aqueous environment terminated research by nuclear waste management on perovskites used for nuclear waste storage.

At approximately the same time as the investigations of  $\text{CaTiO}_3$  as a nuclear waste storage material, ceramists investigated the theoretical stability of  $\text{BaTiO}_3$ .<sup>(49)</sup> The dissolution reactions associated with  $\text{BaTiO}_3$  may be understood in terms of the solubility of the individual metal oxide components,  $\text{BaO}(\text{s})$  and  $\text{TiO}_2(\text{s})$ .<sup>(50)</sup> Figure 2.4 shows the phase stability diagram for  $\text{BaTiO}_3(\text{s})$  in water.<sup>(14,15)</sup>  $\text{BaTiO}_3(\text{s})$  in the  $\text{Ba-Ti-CO}_2\text{-H}_2\text{O}$  system undergoes incongruent dissolution below  $\sim\text{pH } 13$ , with the concentration of  $\text{Ba}^{2+}(\text{aq})$  dependent on the concentration of dissolved  $\text{CO}_2$  in the solution.<sup>(14,15,17-19,35,41-43)</sup> The concentration of  $\text{Ba}^{2+}(\text{aq})$  derived from the  $\text{BaO}(\text{s})$  component is large (as high as 0.1M) and depends upon the surface area of  $\text{BaTiO}_3$  exposed to aqueous solution below about pH 12. In contrast, Figure 2.5 shows that  $\text{TiO}_2(\text{s})$  is only sparingly soluble over the pH range from pH 3 to pH 10.<sup>(20,50-55)</sup> The overall stoichiometric chemical reaction describing the dissolution of  $\text{BaTiO}_3(\text{s})$  is given by,



However, the incongruent dissolution of  $\text{Ba}^{2+}$  is kinetically hindered by the formation of a diffusion barrier of  $\text{TiO}_2$  and/or of the metal salt  $\text{BaCO}_3$ , which is normally present on the surfaces of  $\text{BaTiO}_3$  particles as depicted in Figure 2.6.<sup>(14,35)</sup> However, the milling of the slurry prior to tape casting constantly exposes virgin  $\text{BaTiO}_3$  surface where  $\text{Ba}^{2+}$  has not been dissolved. This continuous new surface exposure saturates the solution

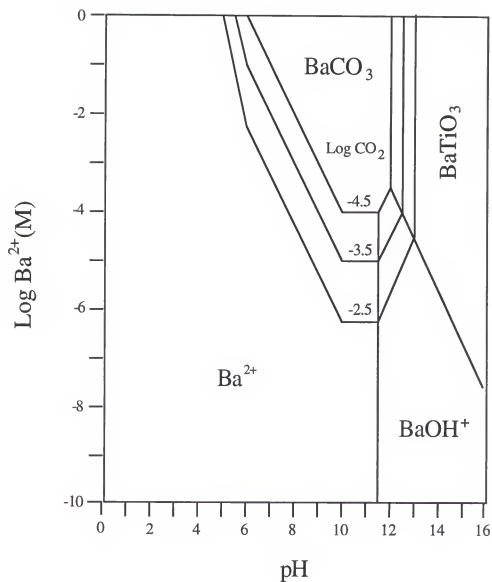


Figure 2.4. Theoretical phase stability diagram for the Ba-Ti-CO<sub>2</sub>-H<sub>2</sub>O system.<sup>(14,15)</sup>

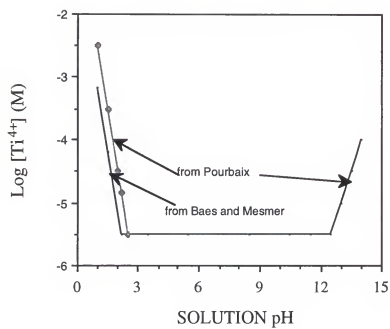


Figure 2.5. The theoretical stability diagram for aqueous  $\text{TiO}_2$  suspensions.<sup>(54,55)</sup>

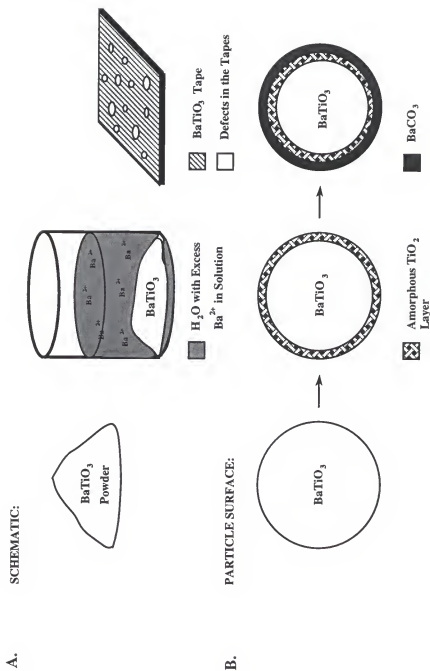


Figure 2.6. Schematic summarizing the problems associated with aqueous processing of barium titanate, specifically the incongruent dissolution of  $\text{Ba}^{2+}$  and the formation of the Ti-rich and Ba-rich surface layer depicted in the corresponding particle diagram. <sup>(14,35)</sup>

with  $\text{Ba}^{2+}(\text{aq})$ .<sup>(35)</sup> It has been demonstrated that most commercial  $\text{BaTiO}_3$  powders have a  $\text{BaCO}_3$  surface layer that forms during storage of the powder or during slurry formulation.<sup>(14,42)</sup> Whether  $\text{TiO}_2$ -rich or  $\text{BaCO}_3$  passivation layers are present on the  $\text{BaTiO}_3$  particle surface depends on the environment to which the powders are subjected during and subsequent to synthesis.<sup>(41)</sup>

The general perovskite structure can be designated as  $\text{ABO}_3$ , with the A ions located at the corners, B ions positioned at the center, and  $\text{O}^{2-}$  ions located at the face centers of the cube.<sup>(1,2,21)</sup> Figure 2.7 depicts the specific perovskite structure for  $\text{BaTiO}_3$ . The A site, a basic cation, is generally soluble over a relatively large pH range while the B site, an acidic cation, is relatively insoluble. This has been shown to be true for  $\text{BaTiO}_3$ , where the A ion is  $\text{Ba}^{2+}$  and the B ion is  $\text{Ti}^{4+}$ .

In summary, the aqueous processing of multicomponent ceramics may lead to the formation of depleted surface layers, deposition of other metastable phases either from saturated solution or via crystallization of surface films, readsorption of the dissolved species, and diffusion of the species through these layers. The presence of  $\text{BaCO}_3$  on the surface or a change in the Ba:Ti ratio due to incongruent dissolution of the surface in aqueous solution can adversely affect sintered microstructures (e.g., exaggerated grain growth) in  $\text{BaTiO}_3$  and, consequently, lead to poor electronic properties of the component. Excess  $\text{Ba}^{2+}$  in solution that dissolves from the  $\text{BaTiO}_3$  particle surface can cross-link the various polymeric additives, or may redeposit onto the particle surface upon drying of the tape, thus changing the surface composition. Polymeric dispersion and sintering of  $\text{BaTiO}_3$  from a Ba:Ti perspective is discussed in more detail in later sections to address the effect of excess  $\text{Ba}^{2+}(\text{aq})$  on the cross-linking of polymeric additives and the final microstructure respectively.

### 2.3.2. Passivation of Thermodynamically Unstable Metals and Glasses

The passivation of metal surfaces has been documented for many years.<sup>(55-57)</sup> Four different types of metal passivation include the formation of an oxide in air, the passivation

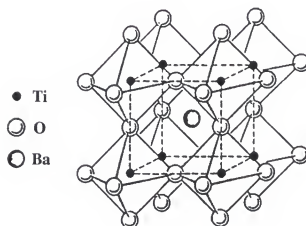
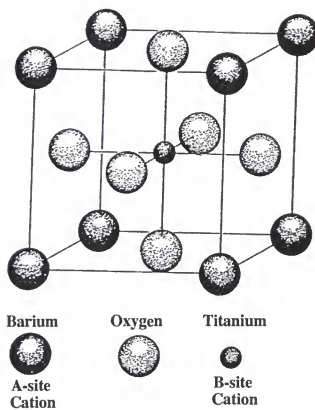


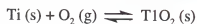
Figure 2.7. Schematic showing two different views of the BaTiO<sub>3</sub> perovskite structure.<sup>(1,2,21)</sup>

of the cathode in solution, the passivation of the anode in solution, and the addition of inhibitors to solution that preferentially interact at the metal/solution interface, protecting the metal (Figure 2.8).<sup>(58)</sup> The formation of an oxide passivation layer on a metal in air via a reaction between the metal and oxygen is dependent on the free energy of formation for the oxide. This is analogous to the formation of  $\text{BaCO}_3$  on the surface of  $\text{BaTiO}_3$  in air. The problem with  $\text{BaCO}_3$  as a passivation layer for  $\text{BaTiO}_3$  is the capricious solubility of  $\text{BaCO}_3$  in water as a function of solution pH.

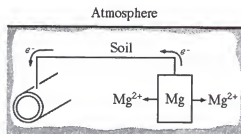
Some metal surfaces react under particular environmental conditions to produce a thin metal oxide passivation layer which is relatively inert in aqueous solution. Cathodic passivation requires a sacrificial anode which supplies electrons to the metal and prevents corrosion. However, the addition of a sacrificial anode to  $\text{BaTiO}_3$  is impractical and will not be considered here. Anodic passivation is commonly used to protect aluminum. In this case, the metal is exposed to a strongly oxidizing solution and a thick oxide layer is produced. The formation of a  $\text{BaO}$  passivation layer on the surface of  $\text{BaTiO}_3$  is not worth pursuing because the solubility of  $\text{BaTiO}_3$ , as discussed in the previous section is based on the solubility of the individual metal oxide components,  $\text{BaO(s)}$  and  $\text{TiO}_2\text{(s)}$ .

The only possible metal passivation technique that could be applied to the passivation of  $\text{BaTiO}_3$  is the addition of inhibitors to the solution phase. Specific ions are added to the solution which preferentially associate with the metal surface and restrict corrosion. The concentration of ions added is critical and must be sufficient to protect all exposed metal surfaces. Insufficient concentrations of inhibitor ions will lead to accelerated corrosion at the unprotected areas. A few possible passivating agents for  $\text{BaTiO}_3$  are proposed in the following section. In principle, the passivation of  $\text{BaTiO}_3$  in an aqueous environment may be achieved in a similar manner to the passivation of metals through the addition of inhibitor ions, in that a surface reaction may be induced between the dissolving  $\text{Ba}^{2+}$  from the surface of the particles and inhibitor ions added to the surrounding media to minimize  $\text{Ba}^{2+}$  dissolution.

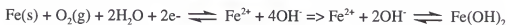
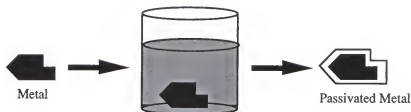
a.



b.



c.



d.

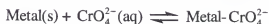
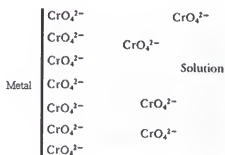


Figure 2.8. A schematic of the various techniques with corresponding reactions to passivate metals where (a) an oxide surface layer forms in the presence of  $\text{O}_2$ , (b) cathodic protection which involves a sacrificial magnesium anode to assure that the galvanic cell makes the pipeline the cathode, (c) anodic protection which passivates through exposure of the metal to a concentrated oxidizing solution, and (d) inhibitor ions associate with the surface to protect the underlying metal from corrosion.<sup>(58)</sup>

The passivation of glasses is due to the formation of a depleted region in solution, the incorporation of multivalent ions into the surface, formation of a crystalline phase at the surface of an amorphous glass, or the deposition of dissimilar materials (i.e. polymer or metal) passivating layer prior to exposure of the glass to the aggressive environment.<sup>(59-62)</sup> The passivation of the  $\text{BaTiO}_3$  surface to minimize the incongruent dissolution modeled after the techniques used to passivate glass is highly unlikely. However, the principles of corrosion may be applied to understanding the incongruent dissolution of  $\text{BaTiO}_3$ . The depleted region in the passivation or corrosion of glass consists of a compositional gradient restricting the diffusion of the dissolving ion to the solution phase. Figure 2.9 shows five different types of corrosion for various glass compositions.<sup>(59)</sup> Type 1 and Type 3 glass corrosion require the coating of the glass surface with an insoluble, compatible coating or the formation of a surface composition via incorporation of multivalent ions that is more chemically resistant than the bulk material, respectively. Type 5 corrosion shows congruent dissolution of the glass surface where all species dissolve until the solution is saturated. The corrosion of  $\text{BaTiO}_3$  is similar to Type 2 glass corrosion, where selective leaching occurs at the surface leaving behind a less soluble passivating layer that restricts the diffusion of the dissolving  $\text{Ba}^{2+}$  ions. Although the formation of a depleted region at the surface of the  $\text{BaTiO}_3$  particle passivates the inner particle core, the excess  $\text{Ba}^{2+}(\text{aq})$  makes this passivation unacceptable in the processing of MLCs.

### 2.3.3. Feasibility of Passivating Barium Titanate

The basic approach in the current work is to create a surface diffusion barrier that is relatively insoluble yet can be easily removed during subsequent processing steps, such as binder pyrolysis and firing. The ideal situation is to precipitate a simple salt with the  $\text{Ba}^{2+}$  ions on the surface of the suspended  $\text{BaTiO}_3$  particles similar to the passivation of metals by the addition of inhibiting ions. The spontaneous formation of a stable compound on the surface will arrest further dissolution and minimize variation in the Ba:Ti ratio. In fact,  $\text{BaCO}_3(\text{s})$  is a natural passivating agent on the surface of the  $\text{BaTiO}_3$  particles.<sup>(19)</sup>

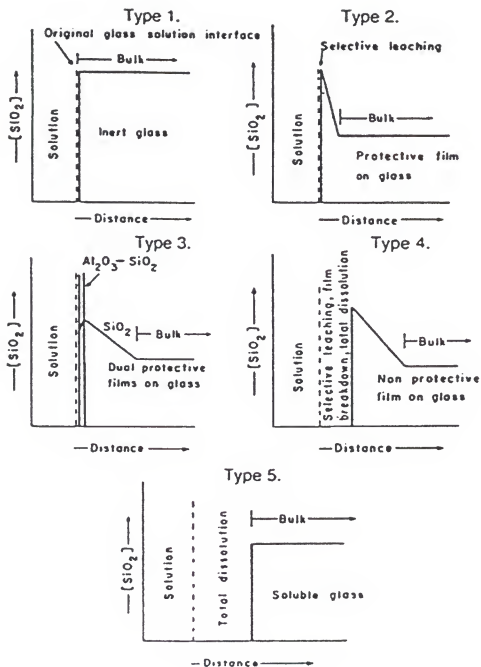


Figure 2.9. Five different types of glass surfaces produced during corrosion.<sup>(59)</sup>

Unfortunately, the solubility of  $\text{BaCO}_3$  varies dramatically with solution pH which reduces the effectiveness of  $\text{BaCO}_3$  as a passivating agent. Moreover, working in the solution pH regime where  $\text{BaCO}_3$  is stable, above pH 9, is not advantageous because many organic additives used as dispersants and binders lose effectiveness in alkaline pH conditions.

There are several sparingly soluble barium salts that have the potential to produce a passivation layer on  $\text{BaTiO}_3$ . A suitable passivating agent should form a sparingly soluble salt with the leached  $\text{Ba}^{2+}$ , and the solubility of the Ba-salt should be relatively insensitive to changes in solution pH. The Ba-salt must be compatible with other organic additives such as dispersants and binders, should experience clean pyrolysis during the organic burnout and sintering processing steps, and should not compromise the electronic properties of the ultimate material. Included among potential anions that form sparingly-soluble barium salts are  $\text{SO}_4^{2-}$  as  $\text{BaSO}_4(\text{s})$ ,  $\text{PO}_4^{3-}$  as  $\text{Ba}_3(\text{PO}_4)_2(\text{s})$ ,  $\text{CO}_3^{2-}$  as  $\text{BaCO}_3(\text{s})$ , and  $\text{C}_2\text{O}_4^{2-}$  as  $\text{BaC}_2\text{O}_4 \cdot \text{H}_2\text{O}(\text{s})$ . Figure 2.10(a) and 2.10(b) shows the solubility of  $\text{BaC}_2\text{O}_4 \cdot \text{H}_2\text{O}(\text{s})$  and a similar compound,  $\text{CaC}_2\text{O}_4 \cdot \text{H}_2\text{O}(\text{s})$ , in water as a function of suspension pH respectively.<sup>(17,63,64)</sup> The solubilities of the passivating solids,  $\text{BaSO}_4(\text{s})$  and  $\text{BaC}_2\text{O}_4 \cdot \text{H}_2\text{O}(\text{s})$  are relatively insensitive to changes in solution pH, while the solubilities of  $\text{Ba}_3(\text{PO}_4)_2(\text{s})$  and  $\text{BaCO}_3(\text{s})$  vary considerably with solution pH because of the respective acid dissociation constants for  $\text{H}_3\text{PO}_4$  and  $\text{H}_2\text{CO}_3$ . Thus  $\text{PO}_4^{3-}$  and  $\text{CO}_3^{2-}$  were rejected as passivating agents. Both acid dissociation constants for oxalic acid ( $\text{H}_2\text{C}_2\text{O}_4$ ) occur below pH 4.5 as discussed below, thus above pH 4.5 the solubility of  $\text{BaC}_2\text{O}_4(\text{s})$  is independent of solution pH similar to that of COM.<sup>(17,63,64)</sup> The  $\text{SO}_4^{2-}$  species was rejected as a passivating agent because of the unfavorable gaseous products produced during the burnout of the organic additives and sintering.  $\text{BaC}_2\text{O}_4(\text{s})$  is sparingly soluble with the solubility relatively constant above pH 4 and should experience relatively clean pyrolysis and leave little or no residue.<sup>(65,66)</sup> Therefore, oxalic acid was chosen as an appropriate passivating agent. Furthermore, it will be shown in future work that dispersant

# SOLUBILITY OF BARIUM OXALATE

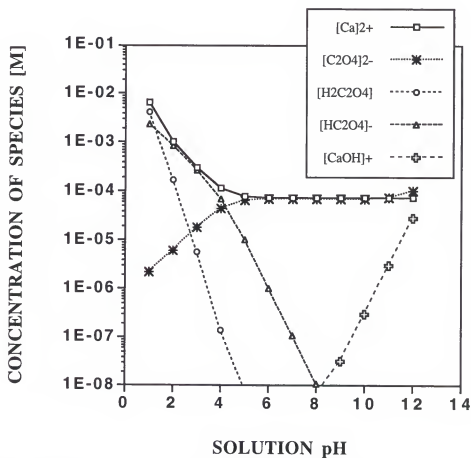
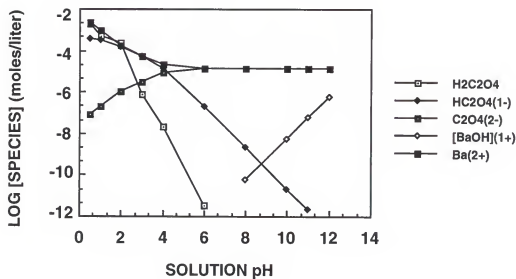


Figure 2.10. Speciation diagrams for (a) the Ba-C<sub>2</sub>O<sub>4</sub>-H<sub>2</sub>O system<sup>(33,58)</sup> and (b) the Ca-C<sub>2</sub>O<sub>4</sub>-H<sub>2</sub>O system.<sup>(63,64)</sup>

and binder systems may be developed that are compatible with the oxalic acid passivation scheme. One of the potential drawbacks in using oxalic acid is the possible formation of  $\text{BaCO}_3(\text{s})$  during pyrolysis. However, this limitation is not expected to have any more impact on sintering and dielectric properties than the levels of  $\text{BaCO}_3(\text{s})$  present in conventional  $\text{BaTiO}_3$  powders.

## 2.4. Dispersion

The colloidal stability and rheological properties of most ceramic particles in aqueous media are dependent upon surface charge formation (i.e. pH, zeta potential, isoelectric point (IEP), ionic strength, and polymeric vis-a-vis electrosteric dispersion) which is affected by both contamination on the particle surface and incongruent dissolution of the surface.<sup>(14,42)</sup> The release of ions from the particle surface into solution can also induce gelation of polymeric additives and impair dispersion, or may deleteriously affect the final microstructure of the sintered body.<sup>(44,45)</sup> These disadvantages can be overcome through a better understanding of the colloidal chemistry, particularly, the chemical reactions at the oxide/solution interface. The colloidal chemistry involved in ceramic processing such as tape casting, extrusion, or slip casting is critical to the fabrication of reliable components from aqueous suspension, but has been virtually ignored by the processing industry.

### 2.4.1. Electrostatic Surface Charge Formation and Stabilization

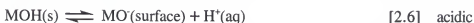
A ceramic dispersion is stable in the colloid chemical sense when particles repel other similar particles and remain unaggregated.<sup>(67)</sup> Suspended particles are constantly moving throughout the liquid due to Brownian motion, gravity (sedimentation), and convection currents. This random motion of the particles leads to particle-particle interactions. If the repulsive forces are not greater than the attractive forces, the particles will agglomerate.<sup>(68)</sup> Larger particles are generally more affected by gravity, whereas smaller particles are influenced by Brownian motion.<sup>(69)</sup> The tendency towards agglomeration results from London or van der Waals forces which are invariably present

and always attractive.<sup>(70)</sup> Thus, a suspension is stable only in the presence of strong, electrostatic repulsive forces, as a result of the electrical double layer and adsorbed layers at the particle surface.

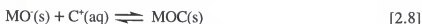
When finely divided metal oxide particles are immersed in water, the charge at the surface controls the stability of the suspension. All metal oxide surfaces carry unsatisfied bonds which may be fully coordinated by reacting with  $\text{OH}^-$  or  $\text{H}^+$  ions in solution. The hydroxyl layer can be represented by the following reaction.<sup>(16)</sup>



The amphoteric dissociation of the hydroxyl groups allows the surface of the oxide to form a positive or negative charge.



Acid dissociation (equation 2.6) leads to negative surface sites, while basic dissociation (equation 2.5), promotes positive surface sites. The magnitude of the surface charge (and therefore the surface potential) is controlled by  $\text{H}^+$  and  $\text{OH}^-$  ions. Therefore, these ions can be considered as the potential determining ions for ceramic oxides in water. The adsorption of any other univalent simple ions cannot increase the stability of oxide dispersions. In fact, they can only decrease the charge as shown in equations 2.7 and 2.8.<sup>(16)</sup>



However, multivalent ions can increase, decrease, or reverse the potential at the surface.<sup>(71,72)</sup>



An important property of these low solubility oxide materials is the dependence of adsorption of simple ions and surfactants, and pH on the oxide acid/base character.<sup>(16)</sup> However, the dissolution of multicomponent compounds (i.e. glasses or cements)<sup>(59-61)</sup> in

any solvent is a complex process which is further complicated by the fact that these systems undergo preferential leaching of certain components, rather than congruent dissolution.<sup>(62)</sup> As the number of components in the ceramic oxide increases, the reaction with water can become correspondingly more complex, raising the possibility that a number of different surface films will form.<sup>(37,59)</sup>

The surface potential,  $\Psi_o$ , is the potential difference between the solid surface and the bulk solution. The potential determining ions alter the surface potential on transfer from the solution phase to the solid surface and vice versa. Theoretical analysis of the double layer shows that the charge density in the aqueous solution decreases rapidly with increasing distance from the solid surface, and that the potential,  $\Psi$ , declines monotonically as a function of distance.

$$\Psi(\text{surface}) = \Psi_o \exp(-Kx) \quad [2.10]$$

The variable  $K$ , referred to as the Debye-Hückel parameter, is the reciprocal of the effective thickness of the diffuse layer. Figure 2.11 shows the difference in separation distance,  $d$ , between two particles with a small  $K$  value and a large  $K$  value (Figure 2.11. (a) and (b) respectively). Larger  $K$  values indicate thinner electrical double layers or smaller counter ion clouds surrounding the solid particle.<sup>(44)</sup> The thickness of the electrical double layer is critical for dispersion of particles and can be approximated by the Debye-Hückel equation,

$$1/K = (\epsilon\epsilon_o RT/F^2 I)^{0.5}, \quad [2.11]^{(67)}$$

where  $\epsilon$ ,  $\epsilon_o$ ,  $R$ ,  $T$ , and  $F$  represent the permittivity of the solution, permittivity of free space, ideal gas constant, temperature, and Faraday's constant respectively, and

$$I = 1/2 \sum (c_i z_i^2). \quad [2.12]$$

The terms  $I$ ,  $c_i$  and  $z_i$  represent the ionic strength of the solution, the bulk concentration and the charge on the  $i^{\text{th}}$  ion, respectively.<sup>(68,70)</sup> Figure 2.12 illustrates the decrease in the

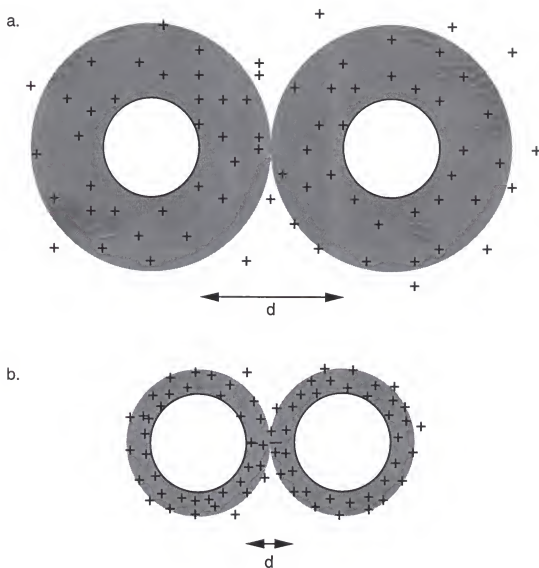


Figure 2.11. The separation distance,  $d$ , between the two pairs of particles is determined at the initial interaction of the surrounding ionic clouds. The effective thickness of the surrounding ionic cloud (diffuse layer) is the reciprocal of the Debye-Hückel parameter where the  $\kappa$  value in (a) is smaller than (b).

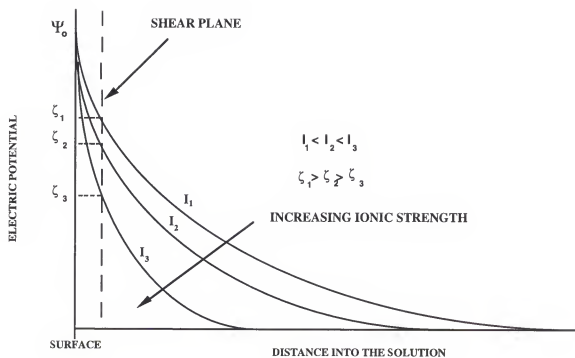


Figure 2.12. The potential distribution near the surface of a particle for different ionic strength values for the simple Gouy-Chapman model of the double layer.<sup>(70)</sup>

double layer thickness with an increase in the ionic strength and is commonly referred to as compression of the double layer. The solubility of  $\text{BaTiO}_3$  produces large concentrations of the divalent ion,  $\text{Ba}^{2+}(\text{aq})$ . Therefore, the ionic strength of aqueous  $\text{BaTiO}_3$  suspensions where the solubility of the particle is not addressed and minimized is large and the colloidal stability is poor.

The charging of the solid surface gives rise to a separation of electric charge where the solid and solution acquire opposite charges at their phase boundary. A number of surface charge models have been proposed in the literature, ranging from simple approximations to more complex and detailed representations.<sup>(73-81)</sup> All surface chemical models may contain two or more of the following components: (1) a surface chemical charging mechanism, (2) an intermediate surface charge layer that accommodates the chemical adsorption that may occur (i.e. the Stern layer or the Helmholtz layers), and (3) a Gouy-Chapman layer or double layer that ensures electroneutrality via a diffuse layer of electrostatically attracted ions labeled as counter ions.<sup>(74,75)</sup> Of these ions, those that are adsorbed only by electrostatic attraction are called indifferent electrolyte ions; those ions which are adsorbed by other means in addition to electrostatic forces are termed specifically adsorbed ions and are located in the Stern plane. Figure 2.13 represents a schematic illustration of the interfacial charge and potential distributions associated with the electrical double layer. The most simple surface charge model is that described by the Nernst relationship. However, the oxide-solution surface is far too complex to be described by this simple model.

In order to quantitatively assess the stability of colloidal dispersions, all the forces acting in the system must be considered. The Derjaguin-Landau-Verwey-Overbeek (DLVO) theory considers the colloid stability in terms of the electrical double layer and London-van der Waals forces.<sup>(81,82)</sup> The energy as a function of interparticle distance is shown in Figure 2.14 (a.). Figure 2.14 (b.) shows the total interaction energy curves for “good”, “moderate”, and “bad” dispersions. The common features for all three curves are

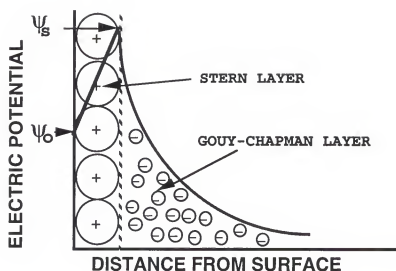


Figure 2.13. The electrical double layer structure showing the strongly adsorbed ions within the Stern plane and the diffuse surrounding cloud of counter ions that decreases in concentration with distance from the particle surface.<sup>(68)</sup>

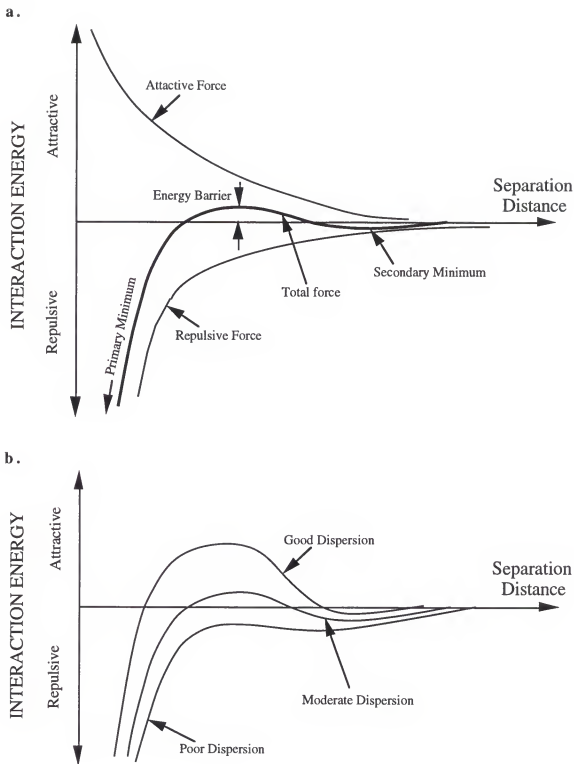


Figure 2.14. (a.) A schematic showing the attractive, repulsive and total electrostatic interaction energy curves for specific solution conditions, and (b.) the total electrostatic interaction energy curves for a poorly dispersed system, a moderately dispersed system, and a well dispersed system.<sup>(68,70)</sup>

(a) the deep primary minimum at small particle separations, (b) the shallow secondary minimum at larger separation distances, and (c) the magnitude of the energy barrier between these two minima which controls stability.<sup>(70)</sup> The stability of the colloidal dispersion breaks down when the total energy barrier becomes of the same order of magnitude as the Brownian motion-associated energy of the particles. The parameters which determine the form of these curves are the surface potential, dielectric constant, ionic charge, ionic strength, temperature, Hamaker constant, and particle dimension. In dilute dispersions it is often sufficient to consider only interactions between pairs of particles, whereas in concentrated systems it is necessary to consider multiparticle interactions.

Whether the dispersion of fine particles is promoted or compromised, it should be clear from the above discussion that simultaneous characterization of the solid phase, the interface, and the aqueous phase is necessary in order to obtain a complete picture of the fundamental charging mechanisms which are dominant.

#### 2.4.2. Polymeric Dispersion

Most ceramic slurries require polymer additives to assist dispersion of the particulate. Steric stabilization of colloidal particles is imparted by macromolecules that are attached by grafting or by physical adsorption to the particle surface.<sup>(38)</sup> The adsorbed polymer molecules form a physical, steric barrier around the particles which acts to prevent close approach of the particles and agglomeration. From an interaction energy versus separation distance perspective, steric stability is achieved as the polymer layer becomes thicker than the distance of the electrostatic energy barrier. Spontaneous redispersion of dried particles is a characteristic feature of most sterically/electrostatically stabilized systems<sup>(38)</sup>, whereas for electrostatic stabilization alone, once the particles come in contact, redispersion is highly unlikely. However, the disadvantage of polymer additions to multicomponent ceramic systems is shown in Figure 2.15 where the polymer molecules can cross-link and form a gel with species in solution that dissolved from the metal oxide surface.<sup>(44,45)</sup> In addition to cross-linking, the formation of soluble dissolved species-

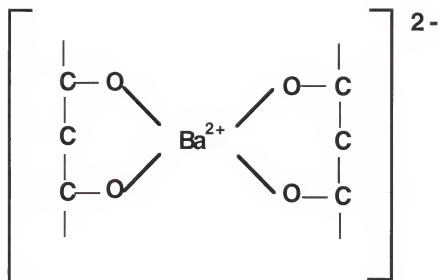


Figure 2.15. Schematic showing a possible interaction between aqueous species, specifically a PVA- $\text{Ba}^{2+}$  interaction.<sup>(44,45)</sup>

polymer complexes increases the solubility of the solid present in solution. Steric stabilization is generally not as important in aqueous/low solubility oxide systems, except under conditions of very high ionic strength. The surface chemistry of oxides in this case controls the generation of charge.<sup>(83)</sup>

Polymer dispersants are typically intermediate length (5,000 to 75,000 molecular weight) organic molecules that may be positive, neutral, or negatively charged depending on the nature of side or backbone functional groups. Polymeric additives can disperse particles by either of the mechanisms shown schematically in Figure 2.16.<sup>(38)</sup> In depletion dispersion shown in Figure 2.16(a), the polymer remains in solution and reduces the interaction energy with which similarly charged particles collide. In the depletion dispersion scenario the polymer is either neutral or exhibits a similar polarity to the surface potential of the particles. The polymeric additive should be soluble in the solution phase and should not enhance deleterious surface reactions or react with species present in solution. The other mechanism shown in Figure 2.16(b) involves the adsorption of the polymer to the particle surface to inhibit particle-particle collisions via electrostatic repulsion, steric hindrance, or a combination of these repulsive mechanisms. Steric stabilization is effective when the polymeric additive adsorbs on the surface of the particle, the thickness of the extended polymer layer is greater than the energy barrier (see Figure 2.14), and the polymer is soluble in the solution phase. The attachment of the polymer molecules to the particle surface can occur by covalent bonding between species in the particle surface and the macromolecule, by electrostatic adsorption of the polymer to the particle surface, or by a combination of covalent and ionic interactions.

#### 2.4.3. Electrophoretic Behavior of Titanium Dioxide and Barium Titanate

Long before any type of solution chemistry studies were performed on BaTiO<sub>3</sub>, titanium dioxide (TiO<sub>2</sub>) was thoroughly investigated because the rutile form of TiO<sub>2</sub> has extensive industrial applications as a pigment. The electrophoretic behavior of rutile and the adsorption of alkaline ions were studied in an effort to try to improve the quality of

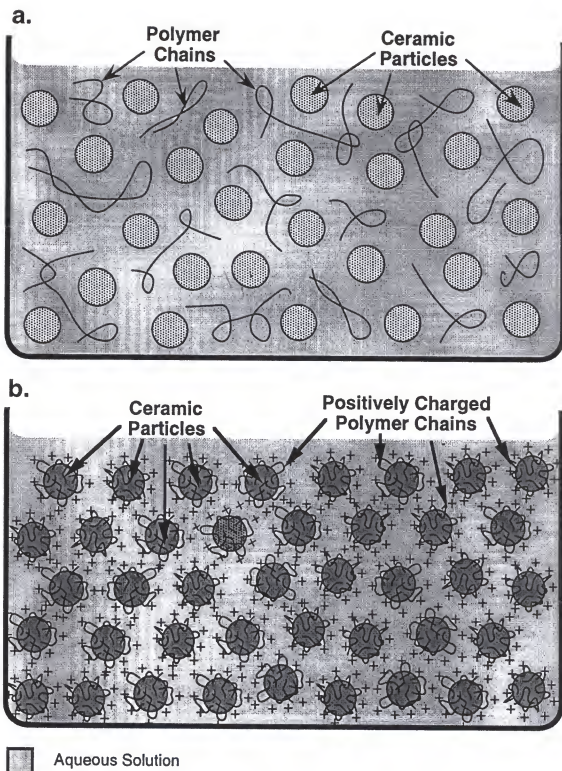


Figure 2.16. Schematic showing two different polymeric dispersing mechanisms for suspensions, (a) depletion dispersion where the polymer remains in solution and prevents particle collisions and (b) adhesion of the cationic polyelectrolyte to the particle surface preventing particle-particle contact by both polymeric and electrostatic repulsion.<sup>(38)</sup>

paint by advancements in colloidal chemistry.  $\text{TiO}_2$  can be considered as a model metal oxide for a number of reasons. It exhibits a reversal of charge at about neutral pH enabling experimental ion adsorption on both a positive and a negative surface. Titania is extremely insoluble in water.<sup>(20,50-55)</sup> The surface properties of rutile have been extensively studied, resulting in the determination of the point-of-zero charge (PZC) and the characterization of the surface charge by electrophoretic and titrimetric methods.<sup>(52)</sup> The PZC is defined as the pH where the adsorption of potential determining ions is equal (i.e.  $\Gamma_{\text{H}^+} = \Gamma_{\text{OH}^-}$ ).<sup>(52)</sup>

Fuerstenau and coworkers<sup>(72)</sup> first determined the PZC for rutile to be pH 6.5, in agreement with several other investigators.<sup>(84-87)</sup>  $\text{NaNO}_3$  and alkaline earth/nitrate complexes were chosen to provide variation in ionic strength and analyze the adsorption behavior of divalent ions at the aqueous/rutile interface since  $\text{Na}^+$  and  $\text{NO}_3^-$  act as indifferent electrolyte ions. Thus, any changes in the electrophoretic behavior of  $\text{TiO}_2$  are due to the adsorption of the metal ions. This allowed the authors to determine the effect of ionic size on the adsorption and surface charge.<sup>(72)</sup> Such electrokinetic experiments provide a clear demonstration of the specific adsorption of nonhydrolyzing multivalent ions on oxides from aqueous solutions.<sup>(88)</sup> The reversal of the zeta potential of rutile to positive values in the presence of barium is much more dramatic than that induced by  $\text{Sr}^{2+}$ ,  $\text{Ca}^{2+}$ , and  $\text{Mg}^{2+}$  (Figure 2.17 (a)). At all concentrations studied (from  $1.67 \times 10^{-3}\text{M}$  to  $1.67 \times 10^{-5}\text{M}$ ), the particles exhibited positive electrophoretic mobility (Figure 2.17 (b)). At  $\text{Ba}^{2+}$  concentrations above  $1.67 \times 10^{-5}\text{M}$ ,  $\text{TiO}_2$  particles appeared to be more positively charged, even at pH values below the PZC. This indicates that  $\text{Ba}^{2+}$  is able to specifically adsorb even when the surface charge of  $\text{TiO}_2$  is positive. The affinity sequence of the alkaline earth ions determined by electrophoretic observations was corroborated by a series of atomic adsorption experiments.<sup>(72)</sup>

The results by Jang and Fuerstenau agreed with the previous electrophoretic mobility behavior, and showed that interaction strength follows the same sequence,  $\text{Ba}^{2+} > \text{Sr}^{2+} \geq \text{Ca}^{2+} > \text{Mg}^{2+}$ .<sup>(84)</sup> Metal ion adsorption from dilute solutions usually occurs at a

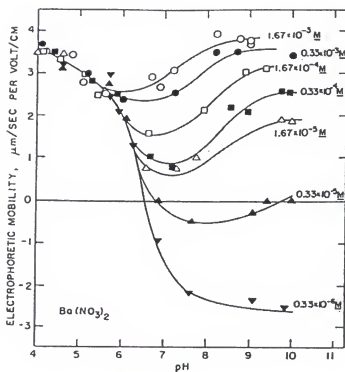
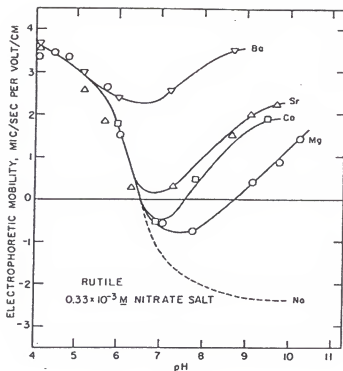
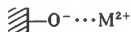


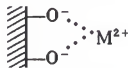
Figure 2.17. (a) Summary of the mobility vs. pH curves for the rutile at different alkaline earth cations at  $0.33 \times 10^{-3} M$  concentration. (b) Electrophoretic mobility vs. pH curves for rutile in the presence of different concentrations of  $Ba(NO_3)_2$ .<sup>(72,84)</sup>

pH below the hydrolysis pH region, and may be considered to take place either through ion exchange (surface complex), in which metal ions replace surface protons, or through the surface-induced hydrolysis of unhydrolyzed bulk metal ions. Three possible schemes for the interaction of alkaline-earth ions or other divalent cations with the oxide surface are represented below:

(a) Monodentate complex



(b) Bidentate complex



(c) Surface-induced hydrolysis complex



Analysis of the ratio,  $r$ , of the number of protons released from the interface to the number of cations adsorbed, indicates that either a bidentate complex formation or a surface induced hydrolysis mechanism is the dominant mode of adsorption for these metal ions at the rutile/water interface.<sup>(72,84)</sup> As the pH of the suspension is increased, the value of  $r$  increases from 1.56 for pH 6.5, to 1.96 for pH 9. If the interaction is dominated by a monodentate-type complex formation, then  $r$  will be close to 1. However,  $r$  will be close to 2 if the interaction is bidentate or surface-induced hydrolysis complex dominated.<sup>(84)</sup>

Initial studies of the electrophoretic behavior for aqueous suspensions of commercial lots of  $\text{BaTiO}_3$  have been performed by Adair et al.<sup>(49)</sup> in the late seventies to early eighties. Substantial differences in the electrophoretic behavior were determined for various lots of commercial  $\text{BaTiO}_3$  powders and  $\text{BaTiO}_3$  powders as a function of solids loading (Figure 2.18 and 2.19 respectively). At a relatively low, constant solids loading, the isoelectric point (IEP) for certain lots of powder ranged from pH 6 to pH 10. The IEP is defined as the pH at which the charge on the solid promoted from all sources is zero.<sup>(47)</sup> That is, the adsorption of positively charged species equals the adsorption of negatively charged species at the particle surface ( $\Gamma_+ = \Gamma_-$ ).<sup>(52)</sup> However, other samples did not exhibit an IEP, exhibiting uniform positive charge over the entire pH range examined. The IEP as

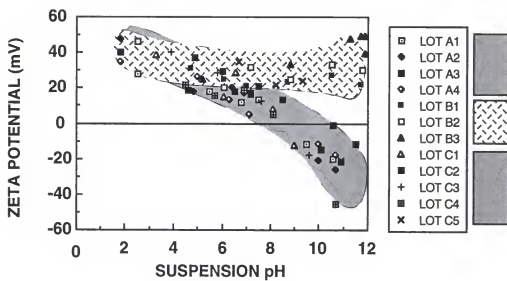


Figure 2.18. Particle electrophoresis data for various lots of commercial BaTiO<sub>3</sub> powder that shows variation in lot to lot behavior as well as the powder supplier.<sup>(49)</sup>

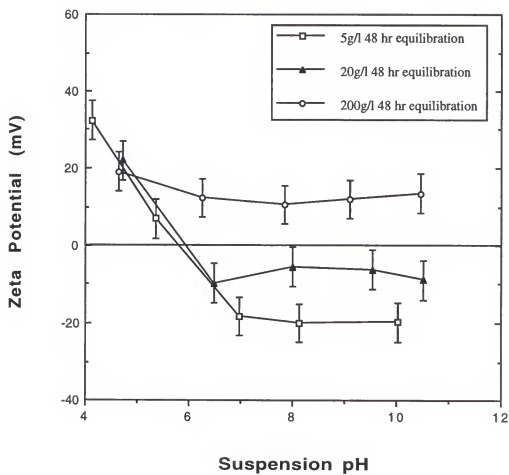


Figure 2.19. Electrophoretic behavior for three  $\text{BaTiO}_3$  suspensions at different solids loading.<sup>(49)</sup>

a function of solids loading also shifted from a pH value of approximately 5, to 8, to a consistently positive zeta potential (no IEP) for 5 g/l, 20 g/l, and 200 g/l respectively (Figure 2.19). The amount of acid or base required to achieve a particular pH for the various BaTiO<sub>3</sub> suspensions was also inconsistent as a function of lot and solids loading.

In summary, current knowledge concerning the BaTiO<sub>3</sub>-H<sub>2</sub>O interface indicates that: (1) at low solids loading, the IEP is similar to that of TiO<sub>2</sub>, and with increased solids loading, the IEP shifts towards a more alkaline pH, (2) the concentration of Ba<sup>2+</sup>(aq) increases with increasing solids loading or a decrease in suspension pH, and (3) Pristine TiO<sub>2</sub> in BaNO<sub>3</sub> solution shows that Ba<sup>2+</sup> ions adsorb onto the TiO<sub>2</sub> surface well below the IEP, causing the magnitude of the charge to become more positive. However, in some cases where the concentrations are large enough, the adsorption of Ba<sup>2+</sup> ions reverses the charge of alkaline suspension of TiO<sub>2</sub> so that the electrophoretic mobility is consistently positive.

#### 2.4.4. Electrophoretic Behavior of Calcium Oxalate Monohydrate

The surface charge imparted to the passivated BaTiO<sub>3</sub> particle surface must be determined to consider the additive as a possible passivating agent. From the section entitled "Feasibility of Passivating Barium Titanate" (2.3.3), the addition of oxalate ions to aqueous BaTiO<sub>3</sub> suspensions was considered a potential candidate to passivate the surface and minimize the concentration of Ba<sup>2+</sup> in solution based upon the solubility data for BOM and CaC<sub>2</sub>O<sub>4</sub>·H<sub>2</sub>O (COM).<sup>(17,64,65)</sup> There are no published studies to date on the electrophoretic behavior for BOM. Since the solubility of BOM and COM are similar, the electrophoretic behavior of the biological compound COM is expected to be similar to BOM and has been well documented.<sup>(64,73)</sup> Figure 2.20 shows the electrophoretic behavior for COM. The importance of the COM electrophoretic behavior to the aqueous processing of BaTiO<sub>3</sub> is the relatively constant surface charge over the pH range from ~pH 4 to pH 10. This is advantageous for the aqueous processing of BaTiO<sub>3</sub> because MLC manufacturers

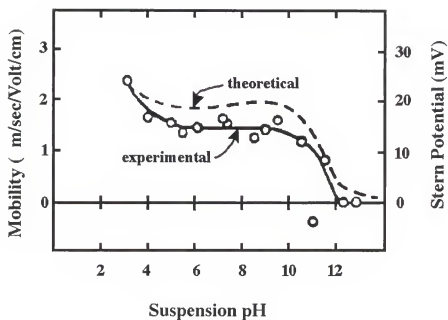


Figure 2.20. Both the theoretical and experimental electrophoretic behavior of COM are illustrated and a relatively constant charge is depicted over the pH range from pH 4 to pH 10.<sup>(64)</sup>

would have a large working pH range where the concentration of  $\text{Ba}^{2+}$  is reduced and the dispersion is most likely favorable.

### 2.5. Binder

Little information has been published on binder/dispersant interactions and binder/particle interactions. This is probably due to highly competitive technical ceramics industry where divulging information could compromise advantages over market competitors. The polymer chosen to add plasticity and strength to the green tapes must meet several requirements that have generally been overlooked in the MLC industry. The aqueous solubility of the polymer, the rheological behavior induced by adding a particular polymer, the crosslinking of the polymeric additives due to the presence of soluble ions, an increase in the solubility of the particle due to the formation of complex polymer/ion species, and the interactions between other polymeric additives need to be addressed before thin ( $< 5 \mu\text{m}$ ) ceramic tapes can be reproducibly cast in an industrial environment.

### 2.6. Variations in the Ba:Ti Ratio on Sintering of Barium Titanate

The importance of addressing the incongruent dissolution and instability of  $\text{BaTiO}_3$  will be emphasized by review of the literature on the sintering of  $\text{BaTiO}_3$ . The Ba:Ti ratio influences the microstructure of the fired ceramic. Variations in the grain size (i.e., abnormal grain growth) as well as the average grain size affect the dielectric properties of the  $\text{BaTiO}_3$  body. These issues will be addressed to strengthen the importance of understanding the surface chemistry issues in aqueous MLC production.

Anderson and coworkers<sup>(35)</sup> investigated the surface chemistry effects on ceramic processing of  $\text{BaTiO}_3$  powder. They determined that milling of  $\text{BaTiO}_3$  powder in deionized water results in the dissolution of  $\text{Ba}^{2+}$  ions from the surface. The amount of barium that dissolved from the particle surface was found to be strongly dependent on the milling pH. As the solution pH became more acidic, significantly more barium was leached from the powder. They also proposed a model that barium dissolves from the surface of the  $\text{BaTiO}_3$  particle under aqueous conditions, and redeposits onto the surface

upon drying leaving a stoichiometric  $\text{BaTiO}_3$  core, encompassed by a Ti-rich layer, circumvented by a Ba-rich surface layer (Figure 2.6 already shown). This  $\text{Ba}^{2+}$  leaching was found to affect the properties of the  $\text{BaTiO}_3$  powder, specifically the amount of exaggerated grain growth which occurred during sintering. Thus, the results from sintering studies which incorporated wet milling are questionable because they may have altered the Ba:Ti ratio at the surface making their results insignificant. The type of binder used to prepare  $\text{BaTiO}_3$  green bodies was also found to affect the amount of exaggerated grain growth which occurred during sintering. An aqueous PVA binder appeared to leach out a significant amounts of  $\text{Ba}^{2+}$  whereas a non-aqueous binder reduced the amount of exaggerated grain growth. Several other studies were performed on the sintering of various  $\text{BaTiO}_3$  formulations to determine the effect excess Ba and excess Ti have on the final microstructure.<sup>(89-95)</sup> However, the validity of these studies is questionable based on the findings on Anderson and coworkers.

The microstructure, grain size and porosity, affect the dielectric properties of sintered  $\text{BaTiO}_3$  ceramics. The dielectric loss is increased by porosity due to the creation of additional surfaces that contain a high concentration of defects. These defects, along with moisture that can condense into the pores, may contribute to leakage currents. In an effort to improve the electrical properties of the MLC, sintering studies have been done to determine optimum dielectric properties as a function of stoichiometry of the powder, microstructure of the sintered body, firing temperature, firing schedule for removal of additives, particle size, particle size distribution, and various dopants to suppress abnormal grain size.

The influence of stoichiometry, Ba:Ti ratio, on the microstructure was investigated by several different researchers. Lin and Hu<sup>(36)</sup> and Kulcsar<sup>(89)</sup> found that fine-grain microstructures are obtained for Ba-rich and stoichiometric  $\text{BaTiO}_3$  ceramics. Several other investigators<sup>(36,89,90)</sup> also found that Ba-rich  $\text{BaTiO}_3$  samples provide a fine grain size with BaO acting as a grain size refiner and forming a second phase identified as barium

orthotitanate,  $\text{Ba}_2\text{TiO}_4$ . The grain size of Ba-rich and stoichiometric samples increases slowly with temperature and time, but is still smaller than  $4\mu\text{m}$  even after sintering at  $1350^\circ\text{C}$  for sixteen hours. Although Ba-rich and stoichiometric  $\text{BaTiO}_3$  samples have similar grain size, the density of the barium-rich samples are generally higher, resulting from the modification defect chemistry of the excess  $\text{Ba}^{2+}$ .<sup>(36)</sup>

The sintering of barium titanate based materials is normally performed with a small excess of  $\text{TiO}_2$  (Ba:Ti atomic ratio  $< 1$ ) as a sintering aid. The excess  $\text{TiO}_2$  (1 to 3 mole percent) reacts with  $\text{BaTiO}_3$  to form what was originally thought to be  $\text{BaTi}_3\text{O}_7$  but later confirmed by microprobe analysis to be  $\text{Ba}_6\text{Ti}_{17}\text{O}_{40}$ .<sup>(89,91,96,97)</sup> This second phase, which forms a eutectic melt between  $1312^\circ\text{C}$  and  $1320^\circ\text{C}$  with  $\text{BaTiO}_3$ , is present in the grain boundaries and triple point regions.<sup>(91,96,97)</sup> The liquid phase, however, not only promotes densification of the polycrystalline ceramic at lower temperatures but also gives rise to pronounced abnormal grain growth through solution-segregation.<sup>(36,91-93,96-98)</sup> This abnormal grain growth of  $\text{BaTiO}_3$  is difficult to control by simple variations of sintering temperature, sintering time, or modification of the chemical composition.<sup>(91)</sup> The microstructure of  $\text{BaTiO}_3$  materials is significantly influenced by the Ba:Ti ratio. As the composition moves from  $\text{TiO}_2$  excess to BaO excess, the amount of enclosed porosity seems to increase, the grain texture changes, the scale of the domain pattern becomes finer, and the grain size becomes smaller.<sup>(36)</sup>

The average grain size of the sintered  $\text{BaTiO}_3$  substrate influences the magnitude of the dielectric constant and loss. The optimum grain size for producing the largest dielectric properties in a relatively uniform structure is approximately  $1\mu\text{m}$  in diameter.<sup>(35,36)</sup> Kinoshita and Yamiji<sup>(94)</sup> showed that, as the grain size of the unmodified  $\text{BaTiO}_3$  decreased from an average size of  $53\mu\text{m}$  to  $1.1\mu\text{m}$ , the dielectric constant increases approximately five fold. Shaikh et al.<sup>(100)</sup>, however, have determined that unmodified  $\text{BaTiO}_3$  with grains smaller than  $0.4\mu\text{m}$  exhibited a decrease in the dielectric constant, possibly due to stresses within the structure. Many researchers have concluded that abnormal bimodal

microstructures or large grained microstructures produce low dielectric properties because large grain ceramics can form  $90^\circ$  twin states much more easily than fine grain ceramics.<sup>(94,100)</sup>

Firing temperature and schedule are critical in producing uniform, fine grained microstructures, which ultimately affect the dielectric properties of the substrate, and less importantly, the cost of production.<sup>(95-101)</sup> Dopants have been used to tailor the curie temperature, suppress abnormal grain growth, and lower the sintering temperature of the sample.<sup>(36,93,98)</sup>

Although several of these studies have provided vital information in improving the electronic properties, the powders in these studies were generally wet milled, dried, and uniaxially pressed into right hand cylinders with atmospheric water present within the compact. A sintering study by Anderson and coworkers<sup>(35)</sup> may question the validity of the previous sintering studies because they determined that  $\text{BaTiO}_3$  is unstable in aqueous conditions (i.e. wet milling), which affects the grain size and uniformity of the final microstructure. The instability of  $\text{BaTiO}_3$  in aqueous environments is one of the difficulties plaguing aqueous tape casting and will be discussed in more detail in a following section.<sup>(33)</sup>

## 2.7. Characterization Techniques

### 2.7.1. Solution Chemistry

The concentration of soluble species in the sample supernatant may be detected by inductively coupled plasma spectroscopy. The supernatant is atomized via argon plasma excitation and sustained by inductive coupling to a radio-frequency electromagnetic field.<sup>(102)</sup> Detection limits for most elements are generally in the parts per billion regime. However this limit is dependent on the instrument model as well as the specific ion being determined. Experimentally determined concentrations can corroborate theoretical stability diagrams.

### 2.7.2. Surface Charge Analysis

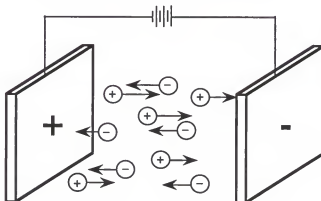
Solid oxides in aqueous suspension are electrically charged and may be observed most directly by electrokinetic measurements.<sup>(83)</sup> As a result of the charge on their surfaces, colloidal particles immersed in water can move via an electrical potential gradient as depicted in Figure 2.21. The electrophoretic mobility,  $\mu_E$ , is defined as the particle velocity per unit static electric field. It can be determined by measuring the electrical potential at the plane of shear surrounding the particle. The shear plane is defined as the boundary between the bulk solution, where the ions are free to move, and the inner layer of strongly adsorbed ions which move with the particle under the influence of the applied field. The zeta potential is calculated from the experimentally determined electrophoretic mobility according to the Smoluchowski equation,

$$\zeta = \frac{\eta \mu_E}{k \epsilon_o} \quad [2.13]$$

whereby  $\eta$  represents the viscosity of the solution ( $\eta_{\text{water}} = 1 \text{ cP} = 1 \times 10^{-3} \text{ Kg/Msec}$ ),  $k$  represents the dielectric constant of the solution ( $k_{\text{water}} = 79.9$ ), and  $\epsilon_o$  represents the permittivity of free space ( $8.854 \times 10^{-12} \text{ F/m}$ ).<sup>(68)</sup>

Electrophoresis measurements offer a convenient method to study the double layer properties for a particle under specific solution conditions.<sup>(67)</sup> In the absence of strongly absorbing species other than protons, the pH of the solution will determine the magnitude and polarity of the surface charge, and thus the stability. The adsorption of most soluble ions from water onto the oxide surface is relatively fast.<sup>(71)</sup> Changes in the polarity of the zeta potential as a function of salt concentration are useful in evaluating chemical adsorption of ionic species at the particle surface.<sup>(68,72)</sup> Electrokinetic experiments have long been known to provide a clear demonstration of the specific adsorption of nonhydrolyzing multivalent ions on oxides from aqueous solutions.<sup>(70)</sup>

## a. ELECTROPHORESIS MEASUREMENTS



$$\zeta = \frac{4\pi\eta\mu}{k\epsilon\epsilon_0} \quad \mu = \frac{P(V)}{\text{time}} \quad P(V) = \frac{\text{Graticle distance}}{\text{Applied Voltage} / l}$$

LEGEND:

$\zeta$  = Zeta Potential (mV)     $\eta$  = Viscosity ( $\text{Nm}^{-2} \text{s}$ )     $k$  = Dielectric constant of medium

$\epsilon_0$  = Permittivity of free space =  $8.854 \times 10^{-12} \text{ Fm}^{-1}$     time = time to traverse one graticle unit

$\mu$  = Electrophoretic mobility ( $(\mu\text{m}/\text{sec})(\text{V}/\text{cm})$ )     $l$  = cell constant (cm)

## b. ELECTROPHORETIC BEHAVIOR

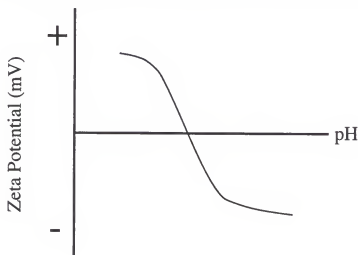


Figure 2.21. (a.) Schematic representing the particle movement in an applied electric field to determine the electrophoretic mobility. (b.) The electrophoretic mobility can be plotted as a function of pH or used to calculate the zeta potential and plotted as a function of pH.

### 2.7.2.1. Light Scattering Techniques

Light scattering techniques<sup>(103)</sup> to determine the electrophoretic mobility require low concentration suspensions that are optically transparent with ionic strengths below 0.01M. Samples that are higher in concentration than permissible for detection by the instrument have to be reconstituted by sequestering a small amount of sediment and redispersing the sediment in the supernatant. The monochromatic light source is split to provide a reference beam and a sample detection beam. The shift in frequency of the sample light source with respect to the reference beam determines the magnitude and polarity of the charge at the particle surface. Variations in the output from the a light scattering, electrophoretic mobility measuring instrument can be used to discern whether the particles are similarly charged or two differently charged particles are present in solution. A single narrow peak output is indicative of a suspension with similarly charged particles, whereas a multipeak output describes suspensions with two or more differently charged particles in suspension, where each peak describes a specifically charged particle.<sup>(103)</sup> In general, the electrophoretic characterization of BaTiO<sub>3</sub> suspensions with various passivating agents was used to determine whether the association of the dissolved Ba<sup>2+</sup> ion after leaving the BaTiO<sub>3</sub> particle surface forms either a passivation layer at the particle surface (single peak output) or a barium precipitate with a different surface charge than the incongruently dissolved BaTiO<sub>3</sub> (multiple peak output).

### 2.7.2.2. Electroacoustic Analysis

In contrast to the light scattering technique to determine the electrophoretic mobility of low concentration suspensions, electroacoustic methods use the interaction of electric fields and sounds waves to deduce the charged particles in highly concentrated suspensions.<sup>(104)</sup> Other advantages of electroacoustic characterization include the measurement of stirred samples to reduce settling or analyze viscous samples, and the continuous determination of charge over a wide pH range via an automated titrator. The

electroacoustic analyzer was used in the current research to confirm or refute the surface charge determined at lower solid concentrations.

### 2.7.2.3. Sedimentation analysis

Sedimentation analysis in conjunction with surface charge determination can provide insight to the stability of a suspension. Figure 2.22 shows the recorded sediment heights for various suspensions as denoted by the arrows. The sediment height was recorded for the opaque region in the test tube. The opacity region was determined by visual inspection through the test tube where a finger could not be visually discerned, as also depicted in Figure 2.22. Highly agglomerated or poor dispersion suspensions displayed a sedimentation behavior similar to that shown in Figure 2.22(a) where the sediment height was easily discerned from the supernatant. As the dispersion improved, the sediment height was harder to determine. Figure 2.22(b) and 2.22(c) show variations of improved dispersion where fine particles remained in suspension and the larger, agglomerate particles settled. Lastly Figure 2.22(d) illustrates a well dispersed suspension.

### 2.7.3. Particle Observation

#### 2.7.3.1. Scanning Electron Microscopy

The most common operation of the scanning electron microscope (SEM) uses emission of secondary electrons to provide two-dimensional images of particle characteristics such as size and morphology, and pseudo-tape characteristics such as uniformity, the presence of agglomerates, voids, and other defects within the cast pseudo-tapes.<sup>(102)</sup> Surface features are discerned by the yield of electrons that reach the detector. Features projected toward the detector are brighter or more white than features facing away from the detector. Hence, imaging an atomically flat sample would provide no detail or an all white image due to lack of contrasting electron yield to the detector. In addition to particle electrophoresis and sedimentation studies at low solids loading, dispersion of the various slurry formulations (high solids loading) in the current research was assessed via rheological properties in conjunction with SEM analysis of the pseudo-tapes.

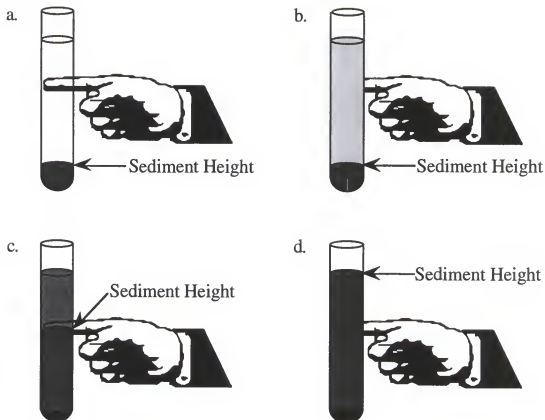


Figure 2.22. Schematic showing variations in the sedimentation of the suspensions and the sediment height recorded in the sedimentation analysis. Finger shows variations in the transparency of the suspensions.

Figure 2.23 (a.) and 2.23 (b.) and shows the contrast between a good and a bad dispersion of the BaTiO<sub>3</sub> particles, respectively.

### 2.7.3.1. Transmission Electron Microscopy

Transmission electron microscopy (TEM) is used to obtain information from specimens that allow the transmission of electrons. Electrons thermionically emitted from the gun are accelerated by a high voltage bias (100 kV- 800 kV), projected on to the specimen by means of a lens system, and scattered as the electrons transverse through the specimen.<sup>(102)</sup> Elastic scattering of the electrons provides a diffraction pattern of the material, whereas inelastic interactions between beam and matrix electrons provide images of the particle geometry, and at higher magnifications the lattice fringes. In the current research, the inelastic scattering mode can be used to image layers present on the particles surface (i.e. amorphous regions and deposited layers).

### 2.7.4. Viscosity

The cone/plate viscometer is a precise torque meter that is driven at discrete rotational speeds.<sup>(105)</sup> The torque is measured via a calibrated beryllium copper spring which is connected to a drive mechanism that rotates the cone. The spring senses the resistance generated by the sample fluid between the rotating cone and a stationary flat plate. The accuracy of the instrument is guaranteed to be within 1% of the full range employed with sample replication within 0.2% of the full scale. Figure 2.24 shows a schematic of the cone/plate viscometer with the variables in the following mathematical expressions defined. The ratio of ( $\omega r$ ) and the gap width ( $C$ ) is a constant for any value of ( $r$ ) due to the angle between the flat plate and the bevel on the cone. The shear stress and shear rate are defined respectively as,

$$\text{Shear Stress (dynes/cm}^2\text{)} = \frac{T}{2/3\pi r^3} \text{ and,} \quad [2.14]$$

$$\text{Shear Rate (sec}^{-1}\text{)} = \frac{\omega}{\sin \theta} \quad [2.15]$$

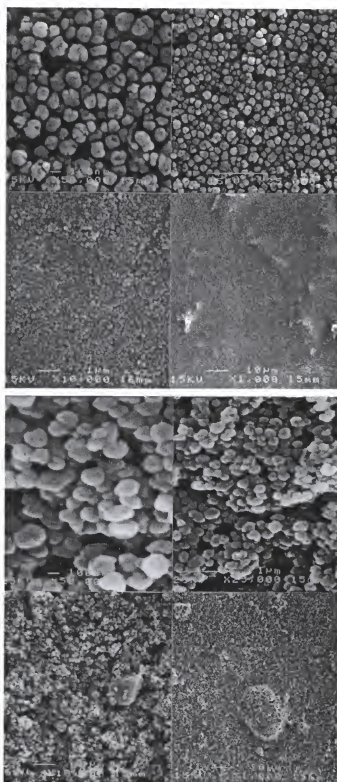
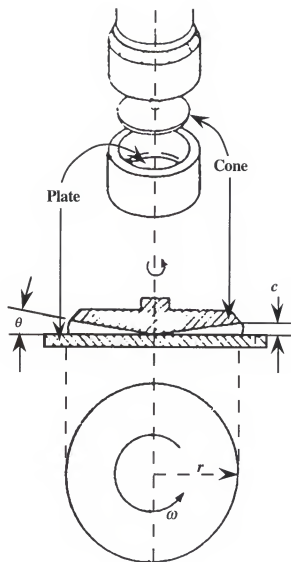


Figure 2.23. Scanning electron micrographs of the particle packing within the hand cast pseudo-tapes showing the difference between (a.) good dispersion and (b.) bad dispersion.



The mathematical expressions for the cone/plate viscometer are:

$$\text{Shear Stress (dynes/cm}^2\text{)} = \frac{T}{2/3\pi r^3}$$

$$\text{Shear Rate (sec}^{-1}\text{)} = \frac{\omega}{\sin \theta}$$

$$\text{Viscosity (cP)} = \frac{(\text{Shear Stress})(100)}{\text{Shear Rate}}$$

Where:

$T$  = % Full Scale Torque (dyne cm)

$r$  = Cone Radius (cm)

$\omega$  = Cone Speed (rad/sec)

$\theta$  = Cone Angle (degrees)

Cone Radius for

CP40 = 2.4 cm

CP52 = 1.2 cm

Figure 2.24. Schematic showing the various components and mathematical variables for the cone/plate viscometer and the corresponding mathematical expressions to determine the shear stress, shear rate, and viscosity.<sup>(105)</sup>

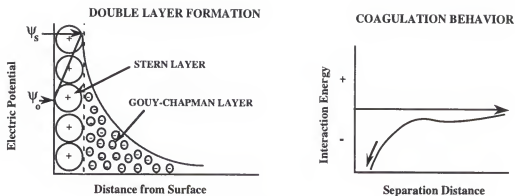
where  $T$  represents the percent of full scale torque in dynes/cm<sup>2</sup>,  $r$  represents the cone radius (cm),  $\omega$  represents the cone speed (rad/sec), and  $\theta$  represents the cone angle (degrees). The two cones used in the current research were CP40 and CP52 with cone radii of 2.4 cm and 1.2 cm, respectively. The viscosity of the fluid is calculated according to,

$$\text{Viscosity (centiPoise)} = \frac{(\text{Shear Stress})(100)}{\text{Shear Rate}} \quad [2.16].^{(105)}$$

## 2.8. Chapter Summary

With the demand of the market to produce of smaller and lighter, yet better electronic equipment in conjunction with increasing governmental regulations concerning the use of hazardous materials, the MLC industry has to produce smaller capacitors with higher capacitance via a more environmentally benign process. As observed in equations 2.1 and 2.2, the MLC industry must reduce the thickness of the ceramic layers in order to increase the capacitance of a MLC. By changing the nonaqueous production of MLCs to an aqueous scheme is the easiest method to circumvent the environmental restrictions. However, the most prolific metal oxide used in the production of MLCs is BaTiO<sub>3</sub> and the ability to produce thinner ceramic layers relies on knowledge of the solution chemistry associated with the aqueous BaTiO<sub>3</sub> MLC process and the use of a smaller particle size to accommodate variations in the particle packing.

A summary of the solution chemistry associated with the aqueous BaTiO<sub>3</sub> MLC production is shown in Figure 2.25. In particular, the solubility of the BaTiO<sub>3</sub> surface in water needs to be addressed to eliminated problems with dispersion and sintering. The incongruent dissolution of the BaTiO<sub>3</sub> particle surface introduces excessive amounts of Ba<sup>2+</sup> in solution which alters the surface and consequently the electrostatic dispersion. The addition of polymeric dispersants and binders can associate the soluble Ba<sup>2+</sup> and phase separate compromising the success of the process. After the solubility of the BaTiO<sub>3</sub>



### ELECTROSTATIC CHARGE FORMATION

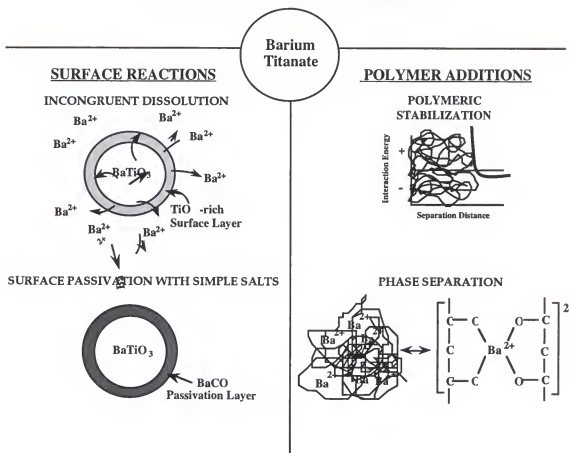


Figure 2.25. A summary of various interactions that can take place  $\text{BaTiO}_3$  particles, water, and polymeric additives.

particle is reduced, the polymeric additives can be tailored to optimize the dispersion of the slurry as well as the rheological properties of the slurry.

Presently, the MLC industry's poor understanding of the solution chemistry associated with the aqueous processing of  $\text{BaTiO}_3$  MLCs suppresses the successful production green ceramic layers  $< 5\mu\text{m}$  thick and fired layers  $< 3\mu\text{m}$ .

## CHAPTER 3

### CHEMICAL PASSIVATION OF THE BaTiO<sub>3</sub> PARTICLE SURFACE VIA OXALIC ACID ADDITIONS

#### 3.1. Introduction

The increasing demand for environmentally benign manufacturing processes dictates the need to develop aqueous processing schemes for a variety of materials including the manufacture of BaTiO<sub>3</sub>-based multilayer capacitors. Perovskite materials such as BaTiO<sub>3</sub>(s) undergo incongruent dissolution in aqueous solutions.<sup>(17,18)</sup> Incongruent dissolution leads to processing problems such as agglomeration of the BaTiO<sub>3</sub> particles, crosslinking of polymer additives (e.g., dispersants and binders) during slurry formulation, and abnormal grain growth during the sintering of the ceramic.<sup>(35)</sup> To satisfy environmental constraints and still maintain the same level of product quality as non-aqueous processing schemes, it will be demonstrated that surface reactions which compromise the processing and ultimate electronic properties of sintered BaTiO<sub>3</sub> ceramics must be eliminated or minimized during aqueous processing.

To a first approximation, the dissolution reactions associated with BaTiO<sub>3</sub> may be understood in terms of the solubility of the individual metal oxide components, BaO(s) and TiO<sub>2</sub>(s). It has been shown that BaTiO<sub>3</sub>(s) in the Ba-Ti-CO<sub>2</sub>-H<sub>2</sub>O system undergoes incongruent dissolution below pH ~13, with the concentration of Ba<sup>2+</sup>(aq) dependent on the concentration of dissolved CO<sub>2</sub> in the solution.<sup>(14,15,17,19,41,42)</sup> The concentration of Ba<sup>2+</sup>(aq) derived from the BaO(s) component is large (as high as 0.1M) and depends upon the surface area of BaTiO<sub>3</sub> exposed to aqueous solution below about pH 12. In contrast, TiO<sub>2</sub>(s) is only sparingly soluble over the pH range from pH 3 to pH 10.<sup>(20,52,53)</sup> The overall stoichiometric chemical reaction describing the dissolution of BaTiO<sub>3</sub>(s) is given by,



However, the incongruent dissolution of  $\text{Ba}^{2+}$  is kinetically hindered by the formation of a diffusion barrier of  $\text{TiO}_2$  and/or of the metal salt  $\text{BaCO}_3$ , which is normally present on the surfaces of  $\text{BaTiO}_3$  particles as depicted in Figure 3.1. It has been demonstrated that most commercial  $\text{BaTiO}_3$  powders have a  $\text{BaCO}_3$  surface layer that forms during storage of the powder or during slurry formulation.<sup>(19)</sup> Whether  $\text{TiO}_2$ -rich or  $\text{BaCO}_3$  passivation layers are present on the  $\text{BaTiO}_3$  particle surface depends on the environment to which the powders are subjected during and subsequent to synthesis.<sup>(42)</sup>

The aqueous processing of multicomponent ceramics may lead to the formation of depleted surface layers, deposition of other metastable phases either from saturated solution or via crystallization of surface films, readsorption of the dissolved species, and diffusion of the species through these layers.<sup>(37,61,72,84)</sup> The presence of  $\text{BaCO}_3$  on the surface or a change in the Ba:Ti ratio due to incongruent dissolution of the surface in aqueous solution can adversely affect sintered microstructures (e.g., exaggerated grain growth) in  $\text{BaTiO}_3$  and, consequently, lead to poor dielectric properties such as low dielectric constant and high dielectric loss factor.<sup>(35,94)</sup>

In addition,  $\text{Ba}^{2+}(\text{aq})$  from the incongruent dissolution of  $\text{Ba}^{2+}$  from the surface of  $\text{BaTiO}_3$  particles can interact in a deleterious manner with various polymeric additives.<sup>(44,45)</sup> The  $\text{Ba}^{2+}$  ions present in solution can induce gelation of the polymeric additives via a salting out mechanism which not only impairs dispersion of the  $\text{BaTiO}_3$  particles, but also leads to holes in the fired tapes because of regions rich in the salted-out polymers. Therefore it is important to minimize the leaching of the  $\text{Ba}^{2+}$  ions from the  $\text{BaTiO}_3$  particle surface, not only to preserve the chemical homogeneity of the powder, but also to prevent deleterious interactions with polymeric dispersants.

Understanding the above fundamental problems associated with the aqueous processing of  $\text{BaTiO}_3$ , allows one to design a solution to passivate the  $\text{BaTiO}_3$  surface exposed to aqueous solution and alleviate the incongruent dissolution. Passivation of metal

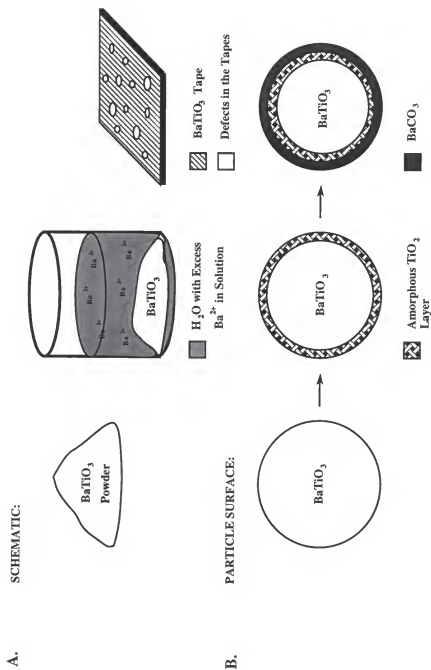


Figure 3.1. (a) Schematic summarizing the problems associated with aqueous processing of barium titanate and (b) a schematic representing the incongruent dissolution of barium from the surface of the barium titanate particle with the formation of an amorphous Ti-rich and Ba-rich layers during fabrication.<sup>(14,35)</sup>

surfaces has been documented for many years.<sup>(55-57)</sup> Some metal surfaces react under particular environmental conditions to produce a thin metal oxide passivation layer which is relatively inert in aqueous solution. The formation of the thin passivation layer protects the bulk material from further corrosion. This is commonly observed for titanium, chromium, and aluminum, with the material forming a thin oxide layer that prohibits corrosion. Stainless steel does not rust due to the presence of chromium which forms a protective oxide barrier to eliminate the corrosion of iron.<sup>(55)</sup> In principle, the passivation of  $\text{BaTiO}_3$  in an aqueous environment may be achieved in a similar manner, in that a surface reaction may be induced between the  $\text{Ba}^{2+}$  leaving the surface of the particles and the surrounding media to minimize  $\text{Ba}^{2+}$  dissolution.

The basic approach in the current work is to create a surface diffusion barrier that is relatively insoluble yet can be easily removed during subsequent processing steps, such as binder pyrolysis and firing. The ideal situation is to precipitate a simple salt with the  $\text{Ba}^{2+}$  ions on the surface of the suspended  $\text{BaTiO}_3$  particles. The spontaneous formation of a stable compound on the surface will arrest further dissolution and minimize variation in the Ba:Ti ratio. In fact,  $\text{BaCO}_3(\text{s})$  is a natural passivating agent on the surface of the  $\text{BaTiO}_3$  particles.<sup>(19)</sup> Unfortunately, the solubility of  $\text{BaCO}_3$  varies dramatically with solution pH which reduces the effectiveness of  $\text{BaCO}_3$  as a passivating agent. Moreover, working in the solution pH regime where  $\text{BaCO}_3$  is stable, above pH 9, is not advantageous because many organic additives used as dispersants and binders lose effectiveness in alkaline pH conditions. Also, the presence of  $\text{BaCO}_3$  can cause significant sintering problems.<sup>35</sup>

There are several sparingly soluble barium salts that have the potential to produce a passivation layer on  $\text{BaTiO}_3$ . A suitable passivating agent should form a sparingly soluble salt with the leachable  $\text{Ba}^{2+}$ , and the solubility of the Ba salt should be relatively insensitive to changes in solution pH. The Ba salt must be compatible with other organic additives such as dispersants and binders, should experience clean pyrolysis during the organic burnout and sintering processing steps, and should not compromise the electronic

properties of the ultimate material. Included among potential anions that form sparingly-soluble barium salts are  $\text{SO}_4^{2-}$  as  $\text{BaSO}_4(\text{s})$ ,  $\text{PO}_4^{3-}$  as  $\text{Ba}_3(\text{PO}_4)_2(\text{s})$ ,  $\text{CO}_3^{2-}$  as  $\text{BaCO}_3(\text{s})$ , and  $\text{C}_2\text{O}_4^{2-}$  as  $\text{BaC}_2\text{O}_4 \cdot \text{H}_2\text{O}(\text{s})$  (BOM). The solubilities of the passivating solids,  $\text{BaSO}_4(\text{s})$  and BOM are relatively insensitive to changes in solution pH, while the solubilities of  $\text{Ba}_3(\text{PO}_4)_2(\text{s})$  and  $\text{BaCO}_3(\text{s})$  vary considerably with solution pH because of the respective acid dissociation constants for  $\text{H}_3\text{PO}_4$  and  $\text{H}_2\text{CO}_3$ . Thus  $\text{PO}_4^{3-}$  and  $\text{CO}_3^{2-}$  were rejected as passivating agents. Both acid dissociation constants for oxalic acid ( $\text{H}_2\text{C}_2\text{O}_4$ ) occur below pH 4.5 as discussed below, thus above pH 4.5 the solubility of BOM is independent of solution pH.<sup>(17)</sup> The  $\text{SO}_4^{2-}$  species was rejected as a passivating agent because of the unfavorable gaseous products produced during the burnout of the organic additives and sintering. Also, any amount of  $\text{PO}_4^{3-}$  or  $\text{SO}_4^{2-}$  that remains would cause sintering problems. BOM is sparingly soluble with the solubility relatively constant above pH 4 and should experience relatively clean pyrolysis and leave little or no residue.<sup>(65)</sup> Therefore, oxalic acid was chosen as an appropriate passivating agent. Furthermore, it will be shown in future work that dispersant and binder systems may be developed that are compatible with the oxalic acid passivation scheme. One of the potential drawbacks in using oxalic acid is the possible formation of  $\text{BaCO}_3(\text{s})$  during pyrolysis. However, this limitation is not expected to have any more impact on sintering and dielectric properties than the levels of  $\text{BaCO}_3(\text{s})$  present in conventional  $\text{BaTiO}_3$  powders.

A schematic diagram of the proposed effect of oxalic acid passivation on  $\text{BaTiO}_3$  in aqueous suspension is shown in Figure 3.2. Aqueous  $\text{BaTiO}_3$  suspensions at tape-casting solid loading levels (i.e., 20 to 35%) are self-buffering to approximately pH 8 or 9. Oxalic acid is fully dissociated ( $\text{pK}_{a_1} = 1.23$  and  $\text{pK}_{a_2} = 4.17$ )<sup>(106)</sup> over this pH range, and is thus present in solution as  $\text{C}_2\text{O}_4^{2-}(\text{aq})$ . Oxalic acid is the simplest of the bifunctional carboxylic acids which makes it easily removable during firing as  $\text{H}_2\text{O}(\text{g})$ ,  $\text{CO}(\text{g})$ , and  $\text{CO}_2(\text{g})$ .<sup>(43)</sup> It will be shown in the present study that  $\text{C}_2\text{O}_4^{2-}$  ions in solution associate with dissolving

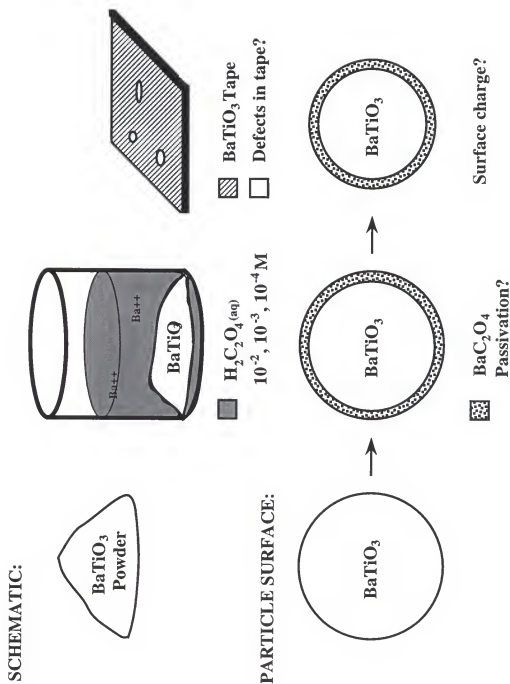


Figure 3.2. Schematic diagram of the proposed additive, oxalate ions, to minimize the dissolution of  $\text{Ba}^{2+}$  with corresponding particles depicting the passivation layer.

$\text{Ba}^{2+}$  ions from the  $\text{BaTiO}_3$  particle surface to form a  $\text{BaC}_2\text{O}_4(\text{s})$  salt on the  $\text{BaTiO}_3$  particle surface. The thermodynamically stable form of barium oxalate at 298K and one atmosphere is the monohydrate ( $\text{BaC}_2\text{O}_4 \cdot \text{H}_2\text{O}$ ), a relatively insoluble simple salt ( $K_{\text{sp}} = 1.6 \times 10^{-7}$ )<sup>(107)</sup> which can passivate the  $\text{BaTiO}_3$  surface as a diffusion barrier against the incongruently dissolving  $\text{Ba}^{2+}$  ions from the bulk of the particles.

The objective of the current work is to confirm the hypothesis that the incongruent dissolution of  $\text{BaTiO}_3$  is inhibited by precipitating a relatively insoluble salt, such as barium oxalate, onto the particle surface in aqueous solution. The experimental results will also be used to corroborate or refute the hypothesis that the magnitude and polarity of the surface charge can be tailored to produce a relatively constant, uniform electrostatic potential over a wide pH range. It will be shown in additional studies that formation and control implied by such a surface state can be used to promote compatibility with organic dispersants and binders for manufacture of multilayer capacitors via tape casting and other multilayer fabrication schemes.

### 3.2. Approach

Experiments were specifically designed to test the hypothesis that the incongruent dissolution of  $\text{BaTiO}_3$  is inhibited by forming a relatively insoluble salt as a barium oxalate on the particle surface. Solution chemistry analysis by inductively coupled argon plasma (ICP) spectroscopy, in concert with high resolution transmission electron microscopy (HRTEM), was used to determine whether oxalic acid minimizes the free  $\text{Ba}^{2+}$  concentration. Solution chemistry analysis by ICP was performed on the supernatant from  $\text{BaTiO}_3$  suspensions as a function of suspension pH to determine the effect of various concentrations of oxalic acid on the concentration of free  $\text{Ba}^{2+}$  ions in solution. A reduction in the amount of  $\text{Ba}^{2+}(\text{aq})$  signifies the precipitation of the aqueous barium ions with other ions such as oxalate in solution. However, a reduction in  $\text{Ba}^{2+}(\text{aq})$  alone does not confirm the location of the barium salt precipitate as a passivation layer on the surfaces of  $\text{BaTiO}_3$  particles. High resolution transmission electron microscopy (HRTEM) was used to

provide visual confirmation of the phase stability diagram proposed by Utech et al. and others<sup>(14,41)</sup> by evaluation of the lattice fringes at the surface of the BaTiO<sub>3</sub> particles after exposure to various aqueous pH conditions (acidic, neutral, and alkaline). HRTEM also was used to confirm whether a BOM layer was formed on the BaTiO<sub>3</sub> particle surface in oxalate containing solutions. Solution chemistry analysis in conjunction with HRTEM was also used to test whether a surface layer of BOM exists on the BaTiO<sub>3</sub> particles exposed to oxalic acid.

Based upon preliminary data confirming that oxalic acid reduces the concentration of Ba<sup>2+</sup>(aq), the surface charge on the BaTiO<sub>3</sub> particles in deionized water was assessed to determine changes with respect to suspension pH in anticipation of dispersion work in a following paper.<sup>(108)</sup> Electrophoretic behavior was initially determined for aqueous BOM and aqueous BaTiO<sub>3</sub> suspensions at the same solids loading as standards against which the oxalate-treated BaTiO<sub>3</sub> powder was compared. Suspensions of BaTiO<sub>3</sub> with various concentrations of oxalic acid were analyzed via electrophoretic light scattering to determine the feasibility of producing a passivating layer of the sparingly soluble salt on the surface of the particles, as well as to monitor surface charge on the particles over a wide pH range. Electrophoretic light scattering was also used to provide additional verification that the oxalate was present as a BaC<sub>2</sub>O<sub>4</sub> precipitate on BaTiO<sub>3</sub> particle surfaces. The absence of doublets in the electrophoretic mobility distribution at a particular pH and oxalate concentration for an aqueous suspension of BaTiO<sub>3</sub> would support the notion that the oxalate is interacting only at the BaTiO<sub>3</sub> particle surface and that BOM precipitates are not formed in the bulk solution. Commercial BaTiO<sub>3</sub> tape casting production uses suspensions with solids loading greater than 20 volume percent (20%). Therefore, electroacoustic analysis at a higher solids content than that possible with electrophoretic light scattering (1%), yet significantly lower than the solids loading used in tape casting formulations (20-25%), was conducted to ensure that the particle electrophoresis results may be extrapolated to higher solids loading.

### 3.3. Materials and Methods

#### 3.3.1. General

All glassware and plasticware were washed with a biodegradable detergent<sup>1</sup>, rinsed thoroughly with tap water to remove residual soap, and subsequently rinsed several times with copious quantities of deionized water<sup>2</sup> before use. Glassware was only used when the solution/suspension pH value of the contents was less than pH 8.5 to minimize soluble silica contamination, whereas plasticware was used over the entire pH range. Unless otherwise noted, deionized water used throughout the current work was boiled for approximately ten minutes while purged with nitrogen to minimize dissolved atmospheric gases, particularly CO<sub>2</sub>, present in solution. Degassed deionized water was stored in glass bottles with rubber-lined caps under a nitrogen atmosphere until required. All constituents were weighed to four decimal places using an analytical balance<sup>3</sup>. The hydrothermally derived BaTiO<sub>3</sub> was supplied by Cabot Performance Materials (Boyertown, PA)<sup>4</sup>. Bulk analysis of the BaTiO<sub>3</sub> powder by the supplier showed concentrations of C, Sr, Fe, and Cl ranging from 500-1000 ppm, 400-800 ppm, 50-200 ppm, and 100-300 ppm respectively. Other bulk contaminants included Al, Si, Cr, Ca, and Ni, of which all concentrations were less than 5 ppm. Pure BaC<sub>2</sub>O<sub>4</sub>·H<sub>2</sub>O was precipitated from equal volumes of 1M BaCl<sub>2</sub>·2H<sub>2</sub>O and 1M K<sub>2</sub>C<sub>2</sub>O<sub>4</sub>·H<sub>2</sub>O solutions, washed three times with deionized H<sub>2</sub>O using 0.22 µm nylon filters<sup>5</sup> to collect filtrate, and finally separated into 1 g/100 ml aqueous suspension for the electrophoretic study. X-ray diffraction was used to confirm the BOM crystal structure and phase purity. All other chemicals used throughout this study are reagent grade and were used without further purification.

---

<sup>1</sup>Sparkleen, Calgon Vestal Laboratories, St. Louis, MS.

<sup>2</sup>Resistivity of the water was greater than 10 Mega ohms.

<sup>3</sup>Fisher Scientific, model A-250, 0.0001 g readability.

<sup>4</sup>Cabot BT-08 and BT-10 powders, Cabot Performance Materials, Boyertown, PA.

<sup>5</sup>Micron Separation Inc., 135 Flanders Rd., Westboro, MA 01581.

### 3.3.2. Barium Titanate Powder Characterization

The as-received  $\text{BaTiO}_3$  powder<sup>4</sup> was characterized in terms of particle size, morphology, surface topography, specific surface area, composition and phase crystallinity to provide a reference state for comparison with experimentally modified particles. As-received  $\text{BaTiO}_3$  powders were characterized using X-ray diffractometry<sup>6</sup> (XRD) for phase crystallinity; scanning electron microscopy<sup>7</sup> (SEM) for particle size, morphology and topography; gas adsorption<sup>8</sup> for specific surface area; and a centrifugal sedimentation technique<sup>9</sup> for particle size distribution. Figure 3.3(a) shows the XRD data for the as-received  $\text{BaTiO}_3$  powder compared with the powder diffraction standard for the tetragonal phase and the cubic phase  $\text{BaTiO}_3$  (JCPDS cards 5-626 and 31-174 respectively). Experimental XRD indicates that the powder exhibits the cubic phase, a finding consistent with previous work on hydrothermally derived  $\text{BaTiO}_3$ .<sup>(109)</sup> The SEM photomicrographs of the as-received powders in Figure 3.3(b) indicate that the particles are equiaxed and approximately 100 nm to 150 nm in diameter with a somewhat irregular topography. A specific surface area of approximately  $8 \text{ m}^2/\text{g}$  was determined for the as-received  $\text{BaTiO}_3$  powder used throughout these studies. A typical cumulative particle size distribution by volume for the powders is shown in Figure 3.4(a). The distribution was fit to a log normal probability distribution in Figure 3.4(b) to give a log normal mean equal to 85 nm with a log normal standard deviation of  $\sigma_z = \log(27)$ <sup>10</sup>.

<sup>6</sup>Philips Electronics APD 3720 X-ray diffractometer, Cu-K $\alpha$ , 40kV-20 mA, Mahwah, NJ.

<sup>7</sup>JEOL JSM 6400 scanning electron microscope, JEOL, Boston, MA.

<sup>8</sup>BET specific surface area

<sup>9</sup>Horiba CAPA-700 particle size analyzer, Horiba, Irvine, CA.

<sup>10</sup> Peakfit , Jandel Scientific.

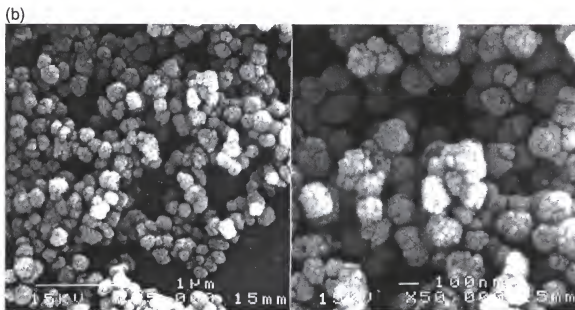
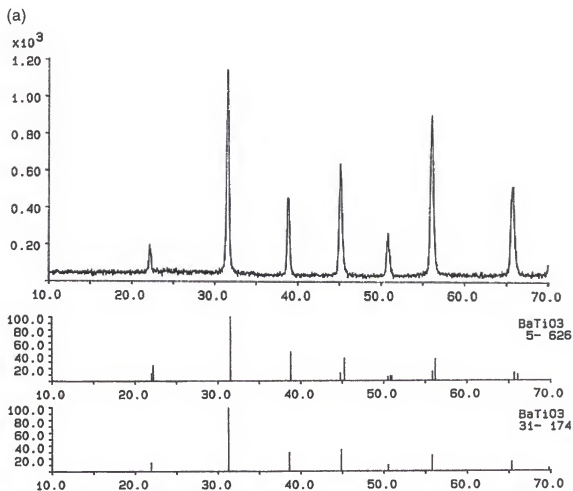


Figure 3.3. (a) X-ray diffraction patterns for the as-received BaTiO<sub>3</sub> powders with JCPDS X-ray diffraction standards for tetragonal and cubic BaTiO<sub>3</sub>, respectively, and (b) scanning electron micrographs of the as-received BaTiO<sub>3</sub> powder.

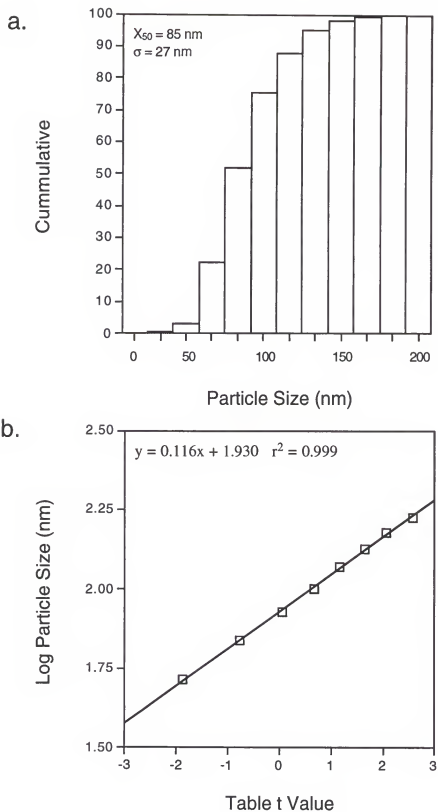


Figure 3.4. (a) Cumulative particle size distribution and (b) log normal probability distribution for the as-received BaTiO<sub>3</sub> powder from Cabot Corporation, Boyertown, PA.

### 3.3.3. Barium Titanate Aqueous Suspension Preparation

Stock solutions of oxalic acid<sup>11</sup> (as  $\text{H}_2\text{C}_2\text{O}_4 \cdot 2\text{H}_2\text{O}$ ) in concentrations of  $10^{-2}\text{M}$ ,  $10^{-3}\text{M}$ ,  $10^{-4}\text{M}$ , and 0 M (deionized water as a control) were prepared using volumetric glassware and deionized water. Suspensions of  $\text{BaTiO}_3$  (~10 g/l or 0.15%) in various concentrations of oxalic acid and BOM (~10 g/l or 0.15%) in deionized water were prepared at various pH values (adjusted using 0.01M or 0.1M tetraethylammonium hydroxide<sup>12</sup> and 0.01M or 0.1M  $\text{HNO}_3$ <sup>13</sup>) and allowed to equilibrate for 24 hours. The suspension pH was readjusted after the 24 hour equilibration period if drift from the initial pH was detected. Initial suspensions that were too high in solids loading to permit optical analysis were diluted by sedimentation and redispersion of a smaller quantity of solid in the decanted supernatant to facilitate electrophoretic light scattering measurements. The supernatant of aqueous  $\text{BaTiO}_3$  suspensions at various concentrations of oxalic acid as a function of suspension pH was analyzed to determine dissolved Ti and Ba concentrations in solution via ICP<sup>14</sup> spectroscopy (wavelengths 336.127 nm and 233.527 nm respectively). The supernatant was obtained by filtration of the  $\text{BaTiO}_3$  suspensions through 0.22  $\mu\text{m}$  using nylon filters. Supernatants were acidified with nitric acid to prevent the formation of  $\text{BaCO}_3(\text{s})$  by reaction with atmospheric  $\text{CO}_2(\text{g})$ . The  $\text{BaTiO}_3$  suspensions were used for electrophoretic mobility and ICP spectroscopy, whereas the BOM suspensions were used only in the electrophoretic mobility study<sup>15</sup>.  $\text{BaTiO}_3$  suspensions at 1% solids loading (60 g/l) with oxalic acid (3% of the solid or  $1.5 \times 10^{-2}\text{M}$ ) present in the deionized water prior to addition of the  $\text{BaTiO}_3$  powder were used in a commercial electroacoustic unit<sup>16</sup>. Details for each suspension are presented in Table 3.1. The pH of

<sup>11</sup>Oxalic acid - Fisher Scientific, lot# 905504.

<sup>12</sup>TEAOH - Tetraethyl ammonium hydroxide, Kodak, lot# A15E.

<sup>13</sup> $\text{HNO}_3$  - Fisher Scientific, 70 wt% in water, lot# 905811.

<sup>14</sup>Perkin-Elmer P2 and P2000, Perkin-Elmer, Norwalk, CT.

<sup>15</sup>Malvern Zetasizer IIc Analyser, 5 mW helium-neon laser ( $\lambda = 632.8 \text{ nm}$ ), Worchester, England.

<sup>16</sup>Matec 8000 signal receiver, Matec SSP-1 ESA sample cell assembly, and Wavetek - model 23,

the suspensions for electroacoustic determinations was adjusted dynamically by an automatic titration device<sup>17</sup> provided with the electroacoustic apparatus using either 0.1M HNO<sub>3</sub> or 0.1M TEAOH solutions. No attempt was made to control the ionic strength of the suspensions by the addition of indifferent electrolytes such as NaCl or KCl.

Table 3.1. Summary of the chemical constituents and pH ranges used for analyzing 1% BaTiO<sub>3</sub> suspensions via electroacoustic analysis.

Suspension	No Oxalate	3.0% Oxalic Acid
<b>Formulation</b>		
Amount of Solids (BaTiO <sub>3</sub> )	1%	1%
Oxalic Acid concentration*	0.0%	3.0%
Oxalic Acid (M)	0.0	1.5 x 10 <sup>-2</sup>
<b>pH range</b>	2.4 - 9.5	2.9 - 11.8

\* added in weight percent of the solids, BaTiO<sub>3</sub> powder

### 3.3.4. Preparation and Characterization of the Various Barium Titanate Powders for High Resolution Transmission Electron Microscopy

High resolution transmission electron microscopy (HRTEM)<sup>18</sup> was used to determine the nature of the surface on BaTiO<sub>3</sub> particles after exposure to various aqueous pH conditions (acidic, neutral, and alkaline: specifically pH 1.3, pH 6.5, and pH 10.2, respectively) and after treatment in ammoniated-water plus oxalic acid solution (pH 7.5). As-received BaTiO<sub>3</sub> powders (~5 g each) were suspended in ~50 ml of either glacial acetic

---

synthesized function generator.

<sup>17</sup>Hamilton - Micro Lab 900, automated titrator.

<sup>18</sup>JEOL JEM 4000FX, JEOL, Boston, MA.

acid<sup>19</sup> (pH 1.3), deionized water, ammoniated deionized water (pH 10.2), or  $10^{-1}$ M oxalic acid solution (pH adjusted to pH 7.5 with ammonium hydroxide) for 24 hours to determine the effect of environment on the particle surface. After the 24 hour equilibration, the suspensions were centrifuged, the suspending media decanted, and the powder resuspended in deionized water to rapidly dilute and wash away unreacted salts such as excess acetate. The particles were immediately concentrated via centrifugation and the excess deionized water was removed before resuspending. The centrifugation, decantation, and resuspension of these particles in deionized water was rapidly performed three times before final suspension of the samples in ethanol for HRTEM sample preparation. Ethanol was used as the final suspending medium because it does not disturb the  $\text{BaTiO}_3$  particle surface,<sup>(13)</sup> in contrast to more conventional HRTEM sample preparation where the particles are dispersed in an epoxy and mechanically dimpled followed by ion milling to produce acceptable samples for HRTEM viewing.<sup>(110)</sup>

After the various powders were suspended in ethanol, several carbon film coated HRTEM specimen grids were dipped into each suspension. Multiple images were taken to obtain a representative perspective on the crystallinity and the lattice fringes of the surface region for each of the various powders. In the preliminary HRTEM work on different commercial powders, it was established that the sample preparation procedure of dipping the carbon film coated specimen holders into well dispersed suspensions produces acceptable HRTEM samples for viewing the particle surface, provided the particles are sufficiently small.

### 3.4. Results and Discussion

#### 3.4.1. Solution Chemistry Analysis

Solution chemistry analysis of the supernatant from various  $\text{BaTiO}_3$  suspensions was performed to determine if oxalate reduces the concentration of  $\text{Ba}^{2+}$  in solution. Chemical analyses for  $\text{Ba}^{2+}(\text{aq})$  via ICP spectroscopy of the supernatant from 10 g  $\text{BaTiO}_3/\text{l}$

---

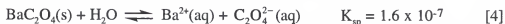
<sup>19</sup>Glacial acetic acid - Fisher Scientific, lot # 905814.

of  $10^{-2}\text{M}$   $\text{H}_2\text{C}_2\text{O}_4$ ,  $10^{-3}\text{M}$   $\text{H}_2\text{C}_2\text{O}_4$ , or  $10^{-4}\text{M}$   $\text{H}_2\text{C}_2\text{O}_4$  solutions are shown in Figure 3.5. The concentration of  $\text{Ba}^{2+}(\text{aq})$  present for the various oxalic acid concentrations is similar and relatively constant from pH 3 to pH 10. The theoretical phase stability diagram for the  $\text{Ba-TiO}_2\text{-CO}_2\text{-H}_2\text{O}$  system<sup>(14)</sup> is shown in Figure 3.6 and includes the experimental barium concentrations from aqueous  $\text{BaTiO}_3$  suspensions for both virgin aqueous suspensions and with  $10^{-4}\text{M}$   $\text{C}_2\text{O}_4^{2-}$  present. In the oxalate-treated suspension, the concentration of  $\text{Ba}^{2+}$  is nearly three orders of magnitude lower than that of the virgin suspension. Furthermore, from  $\sim\text{pH}$  2 to  $\sim\text{pH}$  10, the  $\text{Ba}^{2+}$  concentration is relatively constant, in contrast to the virgin  $\text{BaTiO}_3$  suspension for which  $[\text{Ba}^{2+}](\text{aq})$  decreases from  $\sim 10^{-1}\text{M}$  to  $10^{-4}\text{M}$  over the range from pH 6 to pH 9. Thus, the solution analysis data supports the hypothesis that the oxalate ion is associating with the  $\text{Ba}^{2+}$  via a precipitation reaction to minimize the amount of free  $\text{Ba}^{2+}$  ions in solution.

The concentration of  $\text{Ba}^{2+}$  ions present in solution is reduced by the formation of  $\text{BaC}_2\text{O}_4(\text{s})$ . The oxalate ion is added as oxalic acid and dissociates according to the following reactions:



Figure 3.7(a) and (b) illustrates the speciation diagram for the  $\text{Ba-C}_2\text{O}_4\text{-H}_2\text{O}$  system<sup>(17,63)</sup> and the  $\text{TiO}_2$  stability diagram respectively. At pH values greater than 5, oxalic acid is fully dissociated and present as  $\text{C}_2\text{O}_4^{2-}$ . The oxalate ion reacts with dissolving  $\text{Ba}^{2+}$  from the  $\text{BaTiO}_3$  particle surface according to the following precipitation reaction.



At equilibrium, the stoichiometric solubility<sup>(107)</sup> in an ideal solution where the activity coefficients are assumed to be unity is given by,

$$K_{\text{sp}} = (\text{Ba}^{2+})(\text{C}_2\text{O}_4^{2-}), \text{ and}$$

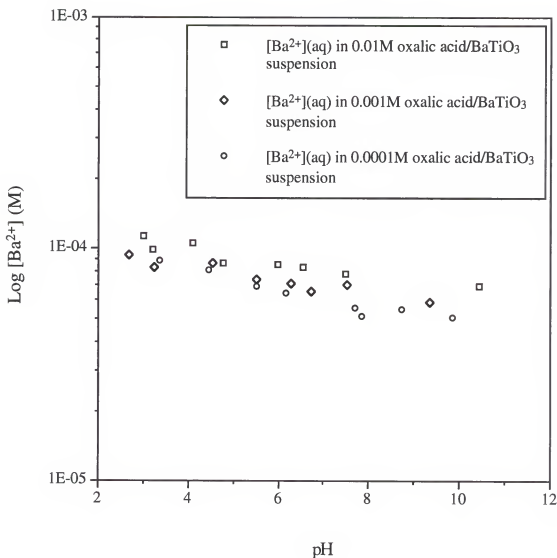


Figure 3.5. ICP data for the Ba<sup>2+</sup>(aq) concentration in solution from three different BaTiO<sub>3</sub> suspensions (10 g of BaTiO<sub>3</sub> powder/l oxalic acid or 0.15%) as a function of oxalic acid (10<sup>-2</sup>M, 10<sup>-3</sup>M, and 10<sup>-4</sup>M) concentration.

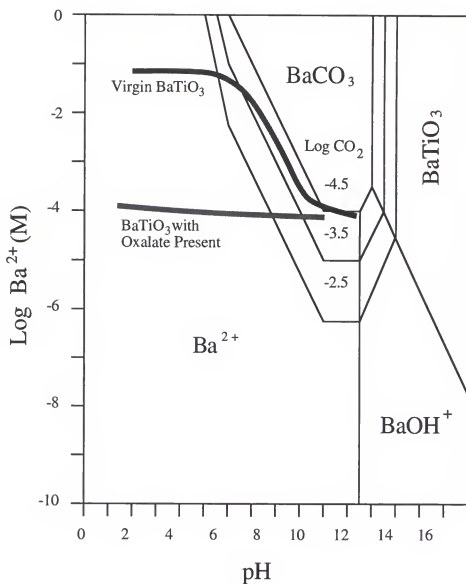


Figure 3.6. Stability diagram for the Ba-TiO<sub>2</sub>-CO<sub>2</sub>-H<sub>2</sub>O system.<sup>(14)</sup> Data lines entitled "Virgin BaTiO<sub>3</sub>" and "BaTiO<sub>3</sub> with Oxalate Present" show the concentration of dissolved Ba<sup>2+</sup> from the supernatants of 10 g BaTiO<sub>3</sub>/l H<sub>2</sub>O (0.15%) and 10 g BaTiO<sub>3</sub>/l 10<sup>-4</sup> M oxalic acid (0.15%), respectively.

# SOLUBILITY OF BARIUM OXALATE

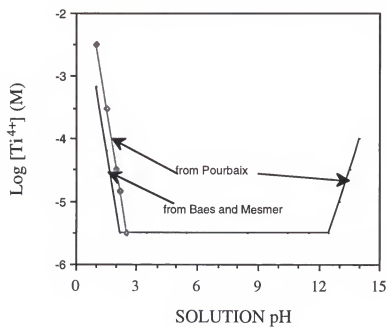
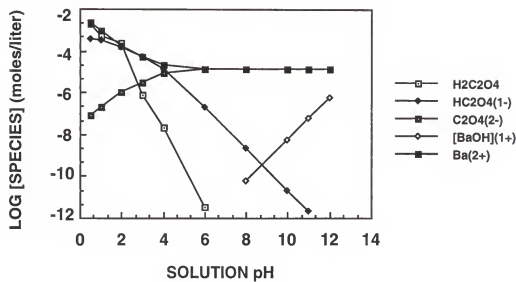


Figure 3.7. (a) Speciation diagram for the Ba-C<sub>2</sub>O<sub>4</sub>-H<sub>2</sub>O system<sup>(17,63)</sup> and (b) the TiO<sub>2</sub> stability diagram.<sup>(54,55)</sup>

$$[\text{Ba}^{2+}] = [\text{C}_2\text{O}_4^{2-}] \approx 4 \times 10^{-4}\text{M} \text{ (from pH 5 to ~pH 11)}$$

Thus, the predicted the amount of  $\text{Ba}^{2+}$  in equilibrium with  $\text{BaC}_2\text{O}_4(\text{s})$  of approximately  $4 \times 10^{-4}\text{M}$  is in relatively good agreement with the experimental solubility of  $\text{Ba}^{2+}$  for the oxalate treated  $\text{BaTiO}_3$  suspensions shown in Figures 3.5 and 3.6.

Furthermore, based on the common ion effect, and assuming ideal solution, the concentration of  $\text{Ba}^{2+}(\text{aq})$  in equilibrium in  $10^{-2}\text{M}$   $\text{C}_2\text{O}_4^{2-}$  and  $10^{-3}\text{M}$   $\text{C}_2\text{O}_4^{2-}$  is approximately  $1.6 \times 10^{-5}\text{M}$  and  $1.4 \times 10^{-4}\text{M}$ , respectively. These values for  $[\text{Ba}^{2+}](\text{aq})$  based on the common-ion effect in the solution with excess  $\text{C}_2\text{O}_4^{2-}(\text{aq})$  are in even better agreement with the measured  $[\text{Ba}^{2+}](\text{aq})$ , which was on the order of  $6 \times 10^{-5}\text{M}$  to  $1 \times 10^{-4}\text{M}$  determined by ICP spectroscopy. While not direct confirmation of the presence of  $\text{BaC}_2\text{O}_4 \cdot \text{H}_2\text{O}(\text{s})$  in equilibrium in the oxalate-treated solutions, the measured concentration of  $\text{Ba}^{2+}$  in the solution is similar to the theoretical BOM solubility. Furthermore, the relative insensitivity of the measured  $[\text{Ba}^{2+}](\text{aq})$  values with respect to solution pH are in good agreement with the expected BOM solubility as a function of solution pH.

### 3.4.2. High Resolution Transmission Electron Microscopy Analysis

High resolution TEM imaging was used to analyze the surface region of the  $\text{BaTiO}_3$  particles subjected to a variety of solution conditions as a function of solution pH and the presence of ions such as oxalate. A reduction in the amount of  $\text{Ba}^{2+}$  ions in solution via the solution analyses is a necessary but insufficient proof that oxalate ions passivate the  $\text{BaTiO}_3$  surface. Chemical analyses do not confirm the physical location of the BOM precipitate which is an additional requirement for the surface passivation. High resolution transmission electron microscopy (HRTEM) was used to provide a visual confirmation of the phase stability diagram proposed by Osseo-Asare et al., Utech et. al, and Lencka and Riman<sup>(14,17,42)</sup> by evaluation of the lattice fringes at the surface of the  $\text{BaTiO}_3$  particles after being exposed to various aqueous pH conditions (acidic, neutral, and basic). HRTEM also was used to confirm whether a BOM layer is present on the  $\text{BaTiO}_3$  particle surface after exposure to pH-adjusted oxalic acid solution.

The four powders examined were acetic acid-washed, water-washed, ammoniated water-washed, and oxalate-treated (Figures 3.8 to 3.11, respectively). The most obvious difference between the various powders was the surface layer, seen as an aura of amorphous material around each of the water-washed particles at a nominal pH 6.5 shown in Figure 3.9. The surface layer (3 nm to 7 nm) on the water-washed  $\text{BaTiO}_3$  particles is most likely due to a barium-depleted region, resulting in an amorphous  $\text{TiO}_2$ -rich layer at the surface of the particle by incongruent dissolution of  $\text{Ba}^{2+}$  ions. The formation of an amorphous surface layer is a common phenomenon observed on corroded soda-lime-silicate glasses.<sup>(61)</sup>

In contrast to the water-washed  $\text{BaTiO}_3$ , the acid-washed and ammoniated water-washed particles have no depleted surface region as shown in Figures 3.8 and 3.10, respectively. The low pH (pH~1) used in the acid-washed sample dissolves the titanium as well as the barium at the surface of the particle, as indicated by the phase stability diagram for  $\text{TiO}_2$  compiled from data in Pourbaix<sup>(55)</sup> and Baes and Mesmer<sup>(54)</sup> and shown in Figure 3.7(b). Therefore at low pH, dissolution of  $\text{BaTiO}_3$  is by congruent dissolution with near stoichiometric concentrations of barium and titanium ions in solution. Under highly alkaline conditions (pH > 12)  $\text{BaTiO}_3$  is theoretically stable as predicted by Osseo-Asare et al. and others.<sup>(14,17,42)</sup> Therefore a depleted surface region is neither expected nor observed for the ammoniated water-washed sample shown in Figure 3.10.

The oxalate-treated  $\text{BaTiO}_3$  particles have a very thin surface layer, as shown in the HRTEM micrograph of Figure 3.11. The layer is approximately 1 nm thick as indicated in the HRTEM micrograph. Such a thin layer is beyond the limits of detection by electron spectroscopic techniques to establish the chemical composition of the layer, but reduction in the amount of aqueous barium present in solution, concurrent with the formation of a surface layer, is compelling experimental evidence that barium is precipitating with oxalate at or near the surfaces of the  $\text{BaTiO}_3$  particles. Furthermore, BOM formation is proposed since the only ions present in solution are from contamination found on the



Figure 3.8. Transmission electron micrograph of the acetic acid-washed  $\text{BaTiO}_3$  particles.

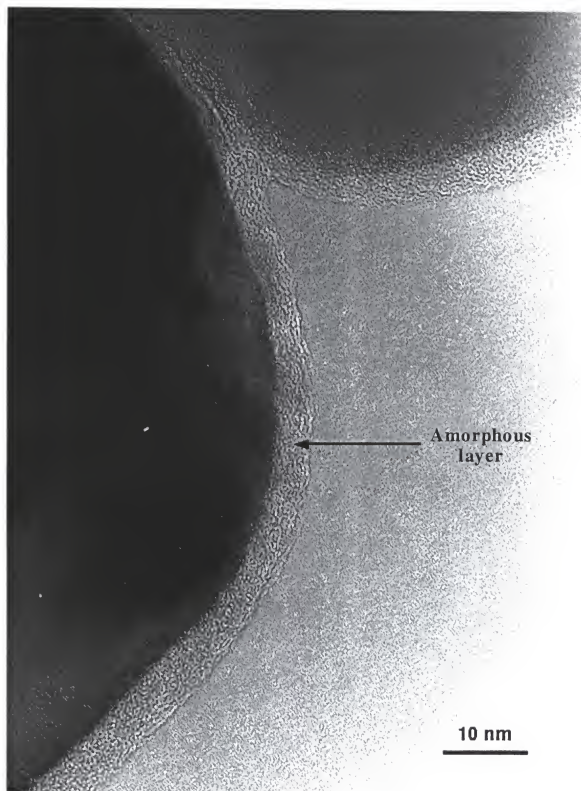


Figure 3.9. Transmission electron micrograph of the water-washed  $\text{BaTiO}_3$  particles.



Figure 3.10. Transmission electron micrograph of the ammoniated water-washed BaTiO<sub>3</sub> particles.

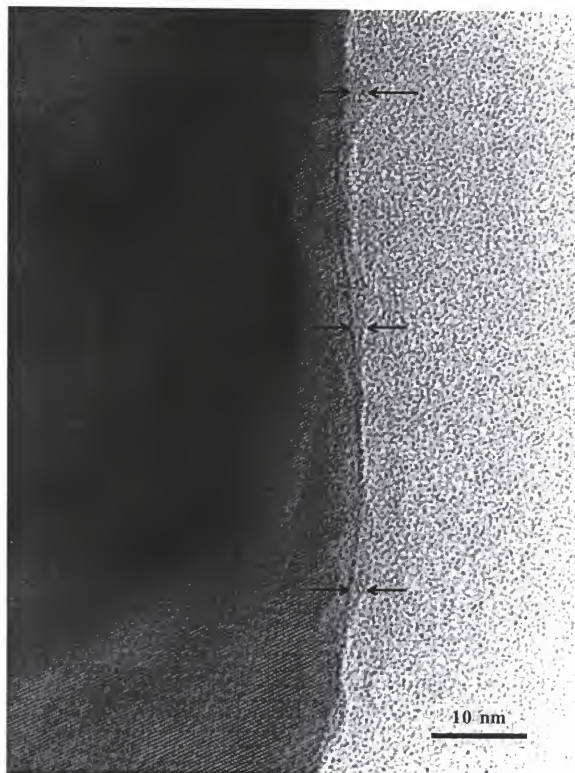


Figure 3.11. Transmission electron micrograph of the oxalate treated  $\text{BaTiO}_3$  particles.

surface of the  $\text{BaTiO}_3$  particles, from exposure to the atmosphere (i.e.  $\text{CO}_3^{2-}$ ), from the addition of oxalic acid, or from the addition of  $\text{HNO}_3$  or tetraethylammonium hydroxide. The lot analysis supplied with the as-received  $\text{BaTiO}_3$  powder showed no significant bulk concentrations of substances that complex with the positively charged  $\text{Ba}^{2+}(\text{aq})$ . The major contaminants include carbon, strontium, iron, and chlorine in the ranges of 500-1000 ppm, 400-800 ppm, 50-200 ppm and 100-300 ppm respectively, with concentrations of silica, aluminum, chromium, calcium, and nickel less than 5 ppm. It is important to note that the contaminant concentrations for the as-received  $\text{BaTiO}_3$  powder represent the bulk material. In the solution phase these concentrations are expected to be significantly lower due to the limited dissolution of the  $\text{BaTiO}_3$  particles. The amounts of acid and base added were relatively small (i.e., less than  $10^{-3}\text{M}$ ) and would not reduce the amount of  $\text{Ba}^{2+}(\text{aq})$  by three orders of magnitude as experimentally observed. Therefore, the only reasonable explanation for the reduction of  $\text{Ba}^{2+}(\text{aq})$  is a reaction between the dissolving barium with the oxalate ions present in solution. Furthermore, the HRTEM results for the oxalic acid-washed  $\text{BaTiO}_3$  indicate that a significant part of this association occurs as deposition on the  $\text{BaTiO}_3$  particle surface. This is in contrast to the formation of a  $\text{Ba}^{2+}$ -depleted amorphous surface region found on the water-washed  $\text{BaTiO}_3(\text{s})$  exposed to aqueous solution at a similar pH, but without oxalate ion present.

Further support for the deposition of BOM or related compounds (e.g., a higher form of a hydrate) on  $\text{BaTiO}_3$  surfaces is provided by an estimation of the thickness of a BOM precipitate on  $\text{BaTiO}_3$  surfaces via a mass balance calculation. It will be assumed that virtually all  $\text{C}_2\text{O}_4^{2-}$  ions reacted with the  $\text{Ba}^{2+}$  ions to form the passivating layer. This assumption ignores the relatively small contribution that the solubility of BOM makes toward partial removal of any  $\text{BaC}_2\text{O}_4$  passivation layer. If the observed layer is thicker than the calculated layer, then the hypothesis that the layer consists of BOM will be compromised.

The theoretical thickness of the BOM passivating layer was calculated for one gram of  $\text{BaTiO}_3$  powder and an oxalic acid dosage of 3% of the solid. One gram of  $\text{BaTiO}_3$  powder has an experimentally determined specific surface area of approximately  $8 \text{ m}^2/\text{g}$  or  $8 \times 10^4 \text{ cm}^2/\text{g}$ . For a 3% oxalic acid dosage, 0.03 g of  $\text{H}_2\text{C}_2\text{O}_4 \cdot 2\text{H}_2\text{O}$  would be added but only  $\sim 0.0214 \text{ g}$  of the  $\text{C}_2\text{O}_4^{2-}$  ions would be present. Assuming all  $\text{C}_2\text{O}_4^{2-}$  ions react with dissolved  $\text{Ba}^{2+}$  ions in solution to form a uniform, continuous passivating layer of  $\text{BaC}_2\text{O}_4 \cdot \text{H}_2\text{O}$  (density,  $\rho = 2.658 \text{ g/cc}$ )<sup>(106)</sup> over the entire surface, and neglecting the solubility of  $\text{BaC}_2\text{O}_4 \cdot \text{H}_2\text{O}$ , the calculated thickness of the BOM layer is approximately 1.6 nm. This value is dependent upon the specific surface area of the powder, the chemical formula of the passivating layer (e.g., whether a higher hydrate is formed- $\text{BaC}_2\text{O}_4 \cdot n\text{H}_2\text{O}$ ), and the solubility of BOM ( $\sim 1.6 \times 10^{-7}$ ). The calculated thickness is in reasonable agreement with the thickness of the layer estimated from the HRTEM micrograph in Figure 3.11 supporting the hypothesis that BOM deposits on the surfaces of the  $\text{BaTiO}_3$  particles and provides a true passivation layer to inhibit incongruent dissolution.

#### 3.4.3. Electrophoretic Behavior of Barium Titanate Suspensions at Various Solids Loading

The objective of this section was to determine the electrophoretic behavior of  $\text{BaTiO}_3$  suspensions at various solids loading. Determining the electrophoretic behavior as a function of solids loading provides information about surface reaction and surface charge formation as well as the mechanism which limits the concentration of  $\text{Ba}^{2+}$  in solution (diffusion or solubility).

The zeta potential of the as-received  $\text{BaTiO}_3$  in aqueous suspension varies with solids loading, as shown in Figure 3.12. The isoelectric point (IEP) (the pH at which the zeta potential changes polarity) of aqueous suspension of  $\text{BaTiO}_3$  increases with increased solids loading. At 5 g/l (0.075% or  $40 \text{ m}^2$  of  $\text{BaTiO}_3$  per liter suspension), the IEP occurs at  $\sim \text{pH } 5$ , while for solids loadings of 20 g/l, 60 g/l, and 200 g/l, the IEPs occur at much more alkaline conditions. This experimental observation for the virgin  $\text{BaTiO}_3$  particles in

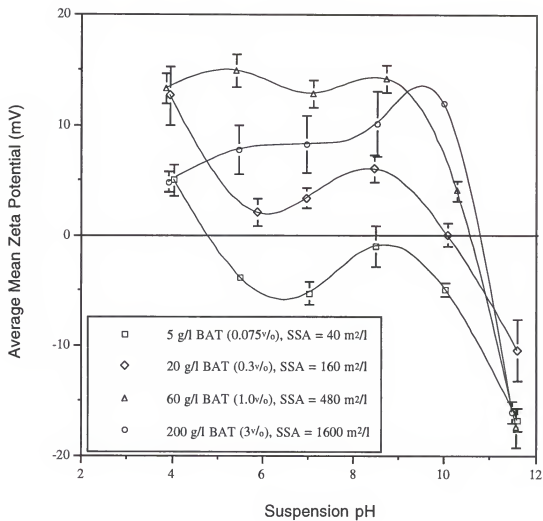


Figure 3.12. Zeta potential measurements as a function of suspension pH for the hydrothermally derived  $\text{BaTiO}_3$  powder as a function of solids loading.

water can be interpreted based on the work by Fuerstenau and co-workers showing specific adsorption of  $\text{Ba}^{2+}(\text{aq})$  on  $\text{TiO}_2(\text{s})$ .<sup>(72,84)</sup> The IEP for the most dilute  $\text{BaTiO}_3$  suspension (5 g/l) is consistent with the presence of a Ti hydrous oxide layer, as indicated for the water-washed  $\text{BaTiO}_3$  particles in Figure 3.9. Various forms of titania are weakly acidic, with an IEP in the pH range from pH 4 to pH 6.<sup>(20,52,53)</sup> The relatively low  $\text{Ba}^{2+}(\text{aq})$  concentration measured at the low solids loading, in contrast to the higher concentrations of  $\text{Ba}^{2+}(\text{aq})$  as the solids loading is increased, as shown in Figure 3.13, is consistent with a system in which incongruent dissolution is taking place. However, as the  $[\text{Ba}^{2+}](\text{aq})$  increases, enough  $\text{Ba}^{2+}(\text{aq})$  is present in solution to support measurable specific adsorption of  $\text{Ba}^{2+}(\text{aq})$  at the amorphous Ti hydrous oxide surface. The conclusion that specific adsorption of  $\text{Ba}^{2+}(\text{aq})$  takes place on the Ti hydrous oxide surface is consistent with the criterion that an ion is specifically adsorbing on a metal hydrous oxide if the adsorption of the ion causes a shift in the IEP of the solid.<sup>(68)</sup> Moreover, Fuerstenau et al.<sup>(72,84)</sup> have observed specific adsorption of  $\text{Ba}^{2+}(\text{aq})$  and other alkaline earth ions on titania in support of the proposed surface charging mechanism for  $\text{BaTiO}_3$  in aqueous suspensions.

While the development and testing of a quantitative surface charge model for  $\text{BaTiO}_3$  in water will be the focus of a later paper, it is proposed that the following surface and solution reactions lead to surface charge formation at a given solids loading or, more precisely, a given surface area of  $\text{BaTiO}_3(\text{s})$  presented to the solution phase. First,  $\text{Ba}^{2+}$  incongruently dissolves at the  $\text{BaTiO}_3$  particle/solution interface. Second, or perhaps concurrent with  $\text{Ba}^{2+}$  incongruent dissolution, the resulting amorphous Ti hydrous oxide takes on surface charge in a manner similar to titania, resulting in a "pristine" IEP at  $\sim\text{pH } 5$ . Third, if there is sufficient  $[\text{Ba}^{2+}](\text{aq})$  in solution, as provided by higher surface areas of  $\text{BaTiO}_3$  exposed to the aqueous phase at higher solid loadings, specific adsorption of  $\text{Ba}^{2+}(\text{aq})$  into the Stern plane on the Ti hydrous oxide surface takes place. Specific adsorption of  $\text{Ba}^{2+}(\text{aq})$  leads to a shift in the IEP toward more alkaline pH values.

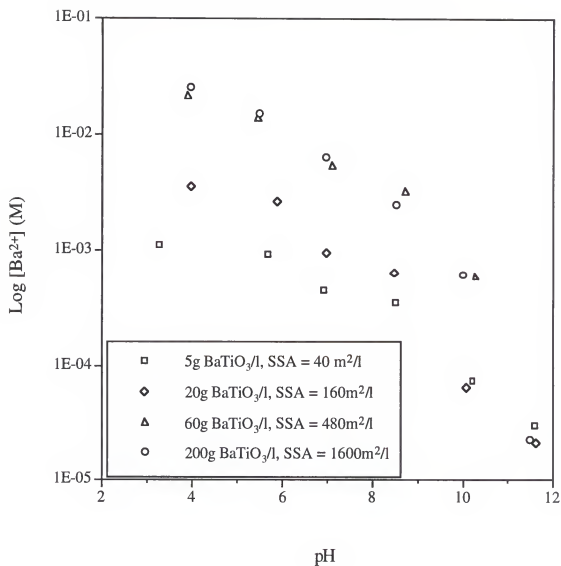


Figure 3.13. ICP analysis for the hydrothermally derived BaTiO<sub>3</sub> powder as a function of solids loading.

The high concentration of  $\text{Ba}^{2+}(\text{aq})$ , particularly at the higher solid loadings, and the relatively modest magnitudes observed for zeta potentials in such suspensions are consistent with the poor stability of  $\text{BaTiO}_3$  aqueous suspensions. In the suspensions used for the electrophoretic light scattering measurements, coagulation manifests as a rapid sedimentation behavior that was observed in all suspensions. As discussed earlier, the addition of an organic dispersant is not sufficient to maintain stability because the relatively high concentrations of  $\text{Ba}^{2+}(\text{aq})$  are capable of cross-linking many of the conventional organic dispersants.

The electrophoretic behavior of  $\text{BaTiO}_3$  as a function of solids loading strongly suggests that increasing the amount of surface area (by increasing the solids content) causes the IEP to shift toward a more alkaline pH. The shift in the IEP towards a more alkaline pH with increased solids ( $\text{BaTiO}_3$ ) implies that the concentration of  $\text{Ba}^{2+}$  in solution is controlled by both the solubility, and a diffusion limiting layer of amorphous  $\text{TiO}_2$ . This layer was also noted in the HRTEM micrograph shown in Figure 3.9.

#### 3.4.4. Electrophoretic Behavior of Barium Oxalate Monohydrate and Barium Titanate Suspensions at Various Oxalic Acid Concentrations

Electrophoretic mobility measurements were made to determine how the presence of oxalate affects the electric potential associated with the surface of  $\text{BaTiO}_3$  particles suspended in an aqueous medium. It will also be shown that the oxalate reacts at the  $\text{BaTiO}_3$  particle surface rather than in the bulk solution. After determining that the oxalate treatment reduces the amount of free  $\text{Ba}^{2+}$  in solution via ICP spectroscopy, the surface charge of  $\text{BaTiO}_3$  suspensions at various oxalic acid concentrations was assessed to ensure uniform coverage. Uniform coverage is characterized by a monomodal distribution of charge, as opposed to a bimodal charge distribution which is indicative of dissimilar particles with various surface charges. Electrostatic charge alone may allow metastable powder dispersion, but for most oxides the charge present on the particle surface is

dependent upon the pH of the suspension. This is because the potential-determining ions for most metal oxides are  $H^+$  and  $OH^-$ .<sup>(68)</sup>

As the pH of the suspension changes, the magnitude and polarity of the charge can also change. A 10 g  $BaTiO_3/l$   $H_2O$  suspension exhibits amphoteric behavior, with the potential changing from a positive to a negative value with increasing pH and an IEP in the intermediate range of pH 8 to pH 9 (Figure 3.14). With the IEP near the processing pH for commercial multilayer capacitors, the particles would have little charge on the surface and would tend to agglomerate much more easily. The ideal situation is to maintain a large potential and constant surface charge polarity over a wide pH range to accommodate any fluctuations in pH during processing.

In contrast to the 10 g  $BaTiO_3/l$   $H_2O$  suspension, the 10 g BOM/ $H_2O$  suspension maintains a constant positive potential ( $\sim 20$  mV) on the particle surface from pH 4 to pH 10, which is similar to the findings of Curreri et. al on a similar compound, calcium oxalate monohydrate (COM).<sup>(64)</sup> This constant positive potential over a wide suspension pH range supports BOM as a potential surface modification agent to tailor the magnitude and polarity of the zeta potential and thus controlling dispersion.

When adding  $BaTiO_3$  (10 g/l or 0.15%) to oxalic acid instead of  $H_2O$ , the pH of the suspension increases. However, the increase in suspension pH is beneficial because it ensures that the  $H_2C_2O_4$  is fully dissociated and present as  $C_2O_4^{2-}$  where it can readily react with  $Ba^{2+}$  ions in solution or  $Ba^{2+}$  ions dissolving from the  $BaTiO_3$  particle surface as shown in equation [1]. Electrophoretic measurements were made over the pH range of  $\sim 3$  to 10 to determine if the BOM is present on the surface and if the oxalic acid concentrations provide uniform coverage. The results (Figure 3.14) show a relatively constant negative charge on the surface, with the magnitude dependent upon the molar concentration of the oxalic acid. At lower oxalic acid concentrations, a small inflection is noted around suspension pH 7 to pH 8 and is probably due to  $BaCO_3$  depositing on the particle surfaces. In contrast to the BOM suspension where the polarity is positive over the pH range from 4

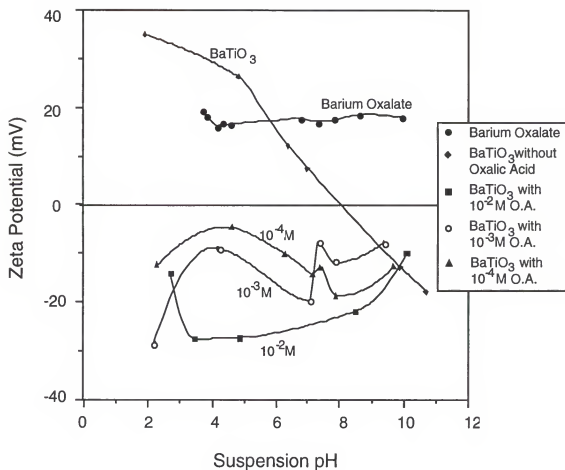


Figure 3.14. Electrophoretic behavior for  $\text{BaC}_2\text{O}_4 \cdot \text{H}_2\text{O}$  and  $\text{BaTiO}_3$  in deionized water and  $\text{BaTiO}_3$  suspensions (10 g/l or 0.15%) in various concentrations of  $\text{H}_2\text{C}_2\text{O}_4 \cdot 2\text{H}_2\text{O}$  ( $10^{-2}$ ,  $10^{-3}$ ,  $10^{-4}$  M).

to 10, the BaTiO<sub>3</sub> particles suspended in oxalic acid exhibit a negative potential over the same pH range. This negative charge is due to the oxalate ion reacting with the dissolving Ba<sup>2+</sup> ion, depositing on the particle surface, and the BOM taking on a net negative surface charge because of excess negatively charged oxalate.<sup>(33)</sup>

Figure 3.15 demonstrates how an increase in the BaTiO<sub>3</sub> solids to one volume percent (1%) with corresponding oxalic acid concentrations affects the electrophoretic behavior of the suspensions. The 60 g/l (i.e., 1%) BaTiO<sub>3</sub> suspensions with various additions of oxalic acid in weight percent of the solids (BaTiO<sub>3</sub> powder) display a behavior similar to BaTiO<sub>3</sub>/oxalic acid suspensions in Figure 3.14 at a lower solids loading. However the 1% addition of oxalic acid does not provide a uniform, negative surface charge over the entire pH range investigated. Larger additions of oxalic acid (2% and 3%) show a relatively constant negative charge on the surface from suspension pH 4 to pH 11.5. Therefore it is necessary to add at least 2% oxalic acid to provide stable zeta potential values as a function of pH.

#### 3.4.5. Electroacoustic Analysis of High Solids Loading Barium Titanate Suspensions

The electrophoretic behavior of low solids loading BaTiO<sub>3</sub> suspensions discussed in a prior section provided some insight into the surface charge at low solid concentrations which are significantly lower than tape casting formulations. The objective of this section was to determine if increasing the BaTiO<sub>3</sub> concentration affects the surface charge associated with the BaTiO<sub>3</sub> particles suspended in either deionized water or oxalic acid. The electroacoustic behavior shown in Figure 3.16 for the two suspensions detailed in Table 3.1 is similar to the electrophoretic behavior for suspensions of similar solids loading with oxalic acid present (Figure 3.15). However, the samples in Figure 3.15 needed to be reconstituted before the electrophoretic behavior could be determined with light scattering, whereas the electroacoustic samples were measured directly at the 1% BaTiO<sub>3</sub> concentration.

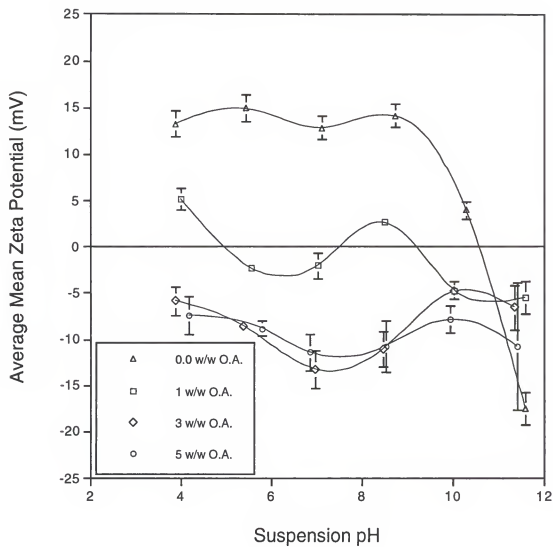


Figure 3.15. BaTiO<sub>3</sub> suspensions (1%) with various amounts of oxalic acid incorporated as a weight percent of the solids (BaTiO<sub>3</sub> powder).

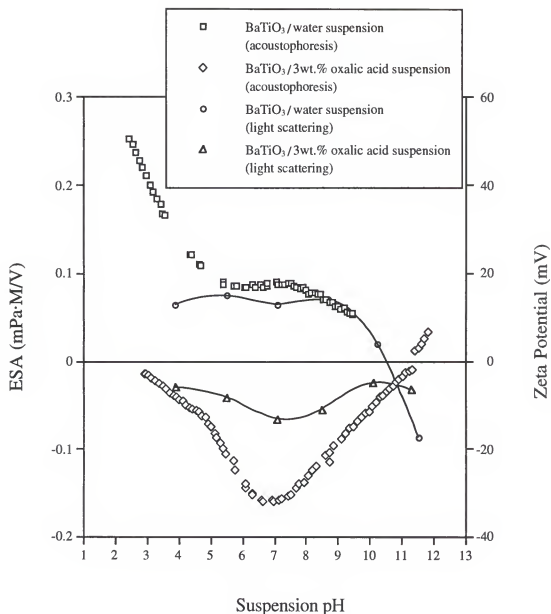


Figure 3.16. Electroacoustic behavior for two different 1% BaTiO<sub>3</sub> suspensions with 0.0 and 3.0% oxalic acid present in comparison with electrophoretic behavior of similar suspensions where the zeta potential determined is determined using a light scattering technique (suspensions 1 through 4 respectively). For additional information about the electroacoustic suspensions see Table 3.1.

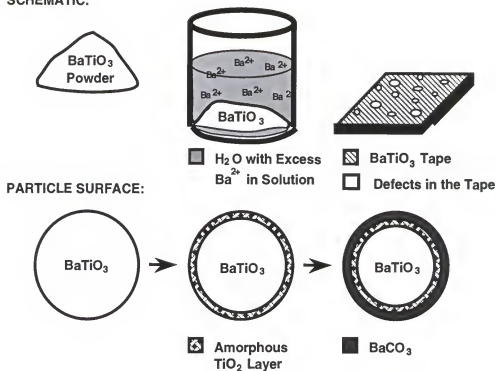
The 1% BaTiO<sub>3</sub> aqueous suspension (analyzed using electroacoustic waves) exhibits a positive charge with no IEP present over the entire pH range (2.5 to 9.5) investigated. Electroacoustic data is given as the electrokinetic sonic amplitude or ESA (mPa-M/V), which can be converted to zeta potential (mV) through a series of equations.<sup>(104)</sup> This electroacoustic data exhibits a similar trend and charge magnitude to the sample in Figures 3.12 and 3.15 with no oxalic acid present over a pH range from pH 4 to pH 10.

The electroacoustic behavior for the 1% BaTiO<sub>3</sub>, 3% oxalic acid exhibits a negative charge ranging between 10 mV and 30 mV over the pH range from pH 4 to pH 10. This corresponds with the particle electrophoretic results for surface potential determined using an electrophoretic light scattering technique. The surface charge measured at low pH ( $1.5 < \text{pH} < 4$ ) and highly alkaline pH values ( $10 < \text{pH} < 12$ ) was not determined using light scattering techniques. However, electroacoustic results show a very small charge at highly acidic and highly alkaline conditions. The low charge exhibited at low pH ( $1.5 < \text{pH} < 4$ ) values may be due to incomplete dissociation of the oxalic acid (present as H<sub>2</sub>C<sub>2</sub>O<sub>4</sub> and HC<sub>2</sub>O<sub>4</sub><sup>-</sup>) and therefore incomplete coverage of the BaTiO<sub>3</sub> particle surface. The low charge noted at highly alkaline conditions ( $10 < \text{pH} < 12$ ) could be due to the formation of Ba(OH)<sup>+</sup>. The formation of Ba(OH)<sup>+</sup> on the particle surface drives the charge towards zero (pH = 11.4) until it eventually becomes positive.

### 3.5. Conclusions

The problems associated with the aqueous processing of BaTiO<sub>3</sub> (incongruent dissolution of Ba<sup>2+</sup> from the BaTiO<sub>3</sub> particle surface) for multilayer capacitors and a solution are summarized in Figure 3.17(a) and 3.17(b) respectively with its validity confirmed by the experimental results. The electrophoretic behavior of aqueous BaTiO<sub>3</sub> suspensions is dependent not only upon batch to batch variations, but also upon solids loading. ICP results confirm the theoretical instability of BaTiO<sub>3</sub>, with high resolution

## a. SCHEMATIC:



## b. SCHEMATIC:

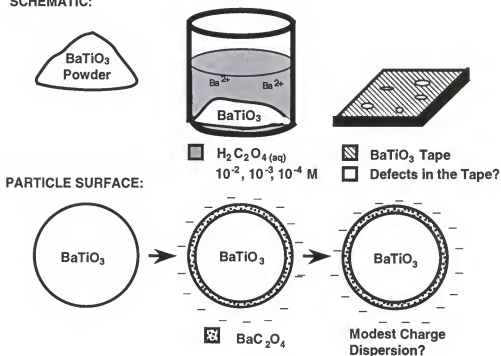


Figure 3.17. (a) Schematic showing the incongruent dissolution of  $\text{Ba}^{2+}$  in deionized water and the formation of Ti-rich and Ba-rich layers which circumvent the stoichiometric  $\text{BaTiO}_3$  core, and (b) the passivation treatment for minimizing the dissolution of  $\text{Ba}^{2+}$  from the  $\text{BaTiO}_3$  particle surface via oxalic acid provides uncertain colloidal stability.

HRTEM corroborating that it is a surface mediated phenomena. In contrast to  $\text{BaTiO}_3$ , electrophoretic measurements for BOM demonstrate a relatively constant, positive zeta potential for a pH range from pH 4 to pH 10. Suspensions of  $\text{BaTiO}_3$  with various concentrations of oxalic acid ( $10^{-2}\text{M}$ ,  $10^{-3}\text{M}$ , and  $10^{-4}\text{M}$ ) show relatively constant, negative zeta potentials over the same pH range, with the magnitude of the charge dependent upon the oxalate ion concentration. Increasing the amount of oxalic acid present increases the magnitude of the charge associated with the surface of the  $\text{BaTiO}_3$  particles. Oxalate additions also minimize the  $\text{Ba}^{2+}$  ion concentration in solution by precipitating the relatively insoluble barium oxalate salt as a diffusion barrier on the surface of the  $\text{BaTiO}_3$  particles. The  $\text{BaC}_2\text{O}_4$  precipitate is the product of the leached  $\text{Ba}^{2+}$  ions from the  $\text{BaTiO}_3$  particle surface and the fully dissociated  $\text{C}_2\text{O}_4^{2-}$  ions present in solution. Calculation of the thickness of this barrier layer was determined to be 1.6 nm, which is reasonably consistent with the surface layer experimentally observed in the HRTEM micrographs of the oxalate-treated powder.

The addition of  $\text{BaTiO}_3$  powder to oxalic acid solution controls the particle surface charge and minimizes the free  $\text{Ba}^{2+}$  ions present in solution over a wide pH range, alleviating the problems associated with small fluctuations in pH during processing. The passivation of the  $\text{BaTiO}_3$  particle surface via oxalic acid was convincingly demonstrated by the experimental results discussed throughout the current work. However, the suspension stability was not improved by the presence of oxalic acid and will be addressed in future experiments.

## CHAPTER 4 DISPERSION OF AQUEOUS BaTiO<sub>3</sub> SUSPENSIONS

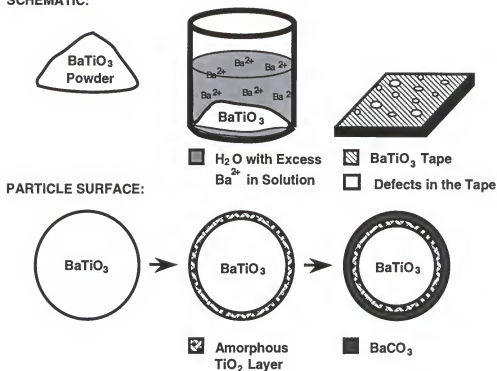
### 4.1. Introduction

The dispersion of fine particles to prepare homogeneous suspensions is critical in ceramic powder processing for the production of uniform green microstructures and reliable fired ceramics.<sup>(6,7,34,67,111-114)</sup> The final microstructure of ceramics is adversely affected when agglomerates of the ceramic particles are present during sintering which consequently increases significantly with the fabrication of thinner layers.<sup>(28,31)</sup> The particles in suspension must be well dispersed, particularly in the highly concentrated slips used in tape casting.<sup>(5,33)</sup> From a handling point of view, excessive thixotropy, dilatancy, and high yield point should be avoided for a tape casting suspension with suitable rheological properties.<sup>(34,115)</sup>

BaTiO<sub>3</sub> suspended in oxalic acid instead of deionized water minimizes the dissolution of the Ba<sup>2+</sup> from the surface of the BaTiO<sub>3</sub> particles as well as providing a relatively uniform, negative surface charge over the pH range from pH 4 to pH 10.<sup>(108)</sup> However, only modest zeta potential magnitudes are provided by the adsorption of the barium oxalate precipitate onto the BaTiO<sub>3</sub> particle surface. Thus, the colloidal stability of the oxalate-treated BaTiO<sub>3</sub> particles is marginal and clearly unsuitable for tape casting. Figure 4.1 summarizes the incongruent dissolution and passivation process with the corresponding particle surface layers depicted.<sup>(14,18,35,43,108)</sup>

Dispersion of a powder, specifically BaTiO<sub>3</sub>, in a liquid must accommodate the various interactions that can take place between the suspending medium and particulate as shown in Figure 4.2. In the BaTiO<sub>3</sub>-H<sub>2</sub>O system, incongruent dissolution of Ba<sup>2+</sup> can lead to deposition of naturally occurring Ba-salts such as BaCO<sub>3</sub>(s), to high ionic strength in

## a. SCHEMATIC:



## b. SCHEMATIC:

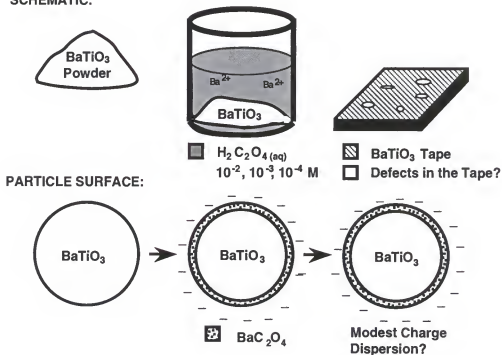


Figure 4.1. (a) Schematic showing the incongruent dissolution of  $\text{Ba}^{2+}$  in deionized water and the formation of Ti-rich and Ba-rich layers which circumvent the stoichiometric  $\text{BaTiO}_3$  core, and (b) the passivation treatment for minimizing the dissolution of  $\text{Ba}^{2+}$  from the  $\text{BaTiO}_3$  particle surface via oxalic acid provides uncertain colloidal stability.<sup>(14,35,108)</sup>

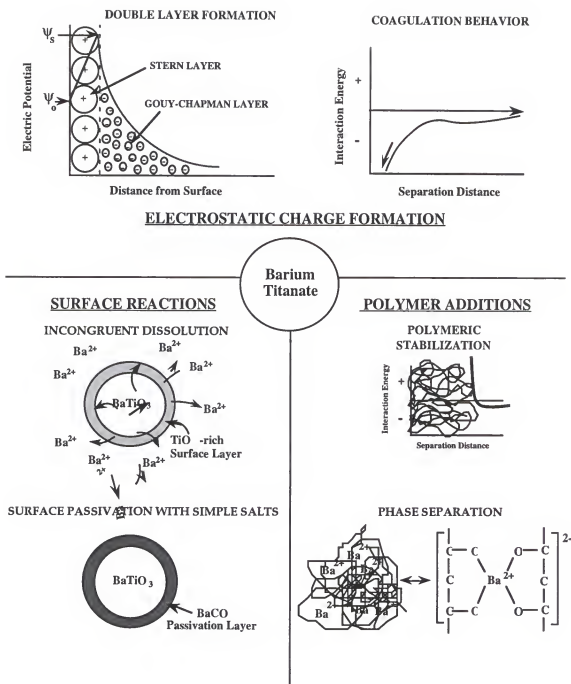


Figure 4.2. A summary of various interactions between  $BaTiO_3$  particles, water, and polymeric additives.<sup>(108)</sup>

solution due to the high solubility of such Ba-salts at low to intermediate pH, and to specific interactions of  $\text{Ba}^{2+}$  with polymeric additives which results in phase separation of the Ba-polymeric moiety.<sup>(44)</sup> In prior work it has been shown that oxalate ( $\text{C}_2\text{O}_4^{2-}$ ) may be used to produce a  $\text{BaC}_2\text{O}_4 \cdot \text{H}_2\text{O}$  (BOM) passivation layer on the surface of the  $\text{BaTiO}_3$  particle.<sup>(108)</sup> The solubility of the BOM passivation layer is much less sensitive to changes in solution pH than either the virgin  $\text{BaTiO}_3$  or the naturally occurring  $\text{BaCO}_3(\text{s})$  passivation layer.<sup>(17,63,64)</sup> The large change in solubility as a function of solution pH for  $\text{BaCO}_3(\text{s})$  increases the ionic strength of the suspension. The  $\text{BaCO}_3(\text{s})$  instability in aqueous solution compromises the dispersion of the  $\text{BaCO}_3$ -passivated  $\text{BaTiO}_3$  in water at low to moderate pH ranges (up to pH 9). The relatively large concentration of  $\text{Ba}^{2+}(\text{aq})$  in either virgin  $\text{BaTiO}_3$  or  $\text{BaCO}_3$ -passivated  $\text{BaTiO}_3$  aqueous suspensions also results in phase separation of many polymeric additives.<sup>(44)</sup> Specific interaction of  $\text{Ba}^{2+}(\text{aq})$  with functional groups such as  $-\text{OH}$  and  $-\text{COO}^-$  in many aqueous polymers used as dispersants or binders results in a less soluble  $\text{Ba}^{2+}$  polymer complex which readily phase separates.<sup>(44)</sup> Thus, the challenge in dispersing the oxalate-passivated  $\text{BaTiO}_3$  in aqueous suspensions is to select an organic dispersant which strongly adsorbs onto the oxalate-treated  $\text{BaTiO}_3$  surface without significant interaction with dissolved  $\text{Ba}^{2+}(\text{aq})$  or  $\text{C}_2\text{O}_4^{2-}(\text{aq})$ .

In the present study, various polymers (cationic, neutral, and anionic) were added to oxalate-treated  $\text{BaTiO}_3$  suspensions to evaluate colloidal stability as a function of polymer characteristics. Polymer dispersants are typically intermediate molecular weight (5,000 to 75,000 molecular weight) organic molecules that may be positive, neutral, or negatively charged depending on the nature of side or backbone functional groups.<sup>(116-119)</sup> Polymeric additives can disperse particles by either of the mechanisms shown in Figure 4.3.<sup>(38)</sup> For depletion dispersion shown in Figure 4.3 (a), the polymer remains in solution and reduces the interaction energy with which similarly-charged particles collide. In the depletion dispersion scenario the polymer is either neutral or exhibits a similar polarity to the surface potential of the particles. The other mechanism shown in Figure 4.3 (b) involves the

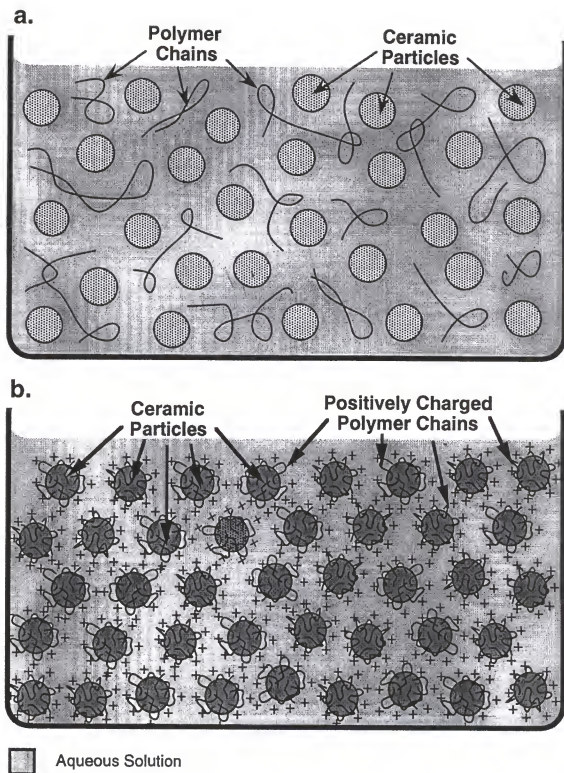


Figure 4.3. Schematic showing two different polymeric dispersing mechanisms for suspensions, (a) depletion dispersion where the polymer remains in solution and prevents particle collisions and (b) adhesion of the cationic polyelectrolyte to the particle surface preventing particle-particle contact by both polymeric and electrostatic repulsion.<sup>(38)</sup>

adsorption of the polymer to the particle surface to inhibit particle-particle collisions via electrostatic repulsion, steric hindrance, or a combination of these repulsive mechanisms. The attachment of the polymer molecules to the particle surface can occur by covalent bonding between species in the particle surface and the macromolecule, by electrostatic adsorption of the polymer to the particle surface, or by a combination of covalent and ionic interactions.

The objective of the current work was to disperse the oxalate-treated  $\text{BaTiO}_3$  particles. The oxalate-treated  $\text{BaTiO}_3$  system with various polymeric dispersants will be investigated to determine the optimum combination of oxalic acid and polymeric dispersant for suspension stability and favorable rheological properties for tape casting.

#### 4.2. Approach

The following experiments were designed and conducted to determine the colloidal stability of the as-received  $\text{BaTiO}_3$  particles, the oxalate-treated  $\text{BaTiO}_3$  particles, and the oxalate-treated  $\text{BaTiO}_3$  particles with various polymeric additives (cationic, anionic, and neutral polymers). Low solids loading solution chemistry analysis, sedimentation, and electrophoretic behavior were used in preliminary studies to screen and eliminate dispersants that increased the concentration of  $\text{Ba}^{2+}(\text{aq})$  concentration, increased the sedimentation rate, or reduced the zeta potential when added to the oxalate-treated  $\text{BaTiO}_3$  suspensions. Dispersants that did not increase the  $\text{Ba}^{2+}(\text{aq})$ , compromise the stability, or reduce the zeta potential were characterized at higher solids loading where stability is more apparent due to the increased number of inter-particle collisions. Higher solids loading slurries, similar to industrial tape casting formulations, were investigated by analysis of the rheological behavior (apparent viscosity and Bingham yield point) of each slurry, by visual assessment of hand cast, “pseudo” tapes for agglomerates, and scanning electron microscopy of the particle packing within the green, pseudo-tapes. The particle packing within the pseudo-tape corresponds to the dispersion of the oxalate-treated  $\text{BaTiO}_3$  suspension with polymeric dispersants present.

### 4.3. Materials and Methods

All glassware and plasticware were washed with a biodegradable detergent<sup>1</sup>, rinsed thoroughly with tap water to remove residual soap, and subsequently rinsed several times with copious quantities of deionized water<sup>2</sup> before use. To avoid contamination by soluble silica species, glassware was used only when the solution/suspension pH of the contents was less than pH 8.5. Unless otherwise noted, the deionized water used throughout the current work was boiled for approximately ten minutes while purged with nitrogen to minimize dissolved atmospheric gases, particularly CO<sub>2</sub>, in solution. Degassed water was stored in glass bottles with rubber-lined caps under a nitrogen atmosphere. All constituents were weighed to four decimal places using an analytical balance<sup>3</sup>. The hydrothermally derived BaTiO<sub>3</sub><sup>4</sup> was supplied by Cabot Performance Materials (Boyertown, PA). Bulk analysis of the BaTiO<sub>3</sub> powder showed concentrations of C, Sr, Fe, and Cl ranging from 500-1000 ppm, 400-800 ppm, 50-200 ppm, and 100-300 ppm, respectively. Other bulk contaminants included Al, Si, Cr, Ca, and Ni which were all less than 5 ppm. Pure BOM was precipitated from equal volumes of 1M BaCl<sub>2</sub>·2H<sub>2</sub>O and 1M K<sub>2</sub>C<sub>2</sub>O<sub>4</sub>·H<sub>2</sub>O solutions, washed twice with deionized H<sub>2</sub>O using 0.22 µm nylon filters<sup>5</sup> to collect filtrate, and dried at ~110°C for sixteen hours. X-ray diffraction was used to confirm the BOM crystal structure. All other chemicals used throughout this study were reagent grade and were used without further purification.

#### 4.3.1. Preparation of Low Solids Loading Barium Titanate Suspensions

BOM suspensions containing various polymers (none - control; 1,3 propanediol; polyvinyl alcohol - PVA; polymethacrylic acid - PMA; ammonium methyl methacrylate -

---

<sup>1</sup>Sparkleen, Calgon Vestal Laboratories, St. Louis, MS.

<sup>2</sup>Deionized water, specific resistivity >10 Megaohms cm.

<sup>3</sup>Fisher Scientific, model A-250, 0.0001 g readability.

<sup>4</sup>Cabot BT-10 BaTiO<sub>3</sub> powder, Cabot Performance Materials, Boyertown, PA.

<sup>5</sup>Micron Separation Inc., 135 Flanders Rd., Westboro, MA 01581.

AmPMMA) were prepared in a 10:1 (BOM:polymer) weight ratio. The pH of the BOM/polymer suspensions was adjusted with 0.1M or 0.2M  $\text{HNO}_3$  and 0.1M or 0.2M KOH to values ranging between pH 2 and pH 11, allowed to equilibrate for 48 hours, and filtered with 0.22  $\mu\text{m}$  filter paper. Supernatants were acidified with nitric acid to prevent the formation of  $\text{BaCO}_3(\text{s})$  by reaction with atmospheric  $\text{CO}_2(\text{g})$ , before assaying for dissolved barium via inductively coupled argon plasma (ICP) spectroscopy.

Preliminary colloidal stability was assessed by adding various amounts of AmPMMA, PEO, and PEI to oxalate treated  $\text{BaTiO}_3$  suspensions. The results warranted that PEI be investigated further. Stock solutions of oxalic acid<sup>6</sup> in concentrations of  $10^{-2}\text{M}$ ,  $10^{-3}\text{M}$ ,  $10^{-4}\text{M}$ , and 0M (deionized water as a control) were prepared using volumetric glassware and deionized water. Sedimentation samples were prepared at 3%  $\text{BaTiO}_3$  (~3.40 g) in 19 ml polypropylene, screw-cap test tubes to evaluate PEI more quantitatively as a dispersant. The appropriate amount of  $\text{BaTiO}_3$  was weighed and placed into a small Nalgene (~50 ml) container with 15 ml of either 0M,  $10^{-2}\text{M}$ ,  $10^{-3}\text{M}$ , or  $10^{-4}\text{M}$  oxalic acid solution and the desired amount of PEI (concentrations from 0 to 5% of the powder). The pH was measured and adjusted to the desired pH value (pH values ranging between pH 3 and pH 11) using 0.01M  $\text{HNO}_3$ <sup>7</sup> and 0.01M tetraethylammonium hydroxide (TEAOH)<sup>8</sup>. The samples were allowed to equilibrate for 15 minutes and the pH was readjusted if necessary. The suspensions were then transferred to the polypropylene test tubes carefully filling the test tubes to the top so that a minimal amount of air was present to reduce the extent of exposure to atmospheric  $\text{CO}_2$ . All suspensions were prepared at a particular pH, oxalate and PEI concentration, and dispersed using an ultrasonic bath followed by mechanical agitation. The samples were then allowed to settle under gravity. Sedimentation heights were recorded at 30 seconds, 1 minute, 5 minutes, 30 minutes, 1 hour, 24 hours, and one week for each sample.

---

<sup>6</sup>Oxalic acid - Fisher Scientific, lot # 905504.

<sup>7</sup> $\text{HNO}_3$  - Fisher Scientific, 70 weight % solution in water, lot# 905811.

BaTiO<sub>3</sub> suspensions (1%<sup>o</sup>) with various concentrations of oxalic acid (10<sup>-2</sup>M, 10<sup>-3</sup>M, 10<sup>-4</sup>M, and 0M) and polyethyleneimine<sup>9</sup> (0, 0.5, 1.0, and 2.0%<sup>o</sup> of the solid BaTiO<sub>3</sub> powder) at various pH<sup>10</sup> values (adjusted using 0.01M and 0.1M TEAOH and HNO<sub>3</sub>) were prepared and allowed to equilibrate for 24 hours. The suspension pH was readjusted after the 24 hour equilibration period if drift in the initial pH was detected. Initial suspensions that were too high in solids loading to permit optical analysis were diluted by sedimentation and redispersion of a smaller quantity of solid in the decanted supernatant to facilitate electrophoretic measurements. Remaining suspensions were stored in Nalgene<sup>11</sup> containers under an argon atmosphere and archived in a frozen state to minimize changes in suspension characteristics over time.

#### 4.3.2. High Solids Loading Barium Titanate Slurries

##### 4.3.2.1 Preparation of Barium Titanate Slurries

Slurries of similar concentrations of BaTiO<sub>3</sub> powder in various concentrations of oxalic acid and PEI were prepared to determine potential formulations as well as an optimum passivation/dispersion dosage. The compositions and visual characterization of the slurries are given in Appendix A, Tables A1 through A5. All initial slurries were prepared according to Figure 4.4 (a). The addition of oxalic acid powder to the deionized water before the addition of BaTiO<sub>3</sub> powder was found to be a critical processing step in controlling the charge of the particles and minimizing the dissolution of Ba<sup>2+</sup> from the surface of the particles. Adding the BaTiO<sub>3</sub> powder directly to deionized water before adding the oxalic acid dihydrate powder, the passivating agent, provided no improvement in the colloidal properties or rheological behavior compared with slurries made with no passivating agent present. Therefore, the desired amounts of oxalic acid dihydrate powder and deionized water were weighed using an analytical balance and placed into a high speed,

---

<sup>8</sup>TEAOH - Aldrich, 35 weight % solution in water, lot# 05498HZ.

<sup>9</sup>Polyethyleneimine (50% in water), Kodak, lot A16B.

<sup>10</sup>pH meter - The London Co. - PHM 64 research pH meter - Cleveland OH.

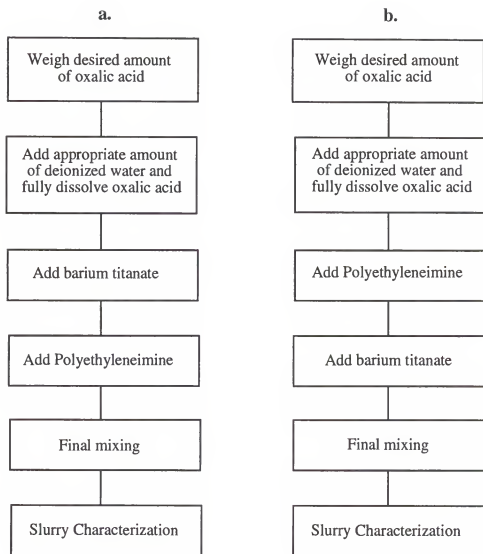


Figure 4.4. (a) Flow diagram for preparing slurries using a stainless steel mixer or polished zirconia mixing media. (b) Revised mixing order use to passivate and disperse the  $\text{BaTiO}_3$  particles simultaneously.

<sup>11</sup>Nalgene Company, subsidiary of Sybron Corporation, Rochester, NY.

stainless steel blender<sup>12</sup>. The oxalic acid was completely dissolved before slowly adding the appropriate amount of BaTiO<sub>3</sub> powder to the stainless steel vessel while continuously mixing at low speed. The appropriate amount of PEI was then added to the vessel containing the oxalate treated BaTiO<sub>3</sub> powder. The constituents of initial slurries were mixed at high speed (~5,000rpm) using the stainless steel blender after each reagent was added. However, it was found that the blender did not provide sufficiently high shear mixing, hence subsequent slurry mixing was performed with polished zirconia<sup>13</sup> mixing media and a vortex mixer. The slurries were characterized as described in the following section (4.3.2.2) and stored in sealed Nalgene containers under a nitrogen atmosphere to minimize atmospheric reactions.

An additional modification to the procedure was the addition of PEI to the oxalic acid solution as shown in Figure 4.4(b). Upon mixing, the passivation agent and dispersion agent crosslinked, forming a metastable gel-like structure. However when BaTiO<sub>3</sub> was added to the passivation/dispersion gel-like structure and a small shear force was applied (mixing with a spatula), a low viscosity slurry was formed similar to when the BaTiO<sub>3</sub> powder was added to the oxalic acid solution followed by the addition of PEI. One possible advantage to mixing the passivation and dispersion agents prior to adding the BaTiO<sub>3</sub> powder is the simultaneous passivation and dispersion of the powder. This processing modification should minimize agglomerate formation by reducing the amount of time in which the oxalate-treated particles can collide and adhere to similar oxalate-treated particles.

---

<sup>12</sup>Waring commercial 7 speed blender, model 7012 with mini-container MC-2, New Hartford, CT.

<sup>13</sup>Highly polished zirconia mixing media.

#### 4.3.2.2 Characterization of the Barium Titanate Slurries

Characterization of the high solids loading samples is essential for interpreting the optimum dosage of oxalic acid and PEI. Small samples were extracted from each slurry for pH measurement, visual inspection, and particle packing. The slurry pH was determined using color-calibrated litmus paper<sup>14</sup>. The second sample was smeared onto a glass microscope slide using a razor blade to create a "pseudo"-tape that could be visually examined for gross defects (agglomerates), topography, and uniformity of the film. Scanning electron microscopy<sup>15</sup> (SEM) was used to examine particle packing within the pseudo tapes. Samples were prepared for SEM by spreading the third small extracted amount of slurry on an aluminum SEM mount and allowing the slurry to air-dry before sputter coating with Au-Pd<sup>16</sup>. Pseudo tapes were examined at 50 kX, 25 kX, 10 kX, and 1 kX.

Initial viscosity measurements were performed on all slurries at 25°C using a cone-plate viscometer<sup>17</sup> at shear rates ranging from  $0.6 \text{ sec}^{-1}$  to  $120 \text{ sec}^{-1}$ . Subsequent measurements were also made using a cone-plate viscometer<sup>18</sup> at 25°C, but with shear rates ranging from  $0.1 \text{ sec}^{-1}$  to  $150 \text{ sec}^{-1}$ . Both the shear stress and the viscosity were determined as a function of shear rate for all samples where the viscosity could be experimentally ascertained. Initially, viscosities were reported at  $24 \text{ sec}^{-1}$  for samples and used as a relative measure of rheological suitability for the suspension in tape casting. Subsequent investigations report the apparent viscosity at shear rates where the viscosity reaches a plateau. However, the viscosity of some samples was larger than the limit of the instrument at  $24 \text{ sec}^{-1}$  (early investigations) and did not achieve a plateau over the range of shear rates investigated (subsequent investigations), and are reported as NA.

---

<sup>14</sup>pHydrion paper, Micro Essential Laboratory, Brooklyn, NY.

<sup>15</sup>JEOL JSM 6400 scanning electron microscope, JEOL, Boston, MA.

<sup>16</sup>Au-Pd sputter, Hummer I, Technics Inc., Alexandria, VA.

<sup>17</sup>Brookfield Viscometer, model #, Brookfield Engineering Laboratory, Inc., Stoughton MA.

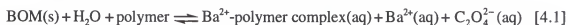
## 4.4. Results and Discussion

### 4.4.1 Preliminary Studies at Low Solids Loading

#### 4.4.1.1 Solution Chemistry

Solution chemistry analysis of the supernatant from aqueous BOM suspensions containing various polymers was performed to determine whether the different polymers increase the dissolved  $\text{Ba}^{2+}$  concentration. Chemical analyses for  $\text{Ba}^{2+}(\text{aq})$  via ICP spectroscopy of the supernatant solutions was used as a criteria for eliminating a potential polymer as additives when it increased the solubility of BOM. Figure 4.5 shows the solubility of BOM (theoretical as well as experimental) and BOM with AmPMMA, PVA, 1,3 propandiol, or PMA as a function of suspension pH. The addition of AmPMMA as well as other organic molecules including polyvinyl alcohol (PVA), 1,3 propandiol, or polymethacrylic acid (PMA) to separate BOM suspensions increases the solubility of BOM by as much as four orders of magnitude.<sup>(17,45,63,108)</sup>

The increase in BOM solubility is due to the formation of a soluble  $\text{Ba}^{2+}$ -polymer complex as depicted in Figure 4.6. The dissolution of BOM is increased by the addition of the polymeric additive according to the following reaction.<sup>(44,45)</sup>



The formation of the polymer complex species drives the reaction to the right based upon Le Chatelier's principle, thus increasing the amount of dissolved  $\text{Ba}^{2+}$  present in solution. The addition of these polymers, particularly AmPMMA, to the oxalate treated  $\text{BaTiO}_3$  suspensions would compromise the passivation of the oxalate treated  $\text{BaTiO}_3$  surface via dissolution of the passivation layer and expose the underlying stoichiometric particle core to aqueous conditions.<sup>(14,35,108)</sup> Thus, AmPMMA and the other polymers described above were eliminated as potential dispersants for the oxalate treated  $\text{BaTiO}_3$  system.

---

<sup>18</sup>Brookfield Viscometer, model # LVTDCP, Brookfield Engineering Laboratory, Inc., Stoughton MA.

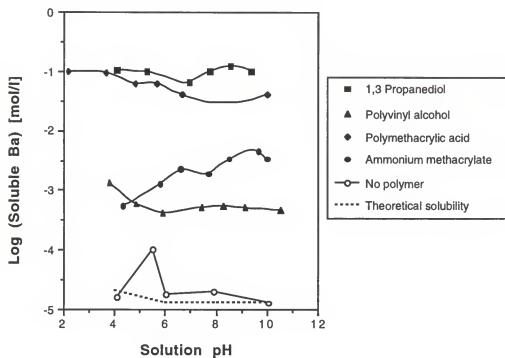


Figure 4.5. The solubility of  $\text{BaC}_2\text{O}_4 \cdot \text{H}_2\text{O}$  (theoretical as well as experimental) and  $\text{BaC}_2\text{O}_4 \cdot \text{H}_2\text{O}$  with various polymeric additives as a function of suspension pH.<sup>(17,45,63,108)</sup>

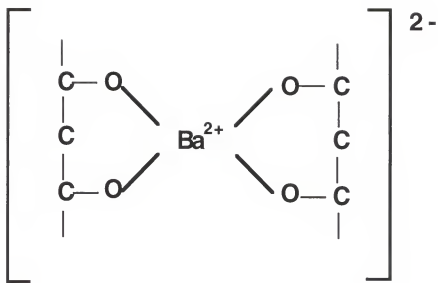


Figure 4.6. Schematic showing a possible interaction between aqueous species, specifically a PVA- $\text{Ba}^{2+}$  interaction.<sup>(44)</sup>

#### 4.4.1.2 Sedimentation Results

Sedimentation studies provide insight into the colloidal stability of suspensions. The addition of PEO to an oxalate treated  $\text{BaTiO}_3$  suspension increased the viscosity and promoted agglomeration of the particles. Due to the deleterious effects of AmpMMA on the solubility of BOM and of PEO on the colloidal stability of the oxalate-treated  $\text{BaTiO}_3$  particles, both of these polymeric additives were eliminated as possible dispersants. However the dispersion of the oxalate-treated  $\text{BaTiO}_3$  suspension with PEI present was promising and warranted a more thorough investigation to determine a range of working dosages as well as an optimum dosage.

Figure 4.7 (a) shows the sediment height for aqueous 3%  $\text{BaTiO}_3$  suspensions as a function of pH and time. Sediment heights are relatively constant after five minutes, demonstrating poor dispersion of the  $\text{BaTiO}_3$  particles under these solution conditions. Without oxalate present to passivate the surface of the  $\text{BaTiO}_3$  particles, the solution conditions favor the agglomeration of the  $\text{BaTiO}_3$  powder.<sup>(14,18,108)</sup> As the incongruent dissolution of the  $\text{BaTiO}_3$  surface occurs, the increased concentration of  $\text{Ba}^{2+}(\text{aq})$  drives the suspension pH toward alkaline conditions, approximately pH 9. Suspension pH 9 is near the isoelectric point of  $\text{BaTiO}_3$  suspensions at this concentration, where the  $\text{BaTiO}_3$  particles exhibit zero net surface charge. The sediment height is easily recorded due to the sharp contrast between the supernatant and the agglomerates. The sedimentation rate shown in Figure 4.7 (b) was calculated at the one hour time interval and is approximately 9 cm/hour. Based on the theoretical phase stability diagram by Utech et al. and others,<sup>(14,18,35,43)</sup> combined with the solution chemistry analysis and the HRTEM micrographs of the surface region discussed in previous work, it can be concluded that the stoichiometric  $\text{BaTiO}_3$  particle core is surrounded by an amorphous  $\text{TiO}_2$ -rich or  $\text{BaCO}_3$  layer depending on the ionic species present in solution and the suspension pH.<sup>(108)</sup> However, both the amorphous, Ba-depleted  $\text{TiO}_2$  surface region and the naturally

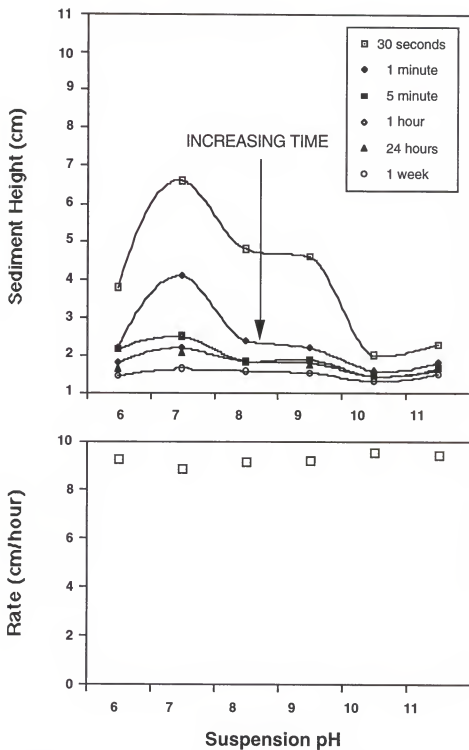


Figure 4.7. (a) Sedimentation results for 3% BaTiO<sub>3</sub> powder as a function of suspension pH and time. (b) Sedimentation rate for the same suspensions calculated at the one hour time period.

occurring, pH sensitive  $\text{BaCO}_3$  surface layer exhibit insufficient charge for electrostatic stabilization.

The sedimentation results for  $\text{BaTiO}_3$  suspended in oxalic acid solution are presented in Figure 4.8 (a) and 4.8 (b). The addition of oxalate ions resulted in no improvement in the suspension stability, as evidenced by the sedimentation rate. In fact, both the suspensions, without and with oxalic acid present, exhibit similar, relatively constant sediment heights after five minutes. In addition, the sedimentation rates for both the as-received  $\text{BaTiO}_3/\text{H}_2\text{O}$  and the oxalate-treated  $\text{BaTiO}_3$  suspensions are approximately 9 cm/hour. The large sedimentation rate is evidence of poor colloidal stability. However, the sediment height was more difficult to discern for the suspensions with oxalic acid present. Each sample containing oxalic acid had a transparent but cloudy region of finely dispersed  $\text{BaTiO}_3$  particles and a relatively opaque region containing agglomerates. The boundary between the transparent but cloudy region and the opaque region was recorded as the sediment height. Reed suggests this is a sign of improved dispersion.<sup>(120)</sup> The presence of the oxalic acid passivates the  $\text{BaTiO}_3$  particle surface and provides a uniform, negative surface charge, as demonstrated via solution chemistry analysis and electrophoretic behavior.<sup>(14)</sup> However, the relatively modest surface charge imparted by oxalate treatment does not provide adequate suspension stability.

Sedimentation plots for aqueous suspensions of 3%  $\text{BaTiO}_3$  with PEI (1% of the solid) but no oxalic acid are shown as a function of pH and time in Figure 4.9. In comparison to the  $\text{BaTiO}_3$  suspensions with oxalic acid present (Figure 4.8), the settling times of more than one week indicate that better dispersion is provided. However this colloidal stability is misleading. Without oxalic acid present, the incongruent dissolution of the  $\text{BaTiO}_3$  particle surface still exists.<sup>(108)</sup> The incongruent dissolution provides excess  $\text{Ba}^{2+}$  ions in solution which can cross-link other polymers added to the slurry (i.e., binder, defoaming agents, or wetting agents) or compromise the ultimate sintered ceramic.<sup>(18,44)</sup> Also, the increase in settling time for the suspensions with only PEI present could be due to

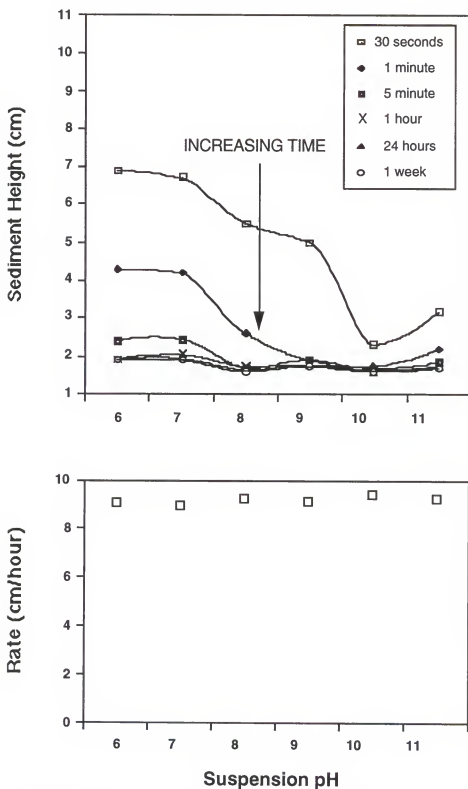


Figure 4.8. (a) Sedimentation results for 3% BaTiO<sub>3</sub> and 5% oxalic acid (w/o of the solids) suspensions as a function of pH and time. (b) Sedimentation rate for the same suspension calculated for the one hour time period.

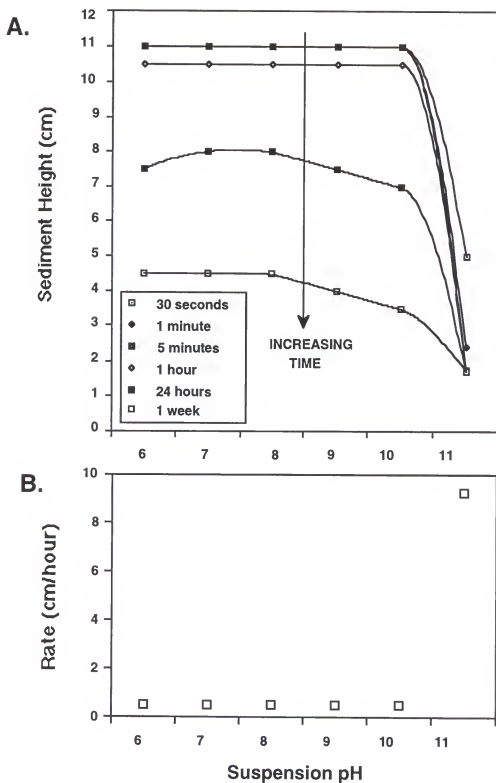


Figure 4.9. (a) Sedimentation results for 3% BaTiO<sub>3</sub> and 1% PEI (% of the solids) suspensions as a function of pH and time. (b) Sedimentation rate for the same suspensions calculated at the one hour time period.

an increase in the viscosity of the suspensions due the addition of the macromolecule, stability induced by electrostatic repulsion between similarly charged bodies (i.e. the positively charged  $\text{BaTiO}_3$  and the positively charged PEI macromolecule), electrostatic effects from the side-walls of the test tubes, or a combination of these two effects. In any case, the stability provided is not adequate for a tape casting formulation that would sit longer than one hour prior to use. More importantly, the incongruent dissolution of the  $\text{BaTiO}_3$  particle would not be addressed.

Figure 4.10 shows the sediment height for 3%  $\text{BaTiO}_3$  suspensions with 5% oxalic acid and 1% PEI present (where both oxalic acid and PEI are added as a weight percent of the  $\text{BaTiO}_3$ ) as a function of pH and time. The sediment height remained constant over one week, and several samples at these conditions remained well dispersed longer than one month. Suspensions made at similar conditions with lower amounts of PEI (<1%) exhibited a similar behavior to the oxalate-treated particles (Figure 4.8), where complete sedimentation occurred in approximately 5 minutes. With less than 1% PEI, there is insufficient PEI present to provide adequate dispersion. Increasing the PEI concentration from 1% to 2% PEI does not change the sedimentation results shown in Figure 4.10.

All sedimentation studies with PEI present, as shown in Figures 4.9 and 4.10, exhibit an instability in the aqueous  $\text{BaTiO}_3$  suspensions above pH 10. The basic dissociation constant for PEI is between pH 10 and pH 11.<sup>(116)</sup> Above the dissociation constant, PEI is no longer positively charged. Without the positive charge associated with the macromolecule, PEI disperses the oxalate-treated  $\text{BaTiO}_3$  in a manner similar to PEO where an increase in agglomeration was noted. Therefore, suspension pH is still critical in the aqueous processing of  $\text{BaTiO}_3$  in oxalic acid with PEI present. However the working pH range is above pH 5, where oxalic acid is fully dissociated and present as  $\text{C}_2\text{O}_4^{2-}$ , and below pH 10, where PEI is positively charged. In any case, this is preferable to the

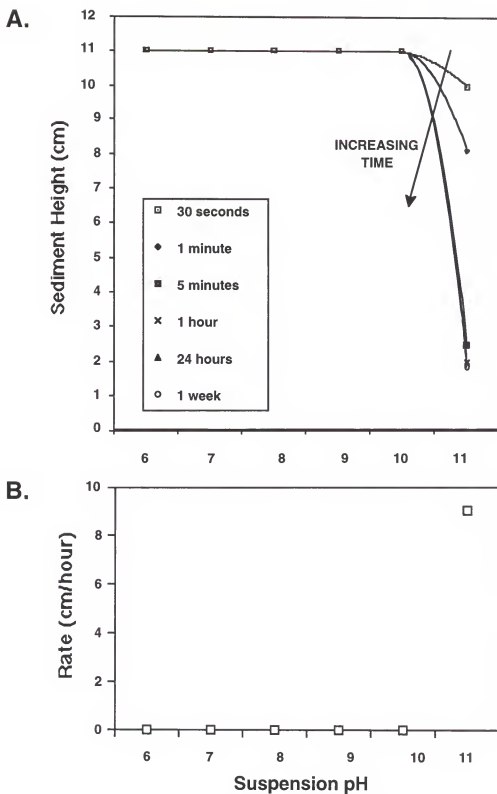


Figure 4.10. (a) Sedimentation results for 3% BaTiO<sub>3</sub>, 5% oxalic acid, and 1% PEI (% of BaTiO<sub>3</sub>) suspensions as a function of pH and time. (b) Sedimentation rate for the same suspensions calculated at the one hour time period.

aqueous processing of BaTiO<sub>3</sub> at pH 12 to 13, which is necessary to minimize the concentration of Ba<sup>2+</sup>(aq) in solution without the addition of oxalic acid.

#### 4.4.1.3 Electrophoretic Behavior

The objective of the electrophoretic behavior study was to corroborate and to provide quantitative analysis of the colloidal stability predicted by the sedimentation study. Electrophoretic analysis will aid in determination of the mechanism by which PEI disperses the oxalate-treated BaTiO<sub>3</sub> particles. Previous studies involved the electrophoretic behavior of BaTiO<sub>3</sub>, BOM, and BaTiO<sub>3</sub> with varying concentrations of oxalic acid.<sup>(108)</sup> The presence of the oxalic acid provides a uniform, negative charge on the surface of the BaTiO<sub>3</sub> particles with the magnitude of the charge dependent upon the oxalate ion concentration.

The electrophoretic behavior of BaTiO<sub>3</sub> powder in oxalic acid solution (5% of the solids) is presented in Figure 4.11. In contrast to the electrophoretic behavior of the oxalate-treated BaTiO<sub>3</sub> suspension are the electrophoretic behavior of similar suspensions with various PEI concentrations. Low concentrations of PEI (0.5%) cause the charge on the particle surface to be more positive at intermediate to alkaline pH (pH > 5.5). However under more acidic conditions (pH < 5), where the oxalate ion may be present as HC<sub>2</sub>O<sub>4</sub><sup>-</sup>, the PEI does not readily affect the surface potential. This phenomenon is not observed for the 1% and 2% PEI suspensions. When PEI is added to the oxalate-treated BaTiO<sub>3</sub> suspension, the pH increases, fully dissociating the oxalic acid and allows the surface passivation reaction to proceed to completion.<sup>(108)</sup> Adding HNO<sub>3</sub> to adjust the pH to more acidic conditions does not seem to affect the BOM passivation layer. As the oxalic acid reacts with the dissolving Ba<sup>2+</sup> from the BaTiO<sub>3</sub> particle surface and the surface becomes more negative, the PEI electrostatically adsorbs onto the Ba-oxalate surface providing a positive zeta potential. From the electrophoretic results, the PEI concentration and suspension pH are critical for providing a large positive surface charge and sufficient dispersion. Corresponding sedimentation studies corroborate the increased stability as a function of increasing PEI concentration and the poor dispersion for samples containing

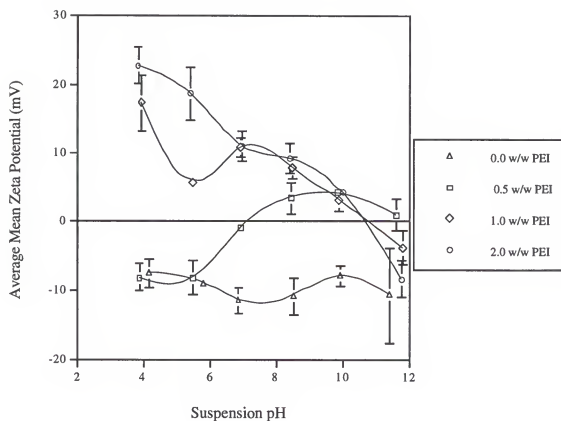


Figure 4.11. Electrophoretic behavior for 3% hydrothermally derived  $\text{BaTiO}_3$  (Cabot Corporation) suspensions with 5% oxalic acid as a function of PEI and suspension pH.

PEI above suspension pH 10 where PEI is no longer positively charged.

The passivated, oxalate-treated  $\text{BaTiO}_3$  particle carries a negatively charged surface whereby the positively charged PEI molecule can electrostatically adsorb, altering the magnitude and polarity of the zeta potential. The sedimentation results, along with the electrophoretic analysis, strongly suggest that steric hindrance is involved in the stabilization of the suspension because over the pH range investigated, the surface charge associated with the oxalate-treated  $\text{BaTiO}_3$  suspensions without and with PEI present (1% or 2%) is very similar ( $\sim 10\text{ mV}$ , negatively and positively charged respectively) as shown in Figure 4.11. However, the settling times for the sedimentation samples at similar pH conditions to the corresponding electrophoretic samples are increased from approximately 5 minutes for suspensions without PEI present to more than one week when PEI is added.

Figure 4.12 shows the molecular structure of PEI and the hypothesized conformation as it adsorbs on the negatively charged, oxalate-treated  $\text{BaTiO}_3$  particle surface. This representation is based on the results of the sedimentation study and corresponding electrophoretic analysis. The PEI molecule (50,000 to 60,000 molecular weight) is a highly branched structure consisting of 25% primary amino groups, 50% secondary amino groups and 25% tertiary amino groups. The highly branched structure of the macromolecule spreads out over the entire particle surface and lies relatively flat with the positively charged functional groups electrostatically adsorbed on the negatively charged oxalate-treated  $\text{BaTiO}_3$  surface. This provides a combination of electrostatic and steric dispersion of the oxalate-treated  $\text{BaTiO}_3$  particles.

#### 4.4.2. High solids loading Barium Titanate Slurries

Dispersing low concentrations of  $\text{BaTiO}_3$  (3%) is relatively easy in comparison to dispersing concentrations similar to tape casting formulations (20% to 30%). The increase in  $\text{BaTiO}_3$  concentration provides more opportunity for particle-particle collisions which leads to the formation of agglomerates. Slurries were prepared at higher concentrations of  $\text{BaTiO}_3$ , similar to industrial tape casting formulations, to evaluate the effectiveness of the

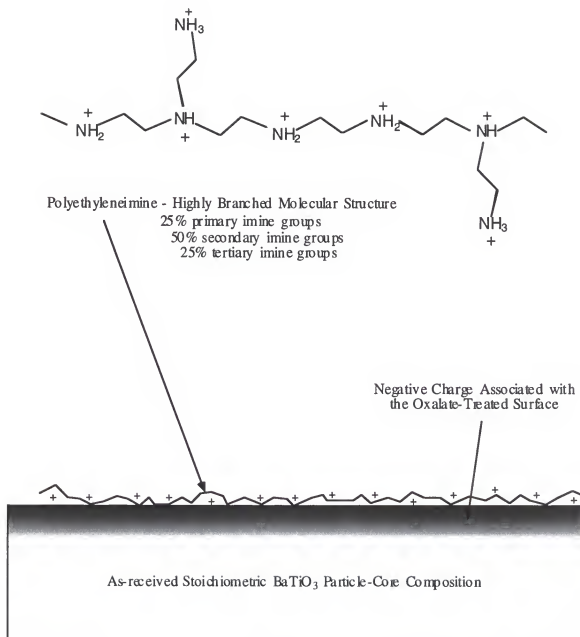


Figure 4.12. Schematic of the PEI molecular structure and its conformation on the negatively charged oxalate-treated  $\text{BaTiO}_3$  surface.<sup>(116)</sup>

oxalate/PEI treatment as well as to determine an optimum oxalate/PEI dosage.

The amount of each constituent, its weight and volume percent in each slurry, and visual characterization of pseudo-tapes cast on a glass microscope slides for several slurries is detailed in Tables A1 through A5 in Appendix A. Oxalic acid concentrations of 0.5, 1, 2, 3, and 5% (weight percent of  $\text{BaTiO}_3$  present) correspond to Tables A1 through A5 respectively. Each table describes five slurries prepared with a similar concentration of oxalic acid and various amounts of PEI (from 0.5 to 5%). Slurry designation 3:1 corresponds to the dosage of passivating agent and dispersing agent (3% oxalic acid and 1% PEI). Rheological data (shear stress and viscosity as a function of shear rate) is plotted only for slurries with 2% oxalic acid and various amounts of PEI in Figure 4.13 to demonstrate how the apparent viscosity and Bingham yield point were ascertained. Data for each slurry was curve fit with a power function which allowed data points to be calculated at shear rates of  $50 \text{ sec}^{-1}$  and  $100 \text{ sec}^{-1}$ . A straight line was plotted through the two calculated viscosities and the apparent viscosity is reported as the y-axis intercept. The Bingham yield point is reported as the shear stress at the lowest shear rate measured. SEM photomicrographs of slurries presented in this section refer to good and rejected formulations on the basis of particle packing within the microstructure of the unfiltered, hand cast pseudo tape.

The data summarized in Table A1 show the effect of 0.5% oxalic acid and 0.5, 1, 2, 3, and 5% PEI (slurries 0.5:0.5, 0.5:1, 0.5:2, 0.5:3, and 0.5:5 respectively) on slurry properties. A summary of the rheological properties (viscosity and Bingham yield point), weight percent of the  $\text{BaTiO}_3$  powder, and passivation/dispersion dosages is presented in Figure 4.14. Rheological properties for slurries 0.5:0.5 and 0.5:1 could not be determined because the slurries exceeded the limitations of the cone-plate viscometer and are denoted as NA. The two formulations are rejected because the rheological properties were offscale and each exhibited a poor microstructure. Both slurries exhibited similar particle packing to the SEM micrographs of slurry 0.5:1 shown in Figure 4.15. These

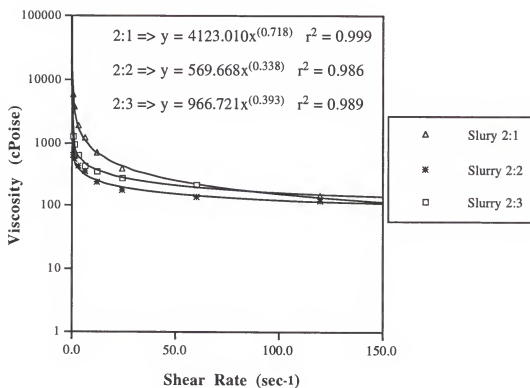
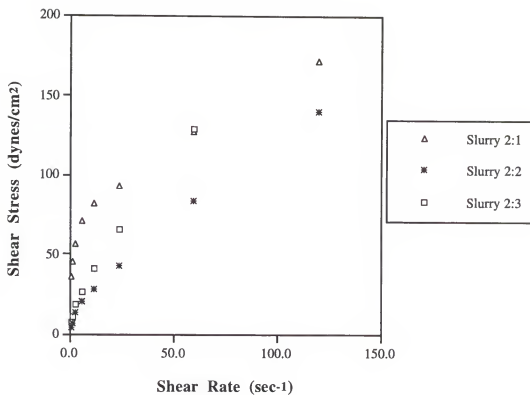


Figure 4.13. Rheological curves for a typical slurry to demonstrate how the viscosity and Bingham yield point were ascertained.

oxalate \ PEI	0.5	1.0	2.0	3.0	5.0
0.5	0.5:0.5 $\eta$ = NA BYP = NA wt.% = 68 OFFSCALE	0.5:1 $\eta$ = NA BYP = NA wt.% = 68 OFFSCALE	0.5:2 $\eta$ = 38.2 cP BYP = 1 wt.% = 65 GOOD	0.5:3 $\eta$ = 64 cP BYP = 1 wt.% = 65 GOOD	0.5:5 $\eta$ = 1225 cP BYP = 82 wt.% = 64 GOOD
1.0	1:0.5 $\eta$ = 308 cP BYP = 43 wt.% = 65	1:1 $\eta$ = 351 cP BYP = 23 wt.% = 68 GOOD	1:2 $\eta$ = 911 cP BYP = 57 wt.% = 67	1:3 $\eta$ = 505 cP BYP = 27 wt.% = 66 GOOD	1:5 $\eta$ = 604 cP BYP = 119 wt.% = 64 GOOD
2.0	2:0.5 $\eta$ = 281 cP BYP = 28 wt.% = 65 AGGLOM.	2:1 $\eta$ = 346 cP BYP = 36 wt.% = 67 GOOD	2:2 $\eta$ = 184 cP BYP = 4 wt.% = 66 GOOD	2:3 $\eta$ = 257 cP BYP = 7 wt.% = 66 GOOD	2:5 $\eta$ = 596 cP BYP = 25 wt.% = 64 GOOD
3.0	3:0.5 $\eta$ = NA BYP = NA wt.% = 65 OFFSCALE	3:1 $\eta$ = 72 cP BYP = 2 wt.% = 67 BEST	3:2 $\eta$ = 397 cP BYP = 17 wt.% = 66 GOOD	3:3 $\eta$ = 471 cP BYP = 17 wt.% = 65 GOOD	3:5 $\eta$ = 826 cP BYP = 33 wt.% = 63 CRACKS
5.0	5:0.5 $\eta$ = NA BYP = NA wt.% = 66 OFFSCALE	5:1 $\eta$ = 648 cP BYP = 225 wt.% = 65 AGGLOM.	5:2 $\eta$ = 15 cP BYP = 1 wt.% = 65 AGGLOM.	5:3 $\eta$ = 52 cP BYP = 1 wt.% = 65 CRACKS	5:5 $\eta$ = 144 cP BYP = 15 wt.% = 63 GOOD

 Rejected Formulations

Figure 4.14. A summary of the rheological properties (viscosity and Bingham yield point), weight percent of the BaTiO<sub>3</sub> powder (wt.%), and passivation/dispersion dosages for possible and rejected (shaded regions) formulations. Criteria for rejected formulations are viscosity ( $\eta$ ) off-scale, or agglomerates noted in the microstructure of hand-cast tapes. Viscosity and Bingham yield point are given in centiPoise and dynes/cm<sup>2</sup>, respectively.

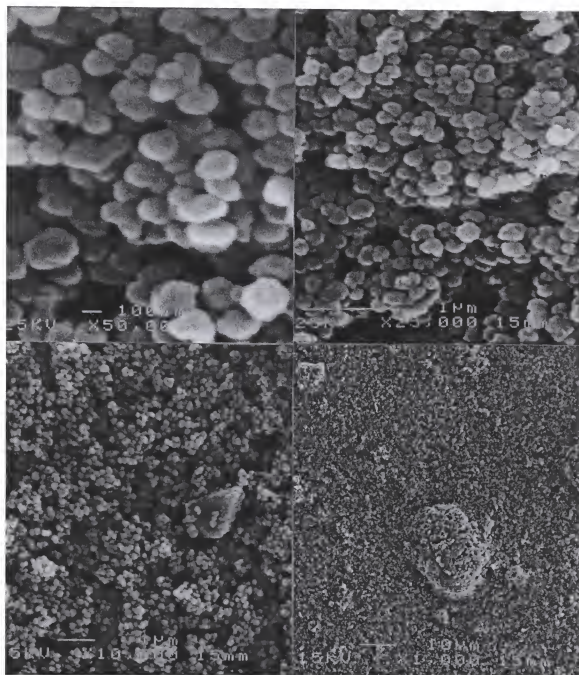


Figure 4.15. Scanning electron micrographs of a smeared sample from slurry 0.5:1 (68%  $\text{BaTiO}_3$ , 0.5% oxalic acid, and 1.0% PEI) at four different magnifications (50 kX, 25 kX, 10 kX, and 1 kX). Oxalic acid and PEI are added as weight percent of the  $\text{BaTiO}_3$ .

features resemble the particle packing of more conventional tape casting formulations as shown in Figure 4.16. The other three slurries at this oxalic acid concentration all exhibited rheological properties (shear thinning) similar to those shown in Figure 4.17 with variations in the viscosity and the shear stress at a minimal shear rate (Bingham yield point). Slurries 0.5:2, 0.5:3, and 0.5:5 exhibited a favorable microstructure (particle packing) similar to the scanning electron micrographs of slurry 2:1 shown in Figure 4.18. However the PEI concentration in slurry 0.5:5 is approaching the alkaline limit (pH 10) where PEI is no longer positively charged and has been found to be ineffective as a dispersant.

The data summarized in Table A2 shows the effect of 1% oxalic acid and 0.5, 1, 2, 3, and 5% PEI (slurries 1:0.5, 1:1, 1:2, 1:3, and 1:5, respectively) on slurry properties. A summary of the rheological properties, viscosity and Bingham yield point, weight percent of the BaTiO<sub>3</sub> powder and passivation/dispersion dosages is presented in Figure 4.14. All five slurries at this oxalate concentration exhibit rheological properties (shear thinning similar to those present in Figure 4.13) in the detection range of the cone-plate viscometer. Slurry 1:0.5 and 1:1 had the lowest viscosity of these five slurries; however, all five slurries exhibit good particle packing similar to Figure 4.18 and are designated as acceptable slurry formulations.

Increasing the oxalic acid concentration to 2% of the solids present (slurries presented in Table 4.3), caused the viscosities of the slurries with corresponding PEI concentrations (Table A2) to decrease. Slurry 2:2 provided the lowest viscosity of an acceptable slurry formulation for the 2% oxalic acid concentration, followed by 2:3, 2:1, and 2:5 (Figure 4.13). A minimum in viscosity is established for intermediate concentrations of PEI at the 2% oxalate concentration. Therefore at a 2% oxalic acid concentration, 1% PEI is not sufficient to establish suspension stabilization. However, excess PEI (2:5) causes the suspension pH to increase near the value where PEI is no longer positively charged and subsequently an increase in the viscosity occurs.

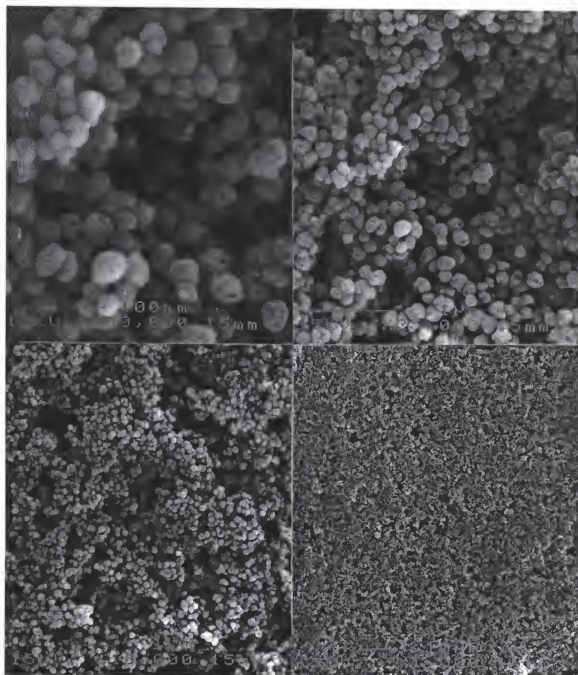


Figure 4.16. Scanning electron micrographs of a smeared sample from an aqueous  $\text{BaTiO}_3$  (Cabot hydrothermally derived powder) slurry prepared with a conventional tape casting formulation at four different magnifications (50 kX, 25 kX, 10 kX, and 1 kX).

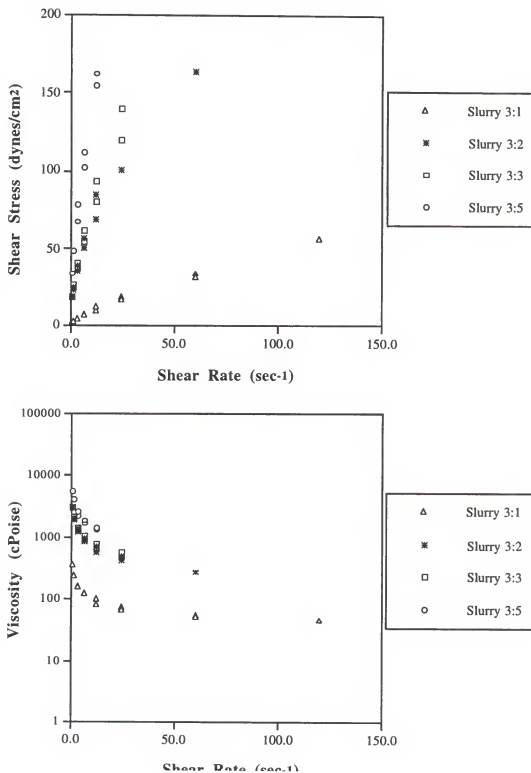


Figure 4.17. Rheological behavior (viscosity and shear stress vs. shear rate) for slurries with ~65%  $\text{BaTiO}_3$ , 3% oxalic acid and 1%, 2%, 3%, and 5% PEI (slurry 3:1, 3:2, 3:3, and 3:5 respectively) where oxalic acid and PEI are added as weight percent of  $\text{BaTiO}_3$ .

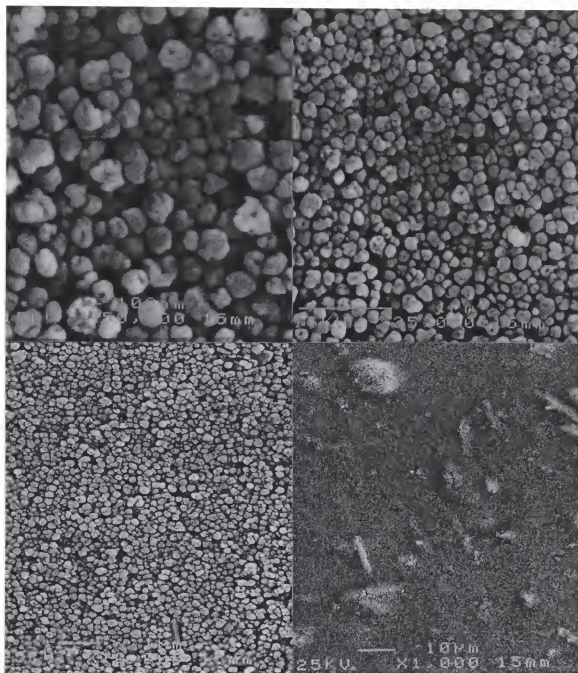


Figure 4.18. Scanning electron micrographs of a smeared sample from slurry 2:1 (67%  $\text{BaTiO}_3$ , 2.0% oxalic acid, and 1.0% PEI) at four different magnifications (50kX, 25kX, 10kX, and 1kX). Oxalic acid and PEI are added as weight percent of the  $\text{BaTiO}_3$ .

The amounts and constituents for each of the various 3% oxalic acid slurries are summarized in Table A4. Figure 4.17 shows a direct relationship between the amount of PEI present and the viscosity. As the PEI concentration is increased the viscosity increases. Four of the five slurries (3:1, 3:2, 3:3, and 3:5) are shear thinning, while the viscosity of slurry 3:0.5 was outside the rheological limitation of the cone-plate viscometer. The lowest viscosity of all slurries is exhibited by slurry 3:1 (3% oxalic acid and 1% PEI), with a viscosity equal to 72 cP and a Bingham yield point of 1.8 dynes/cm<sup>2</sup>. Slurry 3:1 is designated as the "best" slurry based upon the rheological properties and the corresponding particle packing as shown in Figure 4.19. The 3:1% passivation:dispersion agent ratio was found to be the optimum dosage to minimize the amount of Ba<sup>2+</sup>(aq) present and to provide adequate dispersion for future research on tape casting formulations where binders are present.

A concentration limit for oxalic acid is approached when the oxalic acid concentration is increased to 5.0% of the solids present (slurries presented in Table A5). Slurries under 5.0% PEI display agglomerated microstructures, with several micrographs displaying undissolved oxalate crystals present. These formulations were rejected. Only slurry 5:5 (5.0% oxalic acid and 5.0% PEI) provides a favorable viscosity and an acceptable microstructure.

#### 4.5. Conclusions

The problems associated with the aqueous processing of BaTiO<sub>3</sub> (incongruent dissolution of Ba<sup>2+</sup> from the BaTiO<sub>3</sub> particle surface) for multilayer capacitors and a solution which includes passivation and dispersion are summarized in Figure 3.20(a) and 3.20(b) respectively with its validity confirmed by the experimental results. The passivation of the surface and dispersion of the oxalate-treated BaTiO<sub>3</sub> particles will improve the quality of BaTiO<sub>3</sub> ceramic tapes used in the aqueous production of multilayer capacitors. The oxalate treatment to the BaTiO<sub>3</sub> particles creates a negatively charged

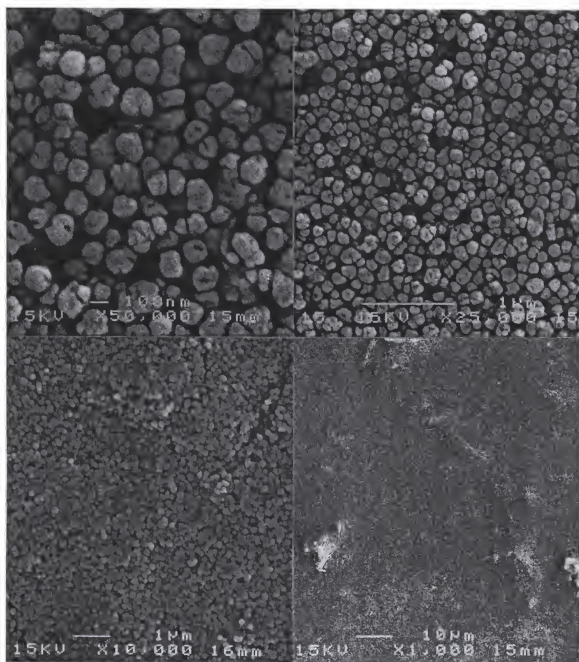
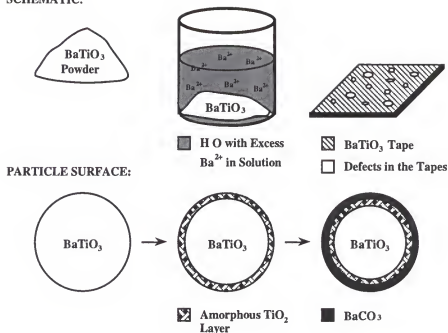


Figure 4.19. Scanning electron micrographs of a smeared sample from slurry 3:1 (67% BaTiO<sub>3</sub>, 3.0% oxalic acid, and 1.0% PEI) at four different magnifications (50kX, 25kX, 10kX, and 1kX). Oxalic acid and PEI are added as weight percent of the BaTiO<sub>3</sub>.

## a. SCHEMATIC:



## b. SCHEMATIC:

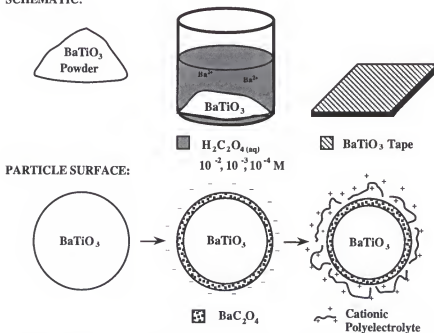


Figure 4.20. (a) Schematic showing the incongruent dissolution of  $\text{Ba}^{2+}$  and the formation of the Ti-rich and Ba-rich layers which circumvent the stoichiometric  $\text{BaTiO}_3$  core. (b) Schematic showing the passivation treatment for minimizing the dissolution of barium from the particle surface and dispersion of the oxalate treated particles with a cationic polyelectrolyte. <sup>(14,35,108)</sup>

surface and the best dispersant for the treated particles is a cationic polyelectrolyte, polyethyleneimine.

Electrophoretic behavior of the aqueous oxalate-treated  $\text{BaTiO}_3$  suspensions with PEI demonstrates that the amount of PEI added is critical for providing a positive charge at the particle surface. Low concentrations of PEI (0.5%) do not provide relatively constant positive charge over the entire pH range (pH 4 to approximately pH 10). In fact at low pH the surface charge is negative and becomes positive as the solution becomes more alkaline. Whereas, when either 1% or 2% PEI is added to the oxalate-treated  $\text{BaTiO}_3$  suspension, a positive surface charge is produced from suspension pH 4 to approximately pH 10 with the magnitude of the charge decreasing as the pH becomes more alkaline. At approximately pH 10, PEI is no longer positively charged. In dispersing the oxalate-treated  $\text{BaTiO}_3$  particles, it is critical to provide sufficient PEI for uniform coverage and to maintain the suspension below pH 10, where PEI is positively charged. Sedimentation results corroborate these findings. Several passivation: dispersion dosages are presented as possible slurry formulations; however slurry 3:1 (3.0% oxalic acid, 1.0% PEI) is designated as the best formulation based upon the favorable rheological properties and microstructure (particle packing) of the green "pseudo" tape.

It has been demonstrated that PEI is an effective dispersant for the oxalate-treated  $\text{BaTiO}_3$  particles. The results presented in this chapter strongly suggest that steric hindrance, in combination with electrostatic forces, is responsible for the colloidal stability of the oxalic acid/PEI/ $\text{BaTiO}_3$  suspension. However further work is required to confirm the dispersion mechanism.

## CHAPTER 5

### BINDER FORMULATIONS FOR THE OXALATE/POLYETHYLENE IMINE-TREATED BaTiO<sub>3</sub> SUSPENSIONS FOR MULTILAYER CAPACITORS

#### 5.1. Introduction

Organic binders are essential additives for processing many commercial ceramics, especially the production of ceramic tapes used in the fabrication of multilayer composites.<sup>(8,10)</sup> Ceramic slurries incorporate organic binders that are dissolved and dispersed in the solution phase (aqueous or nonaqueous) to provide flexibility and mechanical integrity to the dried green structure.<sup>(30,33)</sup> From a hypothetical, ideal prospectus, the binder would be homogeneously dispersed in the liquid phase without electrostatic or chemical interactions with the ceramic particles or the other polymeric additives. In addition, as the cast tapes dry, the binder would remain evenly distributed throughout the structure providing organic bridges and filling the interstices between the ceramic particles. Lastly, the binder should be completely removed prior to sintering as non-volatile gaseous product through the open porosity.<sup>(5)</sup>

An increase in regulations concerning the use of hazardous materials has forced the MLC industry to produce capacitors via a more environmentally benign process. To replace the nonaqueous production of MLCs with an aqueous scheme is an effective method to circumvent the hazardous materials restrictions. However, BaTiO<sub>3</sub> is unstable in water.<sup>(14,15,19,41,47,48)</sup> The incongruent dissolution of the BaTiO<sub>3</sub> particle surface introduces excessive amounts of Ba<sup>2+</sup>(aq) into the solution (more pronounced for finer particles) which affects the surface stoichiometry of the particle, the electrostatic dispersion, and the microstructure of the sintered ceramic layers.<sup>(14,35,68)</sup> Consequently, polymeric additions can associate with the Ba<sup>2+</sup>(aq) to either form a soluble complex which increases the solubility of the Ba<sup>2+</sup> from the BaTiO<sub>3</sub> or phase separate.<sup>(44,45)</sup> The fact that the MLC

industry does not appreciate the solution chemistry associated with the aqueous processing of BaTiO<sub>3</sub> MLCs suppresses the successful production green ceramic layers <5 μm thick and fired layers <3 μm.

The surface charge formation of a single component, metal oxide (e.g. Al<sub>2</sub>O<sub>3</sub>) particle in aqueous solution as a function of pH has been well documented.<sup>(33,53,70)</sup> The polarity and magnitude of the surface potential associated with aqueous ceramic suspensions are dependent upon the solution pH.<sup>(16,83,104)</sup> This is because H<sup>+</sup> and OH<sup>-</sup> are the potential-determining ions for single component metal oxides.<sup>(52)</sup> However, multicomponent ceramics (e.g. BaTiO<sub>3</sub>) are more complex. Surface reactions of most multicomponent oxides have not been well documented. Reactions at the particle surface can manifest as the formation of depleted surface layers, the deposition of metastable phases either from the saturated solution or via crystallization of surface films, the readsorption of dissolved species in solution, and the diffusion of the species through these layers.<sup>(6,13,14,37)</sup>

The passivation of BaTiO<sub>3</sub> via the addition of oxalate ions reduces the concentration of Ba<sup>2+</sup>(aq) and promotes a relatively constant, negative surface charge over a wide pH range from pH 4 to pH 10.<sup>(108)</sup> The addition of polyethylene imine (PEI) to oxalate-treated particles imparts a positive charge over a wide pH range via the adsorption of the positive polymer to the negative oxalate surface.<sup>(121)</sup> Both the passivation agent and the dispersion agent will vaporize as CO(g), CO<sub>2</sub>(g), H<sub>2</sub>O(g), and N<sub>2</sub>(g) during the sintering of the ceramic with no residuals trapped within the microstructure.<sup>(66,116)</sup>

The size and conformation of the polymer additive dictates its purpose, solubility, and rheological behavior.<sup>(115,119)</sup> Polymer dispersants are typically intermediate length (5,000 to 75,000 molecular weight) organic molecules that may be positive, neutral, or negatively charged depending on the nature of side or backbone functional groups.<sup>(116-119)</sup> Both the dispersant and the binder are comprised covalently bonded backbones made of carbon, oxygen, and nitrogen with side groups located periodically along the length of the

molecule. The chemical nature and size of the side groups of a polymer determine the solubility of the polymer in a particular solvent.<sup>(119)</sup> The solubility of the binder can be improved by increasing the size or the number of side groups along the backbone of the polymer. This reduces the amount of interactions that takes place between the solvent/binder molecules. A reduction in the molecular weight of the polymer molecule also increases the solubility.<sup>(119)</sup>

In the literature, little has been documented about the interactions between the aqueous solvent, ceramic particles, and polymeric additives (i.e., dispersants and binders) which can compromise the rheological properties of the system. The location of the binder, whether in solution or adsorbed onto the surface, strongly effects the rheological properties of the ceramic slurry.<sup>(34,122,123)</sup> The addition of a binder changes the rheological properties of water from Newtonian to pseudoplastic in most cases.<sup>(34)</sup> The rheological properties of a ceramic/binder system are dependent on specific interactions between the particle and polymer, and the location of the binder in solution.<sup>(67)</sup> Polyelectrolytes, similar to metal oxides, can form a charge associated with the molecule when introduced to water.<sup>(67)</sup> Interaction between the particle and polymer at the solid-solution interface is dependent on the charge associated with the inorganic and the organic molecule.<sup>(124)</sup> If the polarities are opposite the polymer will electrostatically adsorb to the particle surface.<sup>(125)</sup> Production of a well dispersed slip requires minimization of binder/particle interactions. Thus, the binder and the dispersed particles must maintain a similar polarity.

Figure 5.1 shows the general rheological behaviors associated with polymer solutions.<sup>(34)</sup> When a polymer solution is subjected to a shear force, the polymer chains can align to reduce the solution viscosity and strain produced. When the shear is removed, the viscosity can immediately increase because the alignment of the polymer chains no longer exists. This rheological phenomena is noted as shear thinning or pseudoplastic behavior. The apparent viscosity is the viscosity reported at the plateau region where the viscosity remains relatively constant. The apparent viscosity generally increases with increasing

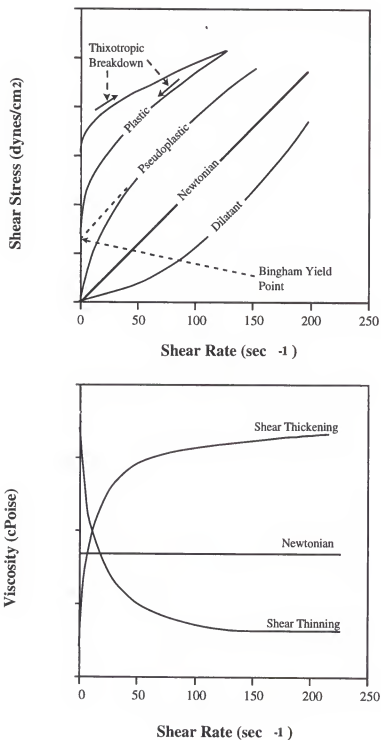


Figure 5.1. Different types of rheological behavior characteristics for various suspensions.<sup>(34)</sup>

polymer concentrations. Thixotropic behavior occurs when the polymer chain alignment gradually dissipates, and the lower viscosity state is retained for some time after the higher shear stresses are removed. Gelation is another rheological condition of importance in binder solutions. Gels can occur when (1) cooling a warm polymer solution, (2) heating a polymer solution (thermal gelation), or (3) reacting the polymer with alkaline earth and heavy metal ions present in solution.<sup>(118,126)</sup> Newtonian fluids exhibit a shear stress that is proportional to the shear rate. Therefore, the shear stress and the viscosity vs. shear rate plots are straight lines with a constant slope since the viscosity equals the instantaneous slope of the shear stress versus shear rate curve. Dilatant fluids show an increase in viscosity with an increase in the shear stress, in which the behavior is opposite to the shear thinning behavior.

The rheological behavior of particle/polymer suspensions can be tailored to meet the demands of various industries. Pseudoplasticity is particularly important to the paint and multilayer capacitor industries.<sup>(33,33)</sup> Colloidal science in the paint industry is employed to inhibit particle settling. Otherwise, manufacturers of these slips would be required to include a shelf life on the packaging label to minimize the chances of slurry containing inhomogeneities.<sup>(67)</sup> Long-chained organic molecules provide control of the rheological behavior that permits the tape casting of thin, uniform ceramic layers. The viscosity of the pseudoplastic fluid at low shear rates must be large and decrease with an applied shear force, as in pouring, spraying, or tape casting. It is desirable to have a low viscosity while casting down a ceramic tape. However, a fast recovery or increase in viscosity is essential when the shear is reduced in order to maximize the uniformity of tape thickness and minimize binder segregation.<sup>(12)</sup>

## 5.2. Approach

In the current work, experiments were specifically designed to determine the colloidal stability of various binder systems (anionic, neutral, or cationic) with the aqueous passivation-dispersion scheme for  $\text{BaTiO}_3$ .<sup>(108,121)</sup> The incongruent dissolution of  $\text{BaTiO}_3$ ,

is inhibited by forming a relatively insoluble salt, barium oxalate, on the particle surface which imparts a relatively constant, negative surface charge over a wide pH range.<sup>(14,19,41,108)</sup> The addition of PEI to the oxalate-treated BaTiO<sub>3</sub> imparts a positive surface charge and colloidal stability.<sup>(121)</sup> Three types of polyelectrolytes (anionic, neutral, and cationic) are evaluated as possible binders for the oxalate/PEI-treated BaTiO<sub>3</sub>. Polyacrylic acid (PAA) which readily takes on negative charge, polyvinyl alcohol (PVA) and polyethylene oxide (PEO) which are neutral polymers, and PEI and polyvinyl pyrrolidone (PVP) which are two cationic polymers.<sup>(116-119,126-128)</sup> It will be shown that the slightly positively charged PVP, added as a combination of two different molecular weights, is the most effective binder composition of the various binders studied for the oxalate/PEI-treated BaTiO<sub>3</sub> particles. Preliminary studies at low solids loading include electrophoresis and sedimentation for oxalate/PEI-treated BaTiO<sub>3</sub> suspension with binder present. Rheological characterization of solutions containing various combinations of the three additives (oxalate, PEI, and binder) without BaTiO<sub>3</sub> present is performed to analyze possible interactions between additives. High solids loading samples were prepared to analyze samples at a concentration where colloidal stability is more critical. Instability or interactions within the suspension will be more obvious at the higher solids loading. Binder compatibility will be assessed at the larger solids content via rheological behavior of the slurry, visual inspection for aggregates within the tape, and SEM of the particle packing within the cast pseudo-tapes. The analysis of various binders at high solids loading is limited by the polymer solubility and complete dissolution in a small amount of water equal to the volume of polymer added. Solubility is an issue since portions of the total water added is needed to separately dissolve the oxalic acid and the binder. These two restrictions limit the choice of polymers, as well as make it difficult to achieve BaTiO<sub>3</sub> solids contents greater than 65 weight percent. However, 65% BaTiO<sub>3</sub> is more concentrated than the ~58% BaTiO<sub>3</sub> solids used in conventional tape casting formulations currently.

It will be demonstrated that the slightly positively charged PVP added as two different molecular weights is compatible and more effective as a binder for the oxalate/PEI-treated BaTiO<sub>3</sub> particles than other investigated binders.

### 5.3. Materials and Methods

#### 5.3.1. General

All glassware and plasticware were washed with a biodegradable detergent<sup>1</sup>, rinsed thoroughly with tap water to remove residual soap, and subsequently rinsed several times with copious quantities of deionized water<sup>2</sup> before use. Glassware was only used when the solution/suspension pH value of the contents was less than pH 8.5 to minimize soluble silica contamination, whereas plasticware was used over the entire pH range. Unless otherwise noted, deionized water used throughout the current work was boiled approximately ten minutes while purged with nitrogen to minimize dissolved atmospheric gases, particularly CO<sub>2</sub>, present in solution. Degassed deionized water was stored in glass bottles with rubber-lined caps under a nitrogen atmosphere until required. All constituents were weighed to four decimal places using an analytical balance<sup>3</sup>. The submicron hydrothermally derived BaTiO<sub>3</sub><sup>4</sup> was supplied by Cabot Performance Materials (Boyertown, PA). The submicron powder is approximately 0.1 μm equiaxed particles with an irregular surface. Bulk analysis of the BaTiO<sub>3</sub> powder by the supplier showed concentrations of C, Sr, Fe, and Cl ranging from 500-1000 ppm, 400-800 ppm, 50-200 ppm, and 100-300 ppm respectively. Other bulk contaminants included Al, Si, Cr, Ca, and Ni which were all less than 5 ppm.

---

<sup>1</sup>Sparkleen, Calgon Vestal Laboratories, St. Louis, MS.

<sup>2</sup>Deionized water, specific resistivity >10 megaohms.cm.

<sup>3</sup>Fisher Scientific, model A-250, 0.0001 g readability.

<sup>4</sup>Cabot Hydrothermally Derived BaTiO<sub>3</sub> powder, Cabot Performance Materials, Boyertown, PA.

The oxalic acid<sup>5</sup> and PEI<sup>6</sup> dosages used as well as the order of addition are similar to previous work on the aqueous passivation and dispersion of BaTiO<sub>3</sub>.<sup>(108,121)</sup> Acidic and alkaline pH adjustments were made using various concentrations of HNO<sub>3</sub><sup>7</sup> and TEAOH<sup>8</sup>. All other chemicals used throughout this study are reagent grade and were used without further purification.

### 5.3.2. Preliminary Studies Low Solids Loading

#### 5.3.2.1. Electrophoretic and Sedimentation Studies

Suspensions for electrophoretic behavior studies were prepared similarly to the recipe reported in earlier work where the oxalic acid was dissolved in deionized water before adding an amount of BaTiO<sub>3</sub> equal to one volume percent (1%v) of the total suspension volume.<sup>(121)</sup> However, only a portion of the total water was used to dissolve the oxalic acid and the remaining water was used to dissolve the polymeric binder additive. PEI was then added in the amount of 1 weight percent (1%w) of the solid BaTiO<sub>3</sub> powder. Various amounts of polyethylene oxide<sup>9</sup> (PEO) (0, 3, 6, 9, and 12%w) were dissolved in the remaining amount of deionized water, added, mixed, and pH adjusted to values between 4 and 12 using HNO<sub>3</sub> and TEAOH. Electrophoretic mobility was determined by the Brookhaven Zeta Plus<sup>10</sup> for comparison to earlier work completed on BaTiO<sub>3</sub> as a function of solids loading, varying concentrations of oxalic acid and PEI, and suspension pH. Sedimentation studies were performed on samples similar to the specimens used for electrophoresis to determine agglomeration/flocculation tendencies of the suspensions. The various samples were prepared and each carefully poured into separate plastic test tubes with a screw tight caps to minimize the amount of trapped air present at the top of the test tube. Sediment height in the test tubes with various concentrations of PEO was recorded as

---

<sup>5</sup>Oxalic acid - Fisher Scientific, lot # 905504.

<sup>6</sup>Polyethyleneimine (50% in water), Kodak, lot A16B.

<sup>7</sup>HNO<sub>3</sub> - Fisher Scientific, 70 weight % solution in water, lot# 905811.

<sup>8</sup>TEAOH - Aldrich, 35 weight % solution in water, lot# 05498HZ.

<sup>9</sup>Polyethylene oxide, Molecular Weights of 600, 1450, and 8000.

function of time for different suspension pH values to determine stability and corroborate the capricious effects determined from the electrophoretic study.

### 5.3.2.2. Polymer Interactions

Rheological behavior was determined on the following solutions: (1) 0.1M oxalic acid solution, (2) 1% PEI solution, and (3) 10% PEO solution. The oxalic acid solution was prepared in a volumetric flask with the oxalic acid dihydrate powder, polymer additives, and deionized water used to make the polymer solutions were weighed out using the analytical balance mentioned in a previous section. These solutions were prepared as reference solutions and made in large quantities to determine possible interactions between any two or possibly all three solutions. Viscosity measurements were performed on all solutions at 25°C using a cone-plate viscometer<sup>11</sup> at shear rates ranging from 0.1 to 300 sec<sup>-1</sup>. Both the shear stress and the viscosity were reported as a function of shear rate for all samples where the viscosity could be determined. An equal quantity of the 0.1M oxalic acid solution was added to the 1% PEI solution. The mixture was divided into three aliquots, and pH adjusted to an acidic, neutral, or an alkaline pH before determining the rheological behavior. The solution pH was adjusted to determine if hydronium or hydroxyl concentration affects rheology. Mixtures of 10% PEO + 0.1M oxalic acid and 10% PEO + 1% PEI were also produced, pH adjusted in a similar manner to the previous mixtures, and rheological properties determined. Finally a mixture of all three solutions was characterized under identical conditions.

Approximately 125 ml of a 1% PEI solution, a 10% - 600 molecular weight PEO solution, and a 10% - 8000 molecular weight PEO solution were titrated to determine possible equivalence points. The initial pH of the three polymer solutions was pH 10.85, pH 4.7, and pH 7.3, respectively. The standard solutions used to titrate each polymer

---

<sup>10</sup>Brookhaven Instrumentation Corporation, ZetaPlus, Holtsville NY.

<sup>11</sup>Brookfield Digital Viscometer, model # LVTDCP, Brookfield Engineering Laboratory, Inc., Stoughton MA.

solution were 0.1M and 0.01M  $\text{HNO}_3$ , and 0.01M TEAOH. The standard solution was added with an adjustable pipette and the pH was measured with a pH meter<sup>12</sup>.

### 5.3.3. High Solids Loading Barium Titanate Slurries

#### 5.3.3.1. Preparation of $\text{BaTiO}_3$ Slurries with Binder Present

$\text{BaTiO}_3$  slurries produced were based upon earlier reports with the desired amount of  $\text{BaTiO}_3$  and other additives.<sup>(108,121)</sup> The appropriate amount of each additive was calculated in grams using a simple computer program. However, the addition of water required special attention. Equal amounts of deionized water and dry binder powder were mixed as a <sup>50/50</sup> binder/deionized water solution (ensuring full polymer dissolution) prior to addition to the oxalate/PEI-treated  $\text{BaTiO}_3$  slurry. The remaining volume of deionized water was used to dissolve the oxalic acid for passivating the surface of the  $\text{BaTiO}_3$  particles.

The desired amount of oxalic acid was completely dissolved before slowly adding the  $\text{BaTiO}_3$  powder to the plastic container. Small volume slurries were mixed with highly polished zirconia mixing media<sup>13</sup> while large volume slurries (1 liter) were mixed with a high speed emulsifier<sup>14</sup>. The appropriate amount of PEI was added to the vessel followed by the desired amount of binder. The constituents were mixed after introducing each reagent to the plastic container. The slurries were stored in these Nalgene containers with lids under a nitrogen atmosphere to minimize reactions between the slurry and atmospheric  $\text{H}_2\text{O}$  or  $\text{CO}_2$ .

#### 5.3.3.2. Characterization of the Barium Titanate Slurries

Characterization of the high solids loading samples is essential to interpret the interactions between the oxalate/PEI treatment and various binders. The larger concentration of  $\text{BaTiO}_3$  particles increases the particle/particle interaction in the sample

---

<sup>12</sup>pH Meter - The London Co. - PHM 64 research pH meter - Cleveland OH.

<sup>13</sup>Zirconia highly polished mixing media - 5 mm.

<sup>14</sup>Kinematic GmbH, type PT 10/35, Switzerland.

which emphasizes the issue of dispersion and colloidal stability more apparent. Three small samples were extracted from each slurry for pH measurement, visual inspection, and particle packing. The slurry pH was determined using color-calibrated litmus paper<sup>15</sup>. The second sample was smeared onto a glass microscope slide using a razor blade to create a "pseudo"-tape that could be visually examined for gross defects (agglomerates), topography, and uniformity of the film. Scanning electron microscopy<sup>16</sup> (SEM) was used to examine the particle packing within the pseudo tapes cast on an aluminum SEM mount. Pseudo tapes were examined at 50kX, 25kX, 10kX, and 1kX where possible.

Viscosity measurements were performed on all slurries at 25°C using a cone-plate viscometer at shear rates ranging from 0.1 to 150 sec<sup>-1</sup>. Both the shear stress and the viscosity were determined as a function of shear rate for all samples where the viscosity could be experimentally ascertained. If the viscosity of the slurry was beyond the limit of the instrument or did not achieve a plateau over the range of shear rates investigated, the suspension "apparent" viscosity was reported as NA and, in any case, would not be suitable for thin tape production. The apparent viscosity and the Bingham yield point were determined by a similar method used in previous work.<sup>(121)</sup>

## 5.4. Results and Discussion

### 5.4.1. Preliminary Studies at Low Solids Loading

#### 5.4.1.1. Electrophoretic and Sedimentation Studies

Electrophoretic studies were performed to evaluate the addition of PEO as a binder for the passivated-dispersed BaTiO<sub>3</sub> system in water. Figure 5.2 shows the electrophoretic behavior of 1% BaTiO<sub>3</sub> suspensions with 5% oxalic acid and 1% PEI as a function of PEO concentration. Electrophoretic analysis shows only minor changes in the magnitude of the potential as a function of PEO concentration and no general increases or decreases in the surface charge with increasing PEO concentrations. The 1% BaTiO<sub>3</sub> solution with

---

<sup>15</sup>pHydron paper, Micro Essential Laboratory, Brooklyn, NY.

<sup>16</sup>JEOL 6400 scanning electron microscope, JEOL, Boston, MA.

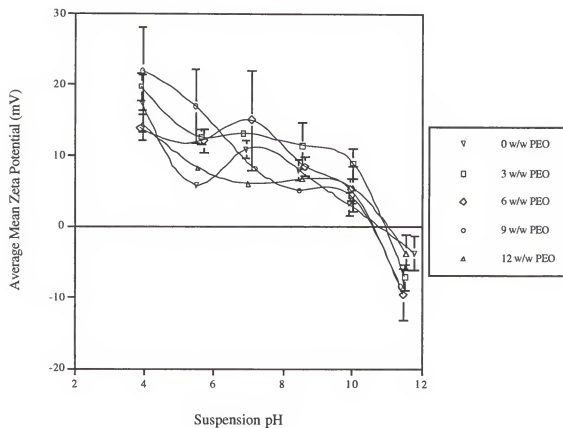


Figure 5.2. Electrophoretic behavior (zeta potential vs. pH) of 1% BaTiO<sub>3</sub>, 5% oxalic acid, and 1% PEI suspension as a function of PEO concentration. All additives are incorporated as a weight percent of BaTiO<sub>3</sub>.

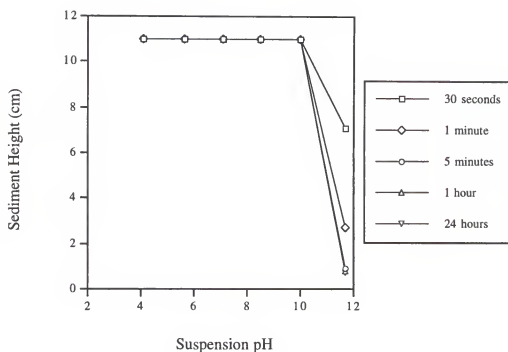
5% oxalic acid and 1% PEI (0% PEO) exhibits a positive charge below the isoelectric point (pH ~10) and slightly negative above the IEP. The magnitude of the potential is ~15 mV at pH 4 and decreases to ~4 mV just below pH 10 before exhibiting a negative 4 mV surface charge at pH 11.7. The influence of the PEO on the surface charge associated with the oxalate/PEI-treated BaTiO<sub>3</sub> seems to be negligible at these solids loading and additive concentrations. The electrophoretic behavior of the 1% BaTiO<sub>3</sub> with 5% oxalic acid, 2% PEI as a function of PEO was similar to the results for the electrophoretic behavior of the 1% BaTiO<sub>3</sub> with 5% oxalic acid, 1% PEI as a function of PEO presented in Figure 5.2.

Sedimentation studies performed in conjunction with the electrophoretic analysis show PEO adversely affects the suspension stability of the passivated/dispersed BaTiO<sub>3</sub> suspensions. Figure 5.3 (a) and 5.3 (b) compare the sedimentation results for suspensions that contain 1% BaTiO<sub>3</sub> with 5% oxalic acid, 1% PEI and either 0% PEO or 12% PEO, respectively. Figure 5.4 (a) and 5.4 (b) compare the sedimentation behavior for similar suspensions containing 2% PEI as opposed to 1% PEI. The overall stability of the suspensions is decreased when 12% PEO binder is present. However the instability is only noted after 24 hours when the particles settled to the base of the test tube. Up to and including the one hour measurement, the various suspensions without and with PEO present were visually similar. For suspensions prepared at pH values above the dissociation of the PEI, the stability decreases dramatically independent of the PEO concentration.<sup>(121)</sup> Therefore, the addition of PEO, a neutral polymer, adversely affects the colloidal stability of the oxalate/PEI-treated BaTiO<sub>3</sub> suspensions.

#### 5.4.1.2. Polymer Interactions

Interaction between the various additives without BaTiO<sub>3</sub> present was investigated using viscosity measurements. The rheological behavior for the three solutions (0.1M oxalic acid, 1% PEI and 10% PEO) is near Newtonian and is shown in Figure 5.5. The viscosity of the 10% PEO solution was ~5 cP and the viscosity of the other two

a.



b.

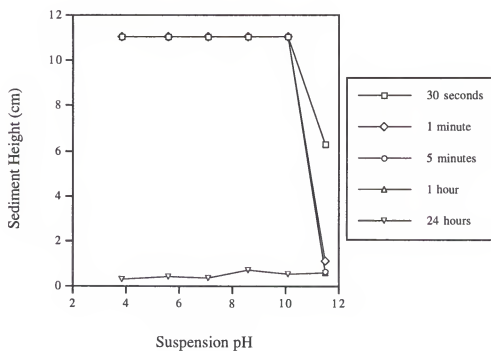
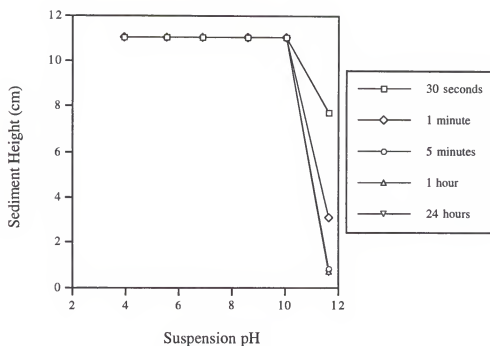


Figure 5.3. Sedimentation results for 1% BaTiO<sub>3</sub>, 5% oxalic acid, 1% PEI, and (a.) 0% PEO or (b.) 12% PEO where all additives are incorporated as a weight percent of BaTiO<sub>3</sub>.

a.



b.

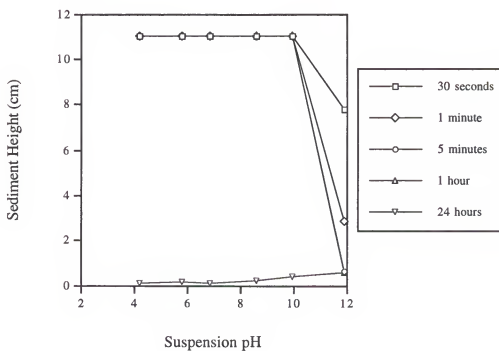


Figure 5.4. Sedimentation results for 1% BaTiO<sub>3</sub>, 5% oxalic acid, 2% PEI, and (a.) 0% PEO and (b.) 12% PEO where all additives are incorporated as a weight percent of BaTiO<sub>3</sub>.

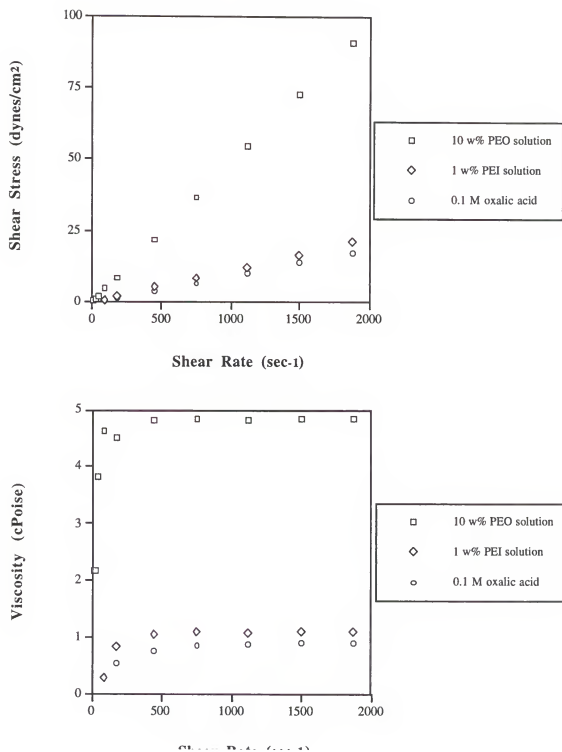


Figure 5.5. Rheological behavior (shear stress and viscosity vs. shear rate) for the following three solutions, 10 w% PEO solution, 1 w% PEI solution, and 0.1 M oxalic acid.

solutions was nearly 1 cP. Figure 5.6 depicts the rheological properties for the three pH adjusted (acidic, neutral, and alkaline) solutions that contain equal amounts of 0.1M oxalic acid and 1% PEI solution. All three pH adjusted solutions to be Newtonian with an approximate viscosity of 1 cP, similar to each single component solution. However, the new total concentration for the mixture of the two suspensions is 0.05M oxalic acid and 0.5% PEI solution. At these low concentrations, no interaction between these two constituents could be confirmed. Figure 5.7 shows the rheological properties for the 0.05M oxalic acid/5% PEO solution as a function of pH. The approximate viscosity for the combination of 0.1M oxalic acid and 10% PEI solution is ~2.25 cP. This change in viscosity from the three single component solutions does not refute or confirm any interaction between oxalic acid and PEO. Similar conclusions can be ascertained for the PEO/PEI (5% and 0.5% respectively) mixture shown in Figure 5.8.

The rheological behavior for the combination of the three solutions as a function of pH is presented in Figure 5.9. The viscosity of the three component solution (0.3M oxalic acid, 0.3% PEI, and 3.3% PEO concentrations respectively) was 2.0 to 2.5 cP and the rheological behavior is similar to both two component solutions. The pH of the mixture has relatively no effect on the rheological behavior. Interaction between these low concentrations of the passivating agent, dispersant, and binder as a function of pH (without BaTiO<sub>3</sub> present) is undetermined at this time.

#### 5.4.1.3. Titration Curves

Figures 5.10, 5.11, and 5.12 depict the titration curves for approximately 125 ml of a 1.0% PEI solution, a 10% PEO (600 MW) solution, and a 10% PEO (8000 MW) solution, respectively. Initial additions of 0.1M HNO<sub>3</sub> to the 1.0% PEI solution produce a titration curve similar to a strong acid-strong base titration. However, as the pH becomes more acidic the titration of the polymer solution behaves more similarly to the titration of a weak base with a strong acid where the pH of the solution slowly decreases with subsequent additions of the acid.<sup>(107)</sup> The final pH was 3.35 after the addition 85 ml of

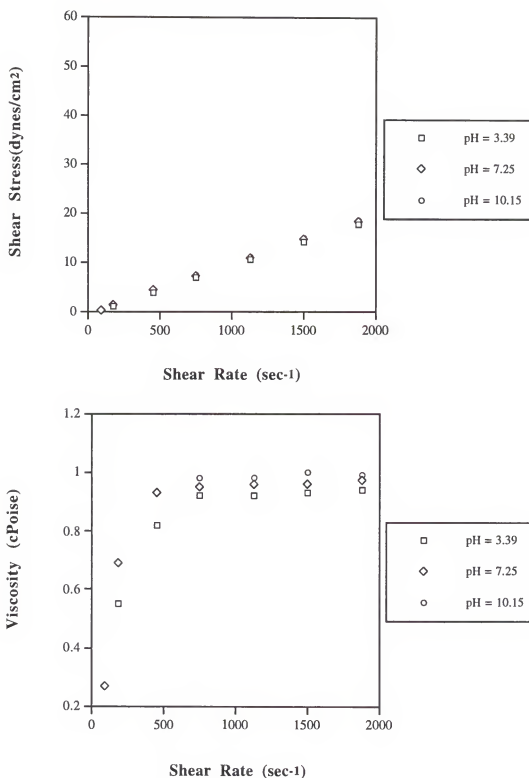


Figure 5.6. Rheological behavior for a mixture of equal amounts of 1% PEI solution and 0.1M oxalic acid at three different pH conditions (acidic, neutral, and alkaline).

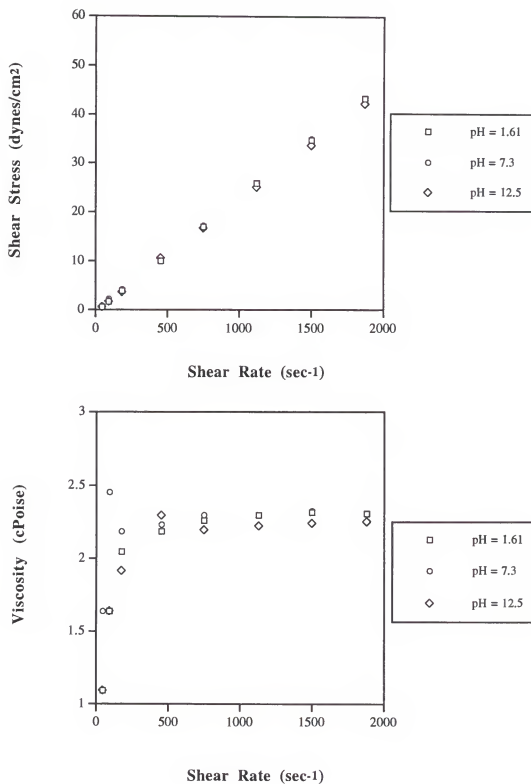


Figure 5.7. Rheological behavior for a mixture of equal amounts of 10% PEO solution and 0.1M oxalic acid at three different pH conditions (acidic, neutral, and alkaline).

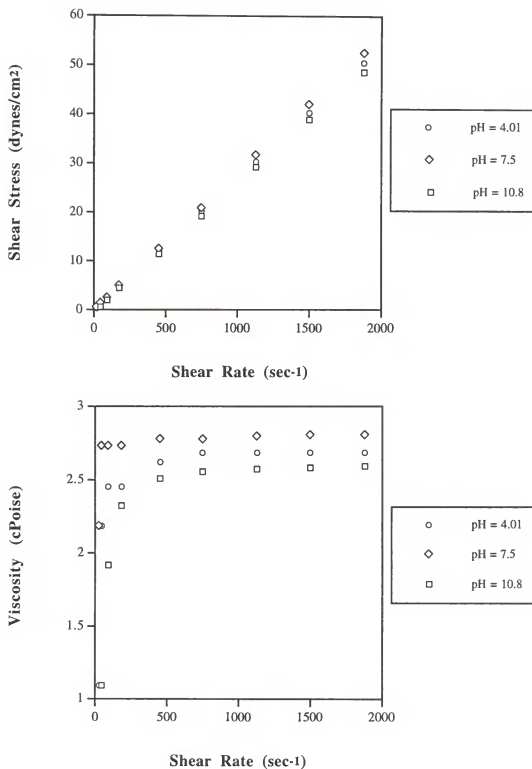


Figure 5.8. Rheological behavior for a mixture of equal amounts of 10% PEO solution and 1% PEI solution at three different pH conditions (acidic, neutral, and alkaline).

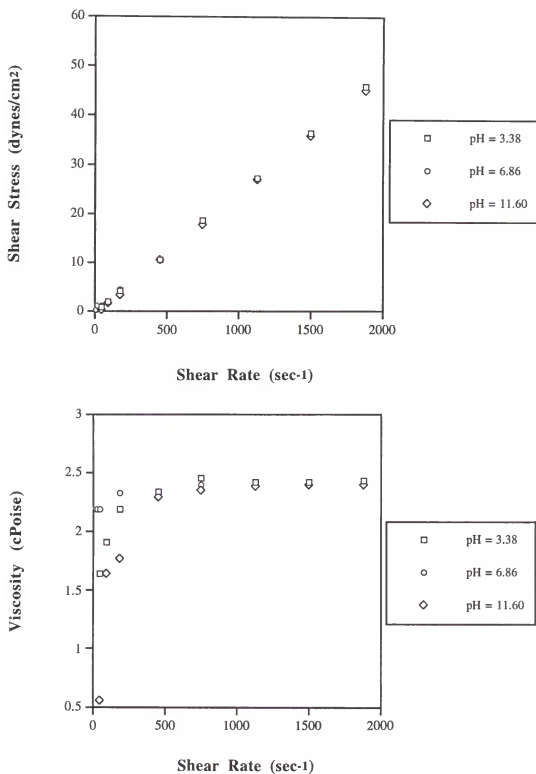


Figure 5.9. Rheological behavior for a mixture of equal amounts of 10% PEO solution, 0.1M oxalic acid, and 1% PEI solution at three different pH conditions (acidic, neutral, and alkaline).

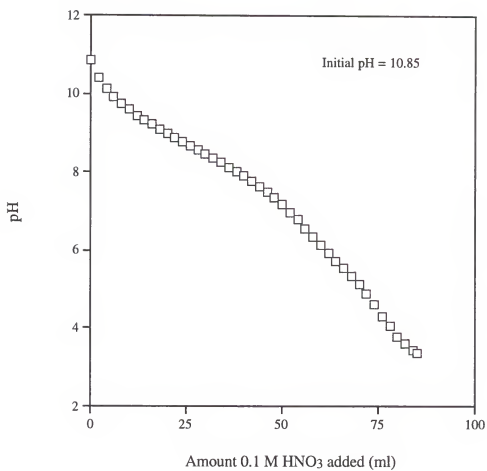


Figure 5.10. Titration curve for 1% PEI solution where 0.1M HNO<sub>3</sub> was used as the titrant.

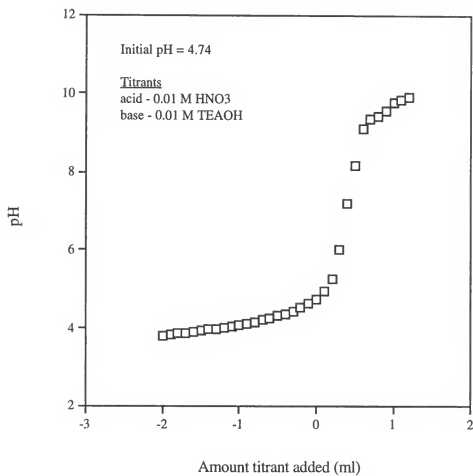


Figure 5.11. Titration curve for 10% 600L PEO solution where 0.01M HNO<sub>3</sub> and 0.01M TEAOH were used as the titrants.

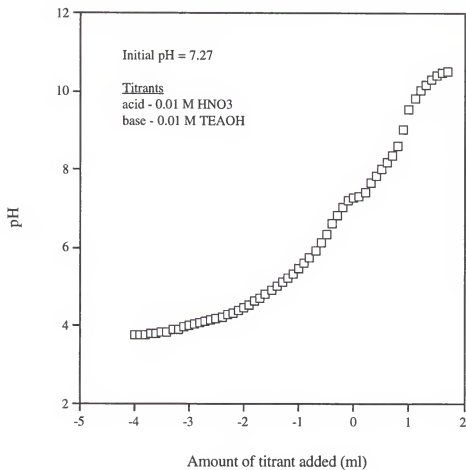


Figure 5.12. Titration curve for 10% 8000 PEO solution where 0.01M HNO<sub>3</sub> and 0.01M TEAOH were used as the titrants.

acid. In agreement with the literature, PEI exhibits a highly positive charge in aqueous conditions below pH 10.<sup>(116)</sup> The titration curve for the 10% 600MW PEO solution is similar to the titration curve produced when a strong base is added to a strong acid. The equivalence point (that is, the point where stoichiometric equivalent quantities of acid and base are present) for the 10% 600MW PEO solution occurs at ~pH 7, whereas the 8000 MW PEO solution shows a gradual in change in the solution pH with additions of either acid or base and no apparent equivalence point.<sup>(107)</sup>

#### 5.4.2. High solids loading BaTiO<sub>3</sub> Slurries

Several slurry formulations were prepared with various binders of different concentrations, with different molecular weights, and with different combinations of two binders to determine the most effective binder for the aqueous oxalate/PEI-treated BaTiO<sub>3</sub> suspensions. The analysis of various binders at high solids loading is limited by the polymer being water soluble and completely dissolved in a small amount of water equal to the volume of polymer added. This is due to the part of the total water added is needed to dissolve the oxalic acid and some of the total water is added with the dispersant, PEI. These two restrictions limit the choice of polymers available, as well as make it difficult to achieve BaTiO<sub>3</sub> solids contents greater than 65 weight percent. However, 65% BaTiO<sub>3</sub> is more concentrated than most conventional tapes casting formulations used in the MLC industry which is believed to currently be ~58% BaTiO<sub>3</sub> solids. SEM analysis shown in Figure 5.13, illustrates the poor particle packing within the green tape when a conventional MLC formulation is employed. No conventional pre-tape casting slurry modification (filtering or degassing) was performed on this slurry or any of the following described formulations.

Table 1 details the slurry formulation (designation, weight percent BaTiO<sub>3</sub> present, and binder composition and concentration) as well as the rheological properties. The number (600,1450, and 8000) and letter (L=liquid, F=flake, and P=powder) before PEO correspond to the molecular weight and as-received form of the PEO, respectively. The

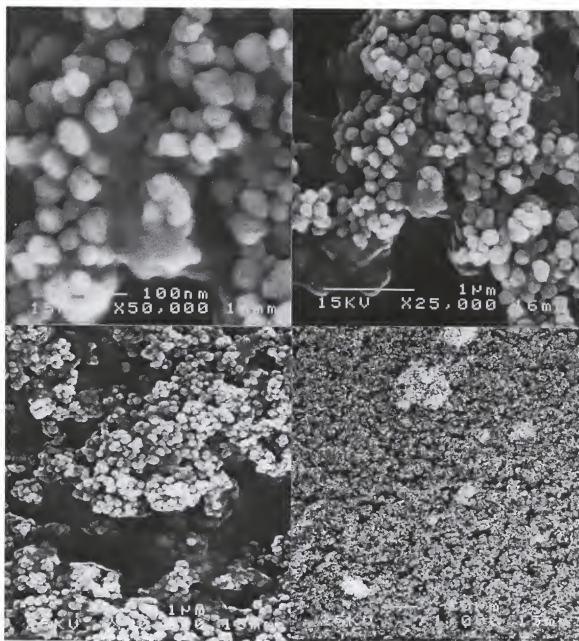


Figure 5.13. Scanning electron micrographs of a smeared sample from an aqueous BaTiO<sub>3</sub> (Cabot hydrothermally derived powder) slurry prepared with a conventional tape casting formulation (57.5% BaTiO<sub>3</sub> and 12% binder) at four different magnifications (50 kX, 25 kX, 10 kX, and 1 kX).

Table 5.1. A summary of the sample designation, weight percent BaTiO<sub>3</sub>, binder composition, and rheological properties (apparent viscosity and Bingham yield point) for the oxalate/polyethylene imine-treated BaTiO<sub>3</sub> slurry formulations.

SAMPLE	WEIGHT % BaTiO <sub>3</sub>	BINDER FORMULATION	OTHER ADDITIVES	APPARENT VISCOSITY (cP)	BINGHAM YIELD POINT (dynes/cm <sup>2</sup> )	PARTICLE PACKING REPRESENTATION
9E-600L	69.8	3w/o 600L PEO	None	NA	NA	Figure 5.14
9E-1450F	69.8	3w/o 1450F PEO	None	428	38	Figure 5.14
9E-8000P	69.8	3w/o 8000P PEO	None	412	34	Figure 5.14
9E-8000F	69.8	3w/o 8000F PEO	None	NA	NA	Figure 5.14
9F-8000F	68.4	6w/o 8000F PEO	None	NA	NA	Figure 5.15
9F-8000P	68.5	6w/o 8000P PEO	None	602	13	Figure 5.15
9G-8000F	65.8	12w/o 8000F PEO	None	NA	NA	Figure 5.16
9G-8000P	65.8	12w/o 8000P PEO	None	NA	NA	Figure 5.16
9G-PVP	59.9	12w/o PVP (40k MW)	None	NA	NA	Figure 5.16
9H-PEI	59.9	12w/o PEI as Binder	None	NA	NA	Figure 5.17
3-1-12-0.5	59.9	12w/o PVP	Darvan C	NA	NA	
D-1	62.5	12w/o 10,000 PVP	None	47	1.0	
J-1	65	12w/o 10,000 PVP	Glycerin	130	2.5	
A-1	60	12w/o PVP	None	119	2	
		10,000/40,000 ( <sup>50/50</sup> )				
C-1	60	12w/o PVP	Glycerin	65	2	
		10,000/40,000 ( <sup>50/50</sup> )				
I-6 A	65	12w/o PVP	Glycerin	902	13	Figure 5.18
		10,000/40,000 ( <sup>50/50</sup> )				
3-1-10 PVP	65	10w/o PVP (40k MW)	Glycerin, Triton X	1583	10	
3-1-10 PVP*	65	10w/o PVP	Glycerin, Triton X	218	2	Figure 5.19
		10,000/40,000 ( <sup>50/50</sup> )				

\*These samples were sent to Cabot Corporation and mixed by Steve Costantino.

apparent viscosity for all slurries prepared with PEO present were higher than ~400 cP. Whereas typical industrial slurry formulations exhibit working viscosities less than 150 cP. The variation in the apparent viscosity and the Bingham yield point for the slurries with PEO incorporated as the binder arises from differences in the molecular weight of the PEO and the as-received form of the binder. The particle packing within the pseudo tapes prepared from slurries 9E-8000P, 9F-8000P, and 9G-8000P is shown in Figures 5.14, 5.15, and 5.16, respectively. Increasing the PEO binder concentration above 6% of the BaTiO<sub>3</sub> powder decreases the particle density. Particle packing displayed from slurries prepared with 600L, 1450F, and 8000F resembled the scanning electron micrographs shown in Figures 5.14, 5.15, and 5.16 for an equal corresponding binder concentration. Although the particle density shown by the slurries with PEO present as a binder were greater than the conventional tape casting formulation (Figure 5.13), the viscosity and Bingham yield point were much higher. However, the slurries with PEO present were prepared with 65% to 70% BaTiO<sub>3</sub> in comparison to conventional formulations with only ~58% BaTiO<sub>3</sub>.

The addition of 12% of a conventional binder, PVP (40,000 molecular weight), or PEI (an additional 12% PEI added as a binder to the already existing 1% PEI added as a dispersant) were all over the range of the viscometer. Figure 5.17 shows the particle packing exhibited slurry 9G-PVP. The addition of Darvan C (3-1-12-0.5) showed no improvement in the slurry's rheological properties or particle packing. However, slurry D-1, where 12% PVP (10,000MW) is incorporated as the binder, exhibited an apparent viscosity of 47 cP and a Bingham yield point of 1 dyne/cm<sup>2</sup> for the 62.5% BaTiO<sub>3</sub> slurry. Increase in the BaTiO<sub>3</sub> solids content to 65% and the addition of glycerin (added as 1% of the BaTiO<sub>3</sub>) as a wetting agent, caused the apparent viscosity and the Bingham yield point to increase to 130 cP and 2.5 dyne/cm<sup>2</sup>, respectively (formulation J-1). The 50 μm thick hand cast tape made with slurry J-1 was relatively agglomerate free even though no pre-cast filtering of the large agglomerates was performed or negative pressure applied to

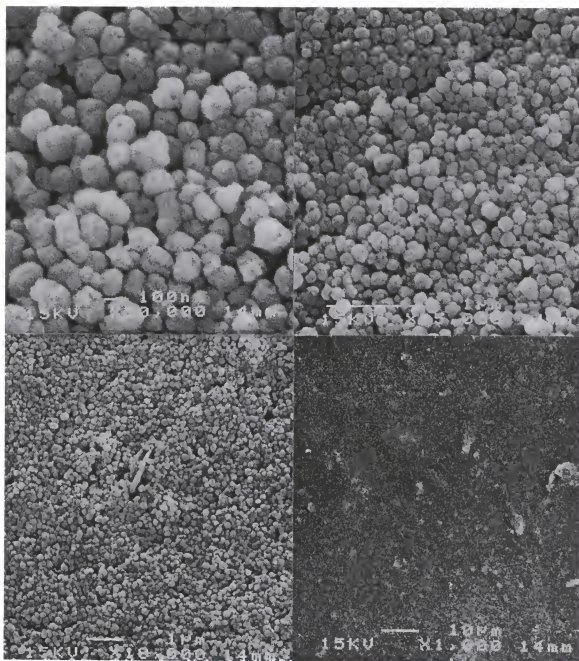


Figure 5.14. Scanning electron micrographs of a smeared sample from slurry 9E-8000P (70%  $\text{BaTiO}_3$ , 3.0% oxalic acid, 1.0% PEI, and 3.0% PEO-powder form) at four different magnifications (50 kX, 25 kX, 10 kX, and 1 kX). Oxalic acid, PEI, and PEO are added as a weight percent of the  $\text{BaTiO}_3$ .

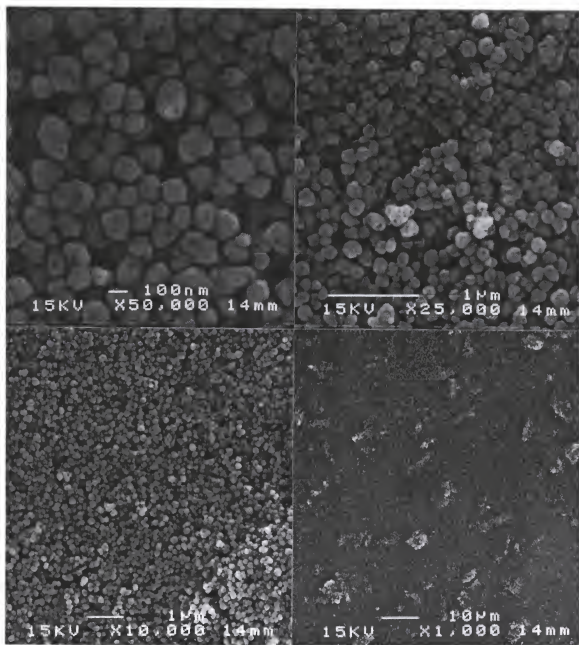


Figure 5.15. Scanning electron micrographs of a smeared sample from slurry 9F-8000P (68% BaTiO<sub>3</sub>, 3.0% oxalic acid, 1.0% PEI, and 6.0% PEO-powder form) at four different magnifications (50 kX, 25 kX, 10 kX, and 1 kX). Oxalic acid, PEI, and PEO are added as a weight percent of the BaTiO<sub>3</sub>.

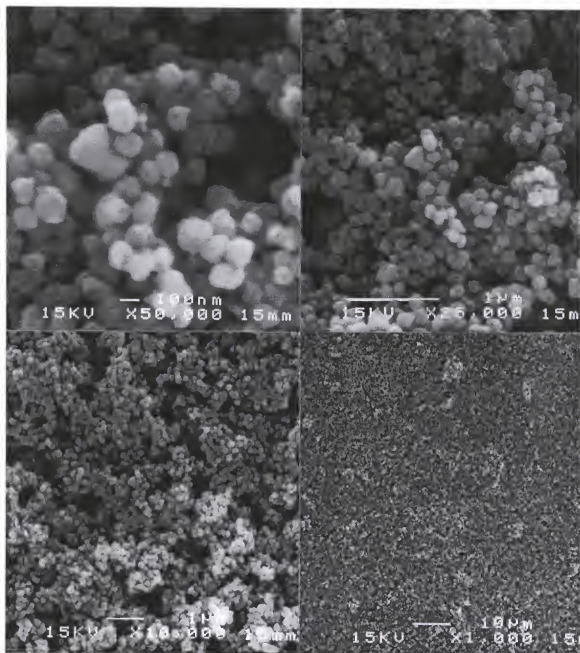


Figure 5.16. Scanning electron micrographs of a smeared sample from slurry 9G-8000P (66% BaTiO<sub>3</sub>, 3.0% oxalic acid, 1.0% PEI, and 12.0% PEO-powder form) at four different magnifications (50kX, 25kX, 10kX, and 1kX). Oxalic acid, PEI, and PEO are added as a weight percent of the BaTiO<sub>3</sub>.

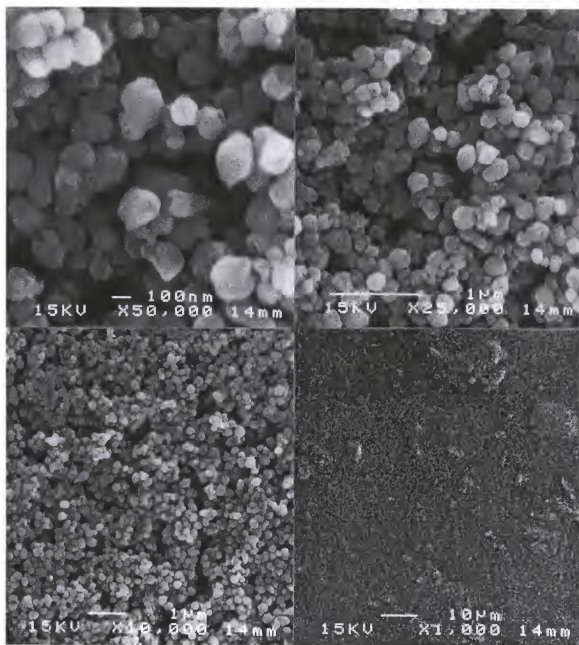


Figure 5.17. Scanning electron micrographs of a smeared sample from slurry 9G-PVP (60% BaTiO<sub>3</sub>, 3.0% oxalic acid, 1.0% PEI, and 12.0% PVP) at four different magnifications (50kX, 25kX, 10kX, and 1kX). Oxalic acid, PEI, and PVP (40k MW) are added as a weight percent of the BaTiO<sub>3</sub>.

remove air within the slurry. After drying, the tape prepared with 12% PVP (10,000MW) remained tacky.

In an effort to reduce the tackiness produced in the hand cast tape from slurry J-1, a 50/50 combination of 10,000MW and 40,000MW PVP was investigated to determine the possibility of using a combination of two binders totaling 12% of BaTiO<sub>3</sub> (6% each). The concept is to increase the T<sub>g</sub> of the binder by adding a larger MW PVP and thus, reduce the tackiness of the cast tape. Figure 5.18 shows the scanning electron micrographs of the particle packing for slurry I-6A with the following formulation, 65% BaTiO<sub>3</sub>, 3.0% oxalic acid, 1.0% PEI, 10.0% PVP, and 1.0% glycerin. The apparent viscosity and Bingham yield point of this slurry were ~900cP and 13 dynes/cm<sup>2</sup>. The viscosity of slurry I-6A is larger than conventional slurry formulations. However, Slurry I-6A was prepared as a 1 liter slurry and no previously used mixing technique adequately homogenize the slurry. Therefore, a similar slurry was prepared with only 10% binder and shipped to Cabot Performance Materials, PA, mixed with a high speed emulsifier, and sent back to the University of Florida for characterization. The apparent viscosity and Bingham yield point of this slurry were ~220cP and 2 dynes/cm<sup>2</sup>. Adequate mixing with a high speed emulsifier and reducing the binder concentration from 12% to 10% reduced the apparent viscosity ~700cP and the Bingham yield point ~10 dynes/cm<sup>2</sup>. Three scanning electron micrographs of the particle packing within the pseudo tape cast from the Cabot mixed slurry are presented in Figure 5.19. The 50kX magnification could not be imaged due to charging at the sample surface. The improvement in the particle packing is easily noted in the 1 kX photomicrograph via the reduction in the size of the agglomerates and in the higher magnifications through increased particle densities.

### 5.5. Conclusions

Several low solids loading and high solids loading experiments were conducted to determine compatible binder systems with the oxalate/PEI-treated BaTiO<sub>3</sub> suspensions which meet tape casting formulation rheological requirements. Electrophoretic behavior

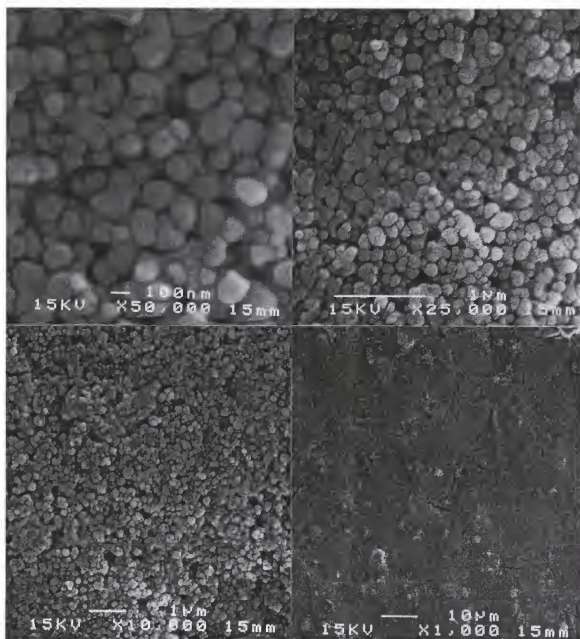


Figure 5.18. Scanning electron micrographs of a smeared sample from slurry I-6, A (65% BaTiO<sub>3</sub>, 3.0% oxalic acid, 1.0% PEI, 10.0% PVP, and 1.0% glycerin) at four different magnifications (50kX, 25kX, 10kX, and 1kX). Oxalic acid, PEI, PVP (<sup>50/50</sup> mixture of 10k and 40k MW), and glycerin are added as a weight percent of the BaTiO<sub>3</sub>.

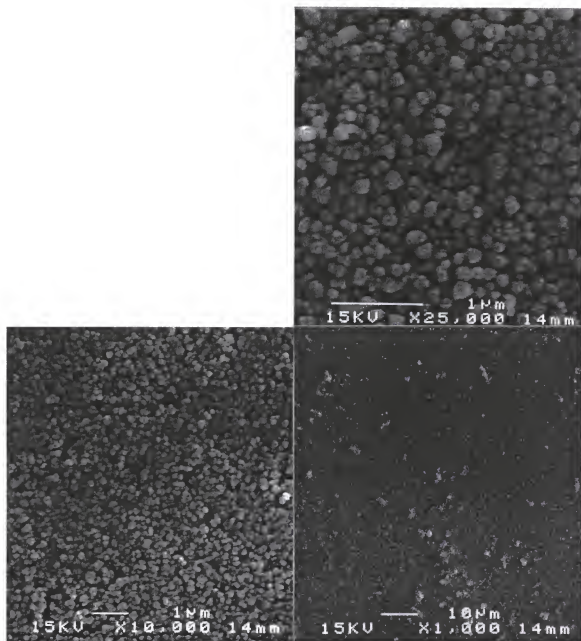


Figure 5.19. Scanning electron micrographs of a smeared sample from slurry 3-1-10 PVP (65% BaTiO<sub>3</sub>, 3.0% oxalic acid, 1.0% PEI, 10.0% PVP, and 1.0% glycerin) at three different magnifications (25 kX, 10 kX, and 1 kX). Oxalic acid, PEI, and PVP (<sup>50</sup>/50 mixture of 10k and 49k MW) are added as a weight percent of the BaTiO<sub>3</sub>. This is the sample sent to Cabot Performance Materials for emulsification.

(zeta potential vs. pH) studies at low solids loading shows that PEO does not affect the polarity or magnitude of the surface potential associated with the oxalate/PEI-treated BaTiO<sub>3</sub> particles. However, corresponding sedimentation studies illustrate PEO adversely affect the colloidal stability by decreasing the sedimentation time from longer than one week to ~24 hours. Rheological characterization of various combinations of the three additives (PEO, PEI, and oxalic acid) as a function of solution pH does not confirm or refute interactions between any two or all three additives.

Slurries that incorporate PEI as the binder and PVP (only 40,000MW) were prepared at 60% BaTiO<sub>3</sub> and rheological properties could not be determined. Therefore, these two specific additives are rejected as compatible binders for the oxalate/PEI-treated BaTiO<sub>3</sub> suspensions. The addition of PEO as a binder system for the oxalate/PEI-treated BaTiO<sub>3</sub> suspensions needs further analysis at lower BaTiO<sub>3</sub> concentrations (~65%) and decreased binder concentrations to either eliminate or accept it as a possible binder. The addition of a 50/50 blend of PVP (10,000MW and 40,000MW) proved to be the most compatible binder system from the various binders analyzed in the current work. The 50/50 blend of PVP as a binder allowed 65% BaTiO<sub>3</sub> solids loading with permissible tape casting rheological properties and far better particle densities over conventional tape casting formulations.

## CHAPTER 6. CONCLUSIONS AND FUTURE WORK

### 6.1. Conclusions

The chemical aspects of MLC aqueous processing are neither trivial nor fully understood by the MLC manufacturers. Industry has relatively ignored the solution chemical reactions which transpire at the particle/solution interface during MLC production. Unfortunately, aqueous-based processing of  $\text{BaTiO}_3$  is difficult due to the incongruent dissolution of the particle surface which supplies large concentrations of  $\text{Ba}^{2+}(\text{aq})$ . The aqueous processing of  $\text{BaTiO}_3$  alters the stoichiometry at the particle surface, compromises the effectiveness of the polymeric additives, and effects the sintering of the ceramic layers which subsequently compromises the dielectric properties of the MLC. The importance of addressing these deleterious effects is significantly increased when a finer particle size needed to produce thinner ceramic layers in the MLC is used.

The current work confirms one of the major problems associated with the aqueous processing of  $\text{BaTiO}_3$  and offers a potential solution, via the use of an organic molecule to passivate the surface. The electrophoretic behavior of aqueous  $\text{BaTiO}_3$  suspensions is dependent not only upon batch to batch variations, but also upon solids loading. ICP results confirm the theoretical instability of  $\text{BaTiO}_3$ , with high resolution HRTEM corroborating that it is a surface mediated phenomena. In contrast to  $\text{BaTiO}_3$ , electrophoretic measurements for BOM demonstrate a relatively constant, positive zeta potential for a pH range from pH 4 to pH 10. Suspensions of  $\text{BaTiO}_3$  with various concentrations of oxalic acid ( $10^{-2}\text{M}$ ,  $10^{-3}\text{M}$ , and  $10^{-4}\text{M}$ ) exhibit a relatively constant, negative zeta potentials over the same pH range, with the magnitude of the charge dependent upon the oxalate ion concentration. Zeta potential analysis via a light scattering

technique showed the Ba-oxalate complex is located at the particle surface by the monomodal output. Increasing the oxalic acid concentration present increases the magnitude of the charge associated with the surface of the  $\text{BaTiO}_3$  particles. Oxalate additions also minimize the  $\text{Ba}^{2+}$  ion concentration in solution by precipitation of the relatively insoluble barium oxalate salt as a diffusion barrier to  $\text{Ba}^{2+}$  dissolution on the surface of the  $\text{BaTiO}_3$  particles. The  $\text{BaC}_2\text{O}_4$  precipitate is the product of the leached  $\text{Ba}^{2+}$  ions from the  $\text{BaTiO}_3$  particle surface and the fully dissociated  $\text{C}_2\text{O}_4^{2-}$  ions present in solution. Calculation of the thickness of this barrier layer was determined to be 1.6 nm, which is reasonably consistent with the surface layer experimentally observed in the HRTEM micrographs of the oxalate-treated powder.

The addition of  $\text{BaTiO}_3$  powder to oxalic acid solution controls the particle surface charge and minimizes the free  $\text{Ba}^{2+}$  ions present in solution over a wide pH range, alleviating the problems associated with small fluctuations in pH during processing. The passivation of the  $\text{BaTiO}_3$  particle surface via oxalic acid was convincingly demonstrated by the experimental results discussed throughout the current work. However, the moderate charge imparted by the oxalate treatment does not provide suspension stability.

Dispersion of the oxalate-treated  $\text{BaTiO}_3$  particles is achieved by the introduction of polyethylene imine. The positively charged polyelectrolyte, polyethylene imine, readily adsorbs onto the negatively charge oxalate-treated particle surface and improves the dispersion by a combination of electrostatic and steric effects. The electrophoretic behavior of the aqueous oxalate-treated  $\text{BaTiO}_3$  suspensions with various concentrations of PEI demonstrates that the PEI concentration is critical for a positive surface charge and colloidal stability. Low concentrations of PEI (0.5%) do not provide relatively constant positive charge over the entire pH range (pH 4 to approximately pH 10). In fact, at low pH the surface charge is negative and becomes positive as the solution becomes more alkaline. Whereas, when either 1% or 2% PEI is added to the oxalate-treated  $\text{BaTiO}_3$  suspension, a positive surface charge is produced from suspension pH 4 to approximately pH 10 with the

magnitude of the charge decreasing as the pH becomes more alkaline. At approximately pH 10, PEI is no longer positively charged and does not improve the colloidal stability. In dispersing the oxalate-treated BaTiO<sub>3</sub> particles, it is critical to provide sufficient PEI for uniform coverage and to maintain the suspension below pH 10, where PEI is positively charged. Sedimentation results corroborate these findings. Several passivation: dispersion dosages are presented as possible slurry formulations; however slurry 9B (3.0% oxalic acid, 1.0% PEI) provides the most favorable rheological properties and microstructure (particle packing) of the green "pseudo" tape.

It has been demonstrated that PEI is an effective dispersant for the oxalate-treated BaTiO<sub>3</sub> particles. The results presented in this chapter strongly suggest that steric hindrance, in combination with electrostatic forces, is responsible for the colloidal stability of the oxalic acid/PEI/BaTiO<sub>3</sub> suspension. However further work is required to confirm the dispersion mechanism.

The addition of a 50/50 blend of PVP (10,000MW and 40,000MW) proved to be the most compatible binder system from the various binders analyzed in the current work. Several low solids loading and high solids loading experiments were conducted to determine compatible binder systems with the oxalate/PEI-treated BaTiO<sub>3</sub> suspensions which meet tape casting formulation rheological requirements. Electrophoretic behavior (zeta potential vs. pH) studies at low solids loading shows that PEO does not seemingly affect the polarity or magnitude of the surface potential associated with the oxalate/PEI-treated BaTiO<sub>3</sub> particles. However, corresponding sedimentation studies illustrate PEO adversely affect the colloidal stability by decreasing the sedimentation time from longer than one week to ~24 hours. Rheological characterization of various combinations of the three additives (PEO, PEI, and oxalic acid) as a function of solution pH does not confirm or refute interactions between any two or all three additives.

Slurries that incorporate PEI as the binder and PVP (only 40,000MW) were prepared at 60% BaTiO<sub>3</sub> and rheological properties could not be determined. Therefore,

these two specific additives are rejected as compatible binders for the oxalate/PEI-treated  $\text{BaTiO}_3$  suspensions. The addition of PEO as a binder system for the oxalate/PEI-treated  $\text{BaTiO}_3$  suspensions needs further analysis at lower  $\text{BaTiO}_3$  concentrations (~65% w/o) and decreased binder concentrations to either eliminate or accept it as a possible binder. The 50/50 blend of PVP as a binder allowed 65% w/o  $\text{BaTiO}_3$  solids loading with permissible tape casting rheological properties and far better particle densities over conventional tape casting formulations.

## 6.2. Future Work

The current research strongly demonstrates the developed passivation/dispersion scheme for aqueous  $\text{BaTiO}_3$  suspensions minimizes the amount of dissolved  $\text{Ba}^{2+}(\text{aq})$  from the  $\text{BaTiO}_3$  particle surface, establishes colloidal stability, and provides uniform particle packing in the pseudo-tapes even at high solids loading. In addition, binder systems compatible with the passivation and dispersion scheme have been produced. However, there are several aspects related to this research that should be examined. First of all, the composition of the passivation layer needs to be confirmed. Theoretical modeling of the surface, based on experimental solution conditions, should be performed to provide insight to the surface charging mechanisms for aqueous  $\text{BaTiO}_3$  suspensions. After successful reproduction of the experimental results for aqueous  $\text{BaTiO}_3$  suspensions, the oxalate additions, as well as PEI additions should be modeled to understand the charging mechanism of the passivation layer and determine the thickness of the adsorbed polymer layer via electroacoustic analysis. Also modeling the oxalate/PEI-treated  $\text{BaTiO}_3$  particle in water may allow further optimization of the passivation/dispersion dosages.

Another unresolved issue concerning this research involves the effect oxalic acid additions have on the presence of  $\text{BaCO}_3$  contamination on the  $\text{BaTiO}_3$  particle surface. When  $\text{BaTiO}_3$  is added to oxalic acid solution, a rigorous reaction takes place giving off a gaseous product. The chemical composition of the gaseous product is unknown at this time. However, it has been speculated to be some form of carbon gas. This issue should

be addressed before transferring the technology to an industrial site because the small oxalate-treated  $\text{BaTiO}_3$  samples prepared at a university research facility may not produce the dangerously large quantities of the gaseous product that would be noted at an industrial MLC plant.

The current research deals with the passivation of only pristine  $\text{BaTiO}_3$ . However, in the MLC industry more complex powder formulation (i.e., dopants, solid solutions, and fluxes) are used to control grain size and dielectric properties. Therefore, it is necessary to determine if the current research concepts can be applied to the various formulated powders.

If the passivation/dispersion scheme presented is to be incorporated into the industrial manufacturing of MLCs, then a firing schedule needs to be determined that removes each additive completely and leaves no residuals. The oxalate ion is proposed to decompose as  $\text{CO}$ ,  $\text{CO}_2$ , and  $\text{H}_2\text{O}$  or from  $\text{BaCO}_3$  prior to evolution as gaseous carbon products. The removal of PEI also needs to be investigated. In addition, the effects of the oxalate passivation layer and PEI on the sintered  $\text{BaTiO}_3$  microstructure and dielectric properties, if any, need to be determined.

Additional issues that warrant analysis are the stability of BOM in air (i.e., when the cast tape dries) with respect to the prevention of carbonate formation. The effect passivation/dispersion additives have on the metal electrode (e.g., wetting, gas formation and removal,) is also unknown. From a powder synthesis and supplier's view, it would be beneficial to determine shelf-life of oxalate/PEI-treated  $\text{BaTiO}_3$  suspensions and whether the chemically passivated and polymerically dispersed particles spontaneously redisperse in water after completely drying. This would allow the synthesized  $\text{BaTiO}_3$  powder to be treated with the passivation and dispersion agents and shipped to the MLC industry as a dry agglomerate-free powder that would be easily dispersed. Therefore the cost of shipping the dry modified powder versus a water based formulation would decrease dramatically.

## APPENDIX A

Table A.1. Summary of the chemical constituents and physical characteristics for BaTiO<sub>3</sub> slurries prepared with 0.5% oxalic acid, and varying amounts of polyethyleneimine (PEI) without binder present.

Formulation	Slurry 0.5:0.5 0.5% PEI	Slurry 0.5:1 1.0% PEI	Slurry 0.5:2 2.0% PEI	Slurry 0.5:3 3.0% PEI	Slurry 0.5:5 5.0% PEI
BaTiO <sub>3</sub> (g)	56.80	56.81	25.00	25.00	56.80
H <sub>2</sub> C <sub>2</sub> O <sub>4</sub> ·2H <sub>2</sub> O (g)	0.28	0.28	0.14	0.13	0.28
PEI (50% in H <sub>2</sub> O) (g)	0.57	1.14	1.01	1.52	5.68
D.I. H <sub>2</sub> O Added (g)	25.32	25.41	12.34	11.86	25.34
<b>Characteristics</b>					
Total Slurry Weight (g)	82.98	83.64	38.48	38.52	88.11
Total Slurry Volume (cc)	35.36	36.02	17.52	17.55	40.49
Total H <sub>2</sub> O Present (g)	25.69	26.06	12.88	12.66	28.26
w% H <sub>2</sub> O	30.96	31.16	33.47	32.86	32.07
v% H <sub>2</sub> O	72.65	72.35	73.54	72.11	69.80
BaTiO <sub>3</sub>					
Weight Percent	68.46	67.92	64.96	64.92	64.47
Volume Percent	26.55	26.07	23.59	23.55	23.19
Slurry pH	~9	10-11	9-10	~10	~10
Observations of Hand Cast Pseudo Tapes	.	.	.	.	.

Table A2. Summary of the chemical constituents and physical characteristics for BaTiO<sub>3</sub> slurries prepared with 1.0% oxalic acid, and varying amounts of polyethyleneimine (PEI) without binder present.

Formulation	Slurry 1:0.5 0.5% PEI	Slurry 1:1 1.0% PEI	Slurry 1:2 2.0% PEI	Slurry 1:3 3.0% PEI	Slurry 1:5 5.0% PEI
BaTiO <sub>3</sub> (g)	25.01	56.80	56.80	56.80	56.81
H <sub>2</sub> C <sub>2</sub> O <sub>4</sub> ·2H <sub>2</sub> O (g)	0.25	0.57	0.57	0.57	0.57
PEI (50% in H <sub>2</sub> O) (g)	0.25	1.14	2.27	3.40	5.68
D.I. H <sub>2</sub> O Added (g)	12.96	25.36	25.39	25.36	25.31
<b>Characteristics</b>					
Total Slurry Weight (g)	38.47	83.87	85.03	86.14	88.37
Total Slurry Volume (cc)	17.42	36.05	37.21	38.31	40.55
Total H <sub>2</sub> O Present (g)	13.16	26.09	26.69	27.22	28.31
w% H <sub>2</sub> O	34.20	31.11	31.38	31.61	32.04
v% H <sub>2</sub> O	75.55	72.37	71.72	71.05	69.83
BaTiO <sub>3</sub>					
Weight Percent	65.01	67.73	66.80	65.95	64.28
Volume Percent	23.74	26.04	25.23	24.51	23.16
Slurry pH	~8	~9	~9	~9	10
Observations of Hand Cast Pseudo Tapes					

Table A3. Summary of the chemical constituents and physical characteristics for BaTiO<sub>3</sub> slurries prepared with 2.0% oxalic acid, and varying amounts of polyethyleneimine (PEI) without binder present.

Formulation	Slurry 2:0.5 0.5% PEI	Slurry 2:1 1.0% PEI	Slurry 2:2 2.0% PEI	Slurry 2:3 3.0% PEI	Slurry 2:5 5.0% PEI
	25.00 0.50 0.26 12.76	56.80 1.14 1.15 25.38	56.80 1.13 2.27 25.36	56.81 1.14 3.40 25.37	56.81 1.14 5.70 25.40
<b>Characteristics</b>					
Total Slurry Weight (g)	38.51	84.47	85.56	86.72	89.04
Total Slurry Volume (cc)	17.29	36.24	37.34	38.49	40.81
Total H <sub>2</sub> O Present (g)	13.03	26.28	26.82	27.40	28.57
% H <sub>2</sub> O	33.82	31.11	31.34	31.60	32.09
% H <sub>2</sub> O	75.36	72.51	71.81	71.18	70.01
BaTiO <sub>3</sub>					
Weight Percent	65.00	67.25	66.39	65.51	63.80
Volume Percent	23.90	25.91	25.14	24.39	23.01
Slurry pH	~8	8-9	~9	~9	9-10
Observations of Hand Cast Pseudo Tapes					

Table A4. Summary of the chemical constituents and physical characteristics for BaTiO<sub>3</sub> slurries prepared with 3.0% oxalic acid, and varying amounts of polyethyleneimine (PEI) without binder present.

Formulation		Slurry 3:0.5 0.5% PEI	Slurry 3:1 1.0% PEI	Slurry 3:2 2.0% PEI	Slurry 3:3 3.0% PEI	Slurry 3:5 5.0% PEI
BaTiO <sub>3</sub> (g)		25.02	56.80	56.80	56.80	56.81
H <sub>2</sub> C <sub>2</sub> O <sub>4</sub> ·2H <sub>2</sub> O (g)		0.75	1.70	1.71	1.70	1.71
PEI (50% in H <sub>2</sub> O) (g)		0.25	1.16	2.27	3.41	5.68
D.I. H <sub>2</sub> O Added (g)		12.58	25.36	25.39	25.37	25.36
<b>Characteristics</b>						
Total Slurry Weight (g)		38.60	85.02	86.17	87.28	89.56
Total Slurry Volume (cc)		17.18	36.39	37.54	38.65	40.92
Total H <sub>2</sub> O Present (g)		12.92	26.42	27.01	27.56	28.69
w/o H <sub>2</sub> O		33.47	31.08	31.35	31.58	32.04
% H <sub>2</sub> O		75.20	72.61	71.97	71.30	70.11
BaTiO <sub>3</sub>						
Weight Percent		64.82	66.81	65.92	65.08	63.43
Volume Percent		24.07	25.80	25.01	24.29	22.95
Slurry pH		~5	8-9	~9	9	~10
Observations of Hand Cast Pseudo Tapes						

Table A5. Summary of the chemical constituents and physical characteristics for BaTiO<sub>3</sub> slurries prepared with 5.0% oxalic acid, and varying amounts of polyethyleneimine (PEI) without binder present.

Formulation		Slurry 5:0.5 0.5% PEI	Slurry 5:1 1.0% PEI	Slurry 5:2 2.0% PEI	Slurry 5:3 3.0% PEI	Slurry 5:5 5.0% PEI
BaTiO <sub>3</sub> (g)		56.81	25.00	25.13	25.17	56.81
H <sub>2</sub> C <sub>2</sub> O <sub>4</sub> ·2H <sub>2</sub> O (g)		2.85	1.25	1.25	1.26	2.84
PEI (50% in H <sub>2</sub> O) (g)		0.56	0.51	1.00	1.52	5.69
D.I. H <sub>2</sub> O Added (g)		25.33	11.75	11.21	10.71	25.35
<b>Characteristics</b>						
Total Slurry Weight (g)		85.55	38.52	38.59	38.66	90.69
Total Slurry Volume (cc)		36.10	16.75	16.72	16.76	41.24
Total H <sub>2</sub> O Present (g)		26.43	12.36	12.07	11.84	29.00
% H <sub>2</sub> O		30.89	32.10	31.27	30.61	31.98
% H <sub>2</sub> O		73.21	73.80	72.17	70.63	70.33
BaTiO <sub>3</sub>						
Weight Percent		66.40	64.92	65.11	65.09	62.64
Volume Percent		26.01	24.68	24.84	24.82	22.77
Slurry pH		2-3	~3	~5	~7	8-9
Observations of Hand Cast Pseudo Tapes						

## REFERENCES

1. B. Jaffe, W.R. Cook Jr., and H. Jaffe, Piezoelectric Ceramics, J.P. Roberts and P. Popper eds., Academic Press, New York, NY, 1971.
2. M.E. Lines and A.M. Glass, "Principles and Applications of Ferroelectric and Related Materials," W. Marshall and D. Wilkinson, Eds., Clarendon Press, Oxford, 1977.
3. Communication with Senior Research Engineer at American Technical Ceramics located in Jacksonville, Florida, 1992.
4. NOVACAP, "Ceramic Chip Capacitors," Technical Brochure, Dover Technologies Company, Valencia, California, Second Edition, Cat. 89-10B, 1990.
5. J.H. Adair, D.A. Anderson, G.O. Dayton, and T.R. Shrout, "A Review of the Processing of the Electronic Ceramics with an Emphasis on the Multilayer Capacitors," *J.M.E.*, **9** (1&2), 71-118, 1987.
6. S. Mizuta, M. Parish, and H. K. Bowen, "Dispersion of BaTiO<sub>3</sub> Powders (Part I)," *Ceramics International*, **10**, 43-48, 1984.
7. S. Mizuta, M. Parish, and H. K. Bowen, "Dispersion of BaTiO<sub>3</sub> Powders (Part II)," *Ceramics International*, **10**, 83-86, 1984.
8. W.G. Burger and C.W. Weigel, "Multi-Layer Ceramics Manufacturing," *IBM J. Res. Develop.*, **27** (1), 1987.
9. H.J. Hagemann, D. Hennings, and R. Wernicke, "Ceramic Multilayer Capacitor," *Phil. Tech. Rev.*, **41**, 89-98, 1983.
10. J.M. Herbert, Chapter 3, Methods of Preparation: Ceramic Dielectrics and Capacitors, Gordon and Breach Science Publishers, New York, NY, 1985.
11. M. Kahn, D.P. Burks, I. Burn, and W.A. Schulze, Ceramic Capacitor Technology in Electronic Ceramics: Properties, Devices and Applications, Edited by L.M. Levison, Marcel Dekker, Inc., New York, NY, 1988.
12. G.N. Howatt, "Method of Producing High Dielectric High Insulation Ceramic Plates," United States Patent, 2,582,993, Jan. 22, 1952.
13. D.V. Miller, J.H. Adair, and R.E. Newnham, "Dissolution of Barium from Barium Titanate in Non-Aqueous Solvents," Proceedings of the Basic Science Meeting of the American Ceramic Society, November 1-4, 1987.
14. B. Utech, "The Effect of Solution Chemistry on Barium Titanate Ceramics," M.S. Thesis in Solid State Science, The Pennsylvania State University, 1990.

15. J.H. Adair, B.L. Utech, and K. Osseo-Asare, "Solubility Relationships in the Coprecipitation Synthesis of Barium Titanate in Aqueous Suspensions," presented at the Fifth US-Japan Seminar on Dielectric and Piezoelectric Ceramics, held in Kyoto, Japan, December 11-14, 1990.
16. K. Osseo-Asare, "Interfacial Phenomena in Leaching Systems," pp. 227-268 in Hydrometallurgical Process Fundamentals, Edited by R.G. Bautista, Plenum Press, New York, NY, 1984.
17. K. Osseo-Asare, F.J. Arriagada, and J.H. Adair, "Solubility Relationships in the Coprecipitation Synthesis of Barium Titanate: Heterogeneous Equilibria in the Ba-Ti-C<sub>2</sub>O<sub>4</sub>-H<sub>2</sub>O System," pp. 47-53 in *Ceramic Transactions, Ceramic Powder Science*, The American Ceramic Society, Inc., Westerville, Ohio, 1988.
18. H. Nesbitt, G. Bancroft, W. Fyfe, S. Karkanis, A. Nishijima, and S. Shin, "Thermodynamic Stability and Kinetics of Perovskite Dissolution," *Nature*, **289**, 358-362, 1981.
19. C.C. Hung, R.E. Riman, and R. Caracciolo, "An XPS Investigation of Hydrothermal and Commercial Barium Titanate Powders," *Ceramic Transactions, Ceramic Powder Science III*, Volume 12, G.L. Messing, S. Hirano, and H. Hausner, Eds., The American Ceramic Society, Inc., Westerville, Ohio, 1990.
20. R.K. Sharma, N.H. Chan, and D.M. Smyth, "Solubility of TiO<sub>2</sub> in BaTiO<sub>3</sub>," *J. Am. Ceram. Soc.*, **64** (8), 448-451, 1981.
21. R.E. Newnham, "Structure Property Relations in Ceramic Capacitors," *JME*, **5**, 941-984, 1987.
22. R.W. Whatmore, "An Introduction to Ferroelectric Ceramics and Their Applications," pp. 223-254 in Fundamentals of Ceramic Engineering, Edited by P. Vincenzini, Elsevier Science Publishers, London, UK, 1991.
23. L.K. Templeton and J.A. Pask, "Formation of BaTiO<sub>3</sub> from BaCO<sub>3</sub> and TiO<sub>2</sub> in Air and CO<sub>2</sub>," *J. Am. Ceram. Soc.*, **42** (5), 212-215 1959.
24. B.J. Mulder, Preparation of BaTiO<sub>3</sub> and Other Ceramic Powders by Coprecipitation of Citrates in an Alcohol," *Ceramic Bulletin*, **49** (11), 990-993, 1970.
25. J. Menashi, R.C. Reid, and L.P. Wagner, "Barium Titanate Based Dielectric Compositions," United States Patent, 4,832,939, May 23, 1989.
26. K.S. Mazdiyasn, R.T. Dolloff, and J.S. Smith II, "Preparation of High-Purity Submicron Barium Titanate Powders," *J. Am. Ceram. Soc.*, **52** (10), 523-526, 1969.
27. K.W. Kirby, "Alkoxide Synthesis Techniques for BaTiO<sub>3</sub>," *Mat. Res. Bull.*, **23**, 881-890, 1988.
28. H.L. Hsieh and T.T. Fang, "Effects of Powder Processing on the Green Compacts of High-Purity BaTiO<sub>3</sub>," *J. Am. Ceram. Soc.*, **72** (1) 142-145, 1989.

29. E. Barringer, N. Jubb, B. Fegley, R.L. Prober, and H.K. Bowen, "Processing Monosized Powders," pp. 315-33 in Ultrastructure Processing of Ceramics, Glasses, and Composites, Edited by L.L. Hench and D.R. Ulrich, John Wiley & Sons, New York, 1984.
30. K. Ettre and G.R. Castles, "Pressure-Fusible Tapes for Multilayer Structures," *Ceramic Bulletin*, **51** (5), 482-485, 1971.
31. J.S. Chappell, Particle Size Distribution Effects on Sintering Rates, 1986.
32. L.L. Hench and J.K. West, Principles of Electronic Ceramics, John Wiley & Sons, New York, NY, 1990.
33. W.H. Morrison, Jr., "Stabilization of Aqueous Oxide Pigment Dispersions," *J. Coatings Tech.*, **57** (721), 55-65, 1985.
34. G.D. Parfitt, Dispersion of Powders in Liquids, 3rd Edition, Applied Science Publishers, Englewood, NJ, 1981.
35. D.A. Anderson, J.H. Adair, D.V. Miller, J.V. Biggers, T.R. Shrout, "Surface Chemistry Effects on Ceramic Processing of BaTiO<sub>3</sub> Powder," Ceramic Transactions, Ceramic Powder Science II, Vol. 1, G.L. Messing, S. Hirano, and H. Hausner eds., The American Ceramic Society, Inc., Westerville, OH, 1987.
36. T.F. Lin and C.T. Hu, "Influence of Stoichiometry on the Microstructure and Positive Temperature Coefficient of Resistivity of Semiconducting Barium Titanate Ceramics," *J. Am. Ceram. Soc.*, **73** (3), 531-536, 1990.
37. S.E. Trolrier, S.D. Atkinson, P.A. Fuierer, J.H. Adair, and R.E. Newnham, "Dissolution of YBa<sub>2</sub>Cu<sub>3</sub>O<sub>(7-x)</sub> in Various Solvents," *Am. Ceram. Soc. Bull.*, **67** (4), 759-762, 1988.
38. D.H. Napper, Polymeric Stabilization of Colloidal Dispersions, Academic Press, New York, 1-91, 1983.
39. L.M. Sheppard, "Advances in Processing of Ferroelectric Thin Films," *Am. Ceram. Soc. Bull.*, **71** (1), 85-95, 1992.
40. G.H. Heartling, Ceramic Materials for Electronics: Processing, Properties, and Applications, Edited by R.C. Buchanan, Marcel Dekkar Inc., New York, NY, 1986.
41. S. Venigalla and J.H. Adair, "Theoretical Modeling and Experimental Verification of Electrochemical Equilibria in the Ba-Ti-C-H<sub>2</sub>O System," accepted in *Chemistry of Materials*.
42. M.M. Lencka and R.E. Riman, "Thermodynamics of the Hydrothermal Synthesis of Calcium Titanate with Reference to Other Alkaline-Earth Titanates," *Chem. Mater.*, **7**, 18-25, 1995.
43. F. Schrey, "Effect of pH on the Chemical Preparation of Barium-Strontium Titanate," *J. Am. Ceram. Soc.*, **48** (8), 401-405, 1965.

44. G.L. Roy, A.L. Laferriere, and J.O. Edwards, "A Comparative Study of Polyol Complexes of Arsenite, Borate, and Tellurate Ions," *J. Inorg. Nucl. Chem.*, **4**, 106-114, 1957.
45. J.H. Adair, R. Sayre, B.L. Utech, and R.E. Chodelka, "The Aqueous Processing of BaTiO<sub>3</sub> for Multilayer Capacitor Fabrication: Crosslinking of Organic Additives by Soluble Species," submitted to the *J. Am. Ceram. Soc.*
46. A.E. Ringwood, S.E. Kesson, N.G. Ware, W. Hibberson, and A. Major, "Immobilisation of High Level Nuclear Reactor Wastes in SYNROC," *Nature*, **278**, 219-223, 1979.
47. H. Nesbitt, G. Bancroft, W. Fyfe, S. Karkanis, A. Nishijima, and S. Shin, "Thermodynamic Stability and Kinetics of Perovskite Dissolution," *Nature*, **289**, 358-362, 1981.
48. S. Myhra, D. Savage, A. Atkinson, and J.C. Riviere, "Surface Modification of Some Titanate Minerals Subjected to Hydrothermal Chemical Attack," *Am. Mineral.*, **69**, 902-909, 1984.
49. J.H. Adair, M.A. Janney, D.V. Miller, G.Y. Onoda Jr., and R.E. Newnham, "The Surface Chemistry of Barium Titanate in Aqueous Suspensions," presented at the 88th Annual Meeting of the American Ceramic Society, Pittsburgh, PA, 1987.
50. H.M. O'Bryan and J. Thompson, Jr., "Phase Equilibria in the TiO<sub>2</sub>-Rich Region of the System BaO-TiO<sub>2</sub>," *J. Am. Ceram. Soc.*, **57**, 522-526, 1974.
51. T. Negas, R.S. Roth, H.S. Parker, and D. Minor, "Subsolidus Phase Relations in the BaTiO<sub>3</sub>-TiO<sub>2</sub> System," *J. Solid State Chem.*, **9**, 297-307, 1974.
52. R.M. Cornell, A.M. Posner, and J.P. Quirk, "A Titrimetric and Electrophoretic Investigation of the PZC and the IEP of Pigment Rutile," *J. Colloid and Inter. Sci.*, **53** (1), 6-13, 1975.
53. G.R. Wiese and T.W. Healy, "Solubility Effects in Al<sub>2</sub>O<sub>3</sub> and TiO<sub>2</sub> Colloidal Dispersions," *J. Colloid and Inter. Sci.*, **52** (3), 452-457, September 1975.
54. C.F. Baes, Jr. and R.E. Mesmer, The Hydrolysis of Cations, John Wiley and Sons, Inc., New York, NY, 1976, reprinted by Krieger Publishing Co., Malabar, FL, 1986.
55. M. Pourbaix, Atlas of Electrochemical Equilibria in Aqueous Solutions, 2nd English edition, 1974, translated by J.A. Franklin, National Association of Corrosion Engineers, Houston, TX.
56. D.A. Jones, "Chapter 4 - Passivity" Principles and Prevention of Corrosion, 2nd edition, Prentice Hall, Upper Saddle River, NJ, 1992.
57. H. Wise and J. Oudar, Material Concepts in Surface Reactivity and Catalysts, 1990, Academic Press, Inc., New York.
58. D.R. Askeline, The Science and Engineering of Materials, 2nd Edition, Edited by J.D. Childress, Jr., PWS-Kent Publishing Company, Boston, MA, 1989.

59. D.E. Clark, C.G. Pantano, Jr., and L.L. Hench, "Summary," Chapter 6 in Corrosion of Glass, The Glass Industry, New York, NY, pp. 64-71, 1979.
60. C.J. Simmons and J.H. Simmons, "Chemical Durability of Fluoride Glasses: I, Reaction of Fluorozirconate Glasses with Water," *J. Am. Ceram. Soc.*, **6** (9), 661-669, 1986.
61. D.E. Clark, C.G. Pantano, Jr., and L.L. Hench, "Auger Spectroscopic Analysis of Bioglass Corrosion Films," *J. Am. Ceram. Soc.*, **59** [1-2] 37-39 (1976).
62. A. Paul, "Chemical Durability of Glasses: a Thermodynamic Approach," *J. Mater. Sci.*, **12**, 2246-2268, 1977.
63. J.H. Adair, Speciation Diagram for  $\text{Ba-C}_2\text{O}_4\text{-H}_2\text{O}$ , unpublished data. See reference 33 for data base used.
64. P. Curreri, G.Y. Onoda, Jr., and B. Finlayson, "An Electrophoretic Study of Calcium Oxalate Monohydrate," *J. Colloid and Inter. Sci.*, **69** (1), 170-182, 1979.
65. W.S. Clabaugh, E.M. Swiggard, and R. Gilchrist, "Preparation of Barium Titanly Oxalate Tetrahydrate for Conversion to Barium Titanate of High Purity," *J. Res. NBS*, **56** (5), 289-291, 1956.
66. A. Hodgkinson, Oxalic Acid in Biology and Medicine, Academic Press, Inc., New York, NY, 1977.
67. J.Th.G. Overbeek, "Recent Developments in the Understanding of Colloid Stability," *J. Colloid Inter. Sci.*, **58** (2), 408-421, February 1977.
68. R.J. Hunter, Zeta Potential in Colloid Science: Principles and Applications, Academic Press, NY, 1981.
69. M. Sacks "Ceramic Processing," class notes for the graduate class, Fall, 1990.
70. R.J. Hunter, Introduction to Modern Colloid Science, Oxford University Press, New York, 1993.
71. W.H. Morrison, Jr., "Aqueous Adsorption of Anions onto Oxides at pH Levels above the Point of Zero Charge," *J. Colloid and Inter. Sci.*, **100** (1), 121-127, 1984.
72. D.W. Fuerstenau, D. Manmohan, and S. Raghavan, "The Adsorption of Alkaline-Earth Metal Ions at the Rutile/Aqueous Solution Interface," Adsorption from Aqueous Solutions, Volume III, P.H. Tewari, Ed., Plenum Press, New York, 93-117, 1981.
73. J.H. Adair, L.A.G. Aylmore, J.G. Brockis, and R.C. Bowyer, "An Electrophoretic Mobility Study of Uric Acid with Special Reference to Kidnet Stone Formation," *J. of Colloid and Inter. Sci.*, **124** (1), July 1988.
74. G. Gouy, *J. Phys.*, **9** (4), 457 (1910).
75. D.L. Chapman, *Phil. Mag.*, **25** (6), 475, 1913.
76. T.W. Healy and L.R. White, "Ionizable Surface Group Models of Aqueous Interfaces," *Advances in Colloid and Interface Science*, **9**, 303-345, 1978.

77. J. Westall and H. Hohl, "A Comparison of Electrostatic Models for the Oxide/Solution Interface," *Advances in Colloid and Interface Science*, **10**, 265-294, 1979.
78. G.R. Wiese and T.W. Healy, "Coagulation and Electrokinetic Behavior of  $\text{TiO}_2$  and  $\text{Al}_2\text{O}_3$  Colloidal Dispersions," *J. Colloid and Inter Sci.*, **51** (3), 427-433, June 1975.
79. G.R. Wiese and T.W. Healy, "Adsorption of Al (III) at the  $\text{TiO}_2$ - $\text{H}_2\text{O}$  Interface," *J. Colloid and Inter Sci.*, **51** (3), 434-442, June 1975.
80. G.R. Wiese and T.W. Healy, "Heterocoagulation in Mixed  $\text{TiO}_2$ - $\text{Al}_2\text{O}_3$  Dispersions," *J. Colloid and Inter Sci.*, **52** (3), 458-467, September 1975.
81. E.J.W. Verwey and J.Th.G. Overbeek, Theory of the Stability of Lyophobic Colloids, Elsevier, New York, Amsterdam, 1948.
82. B.V. Derjaguin, "Some New Aspects of the Conclusions on Theory of Stability of Colloids and their Experimental Verification," *Faraday Disc. Chem. Soc.*, **65**, 306-312, 1978.
83. G.A. Parks, "The Isoelectric Points of Solid Oxides, Solid Hydroxides, and Aqueous Hydroxo Complex Systems," *Chemical Reviews*, **65**, 177-195, 1965.
84. H.M. Jang and D.W. Fuerstenau, "The Specific Adsorption of Alkaline-Earth Cations at the Rutile/Water Interface," *Colloids and Surfaces*, **21**, 235-257, 1986.
85. G. Purcell and S.C. Sun, *Trans.AIME*, **226**, 6, 1963.
86. F.J. Hingston, R.J. Atkinson, A.M. Posner, and J.P. Quirk, *Nature* (London) **215**, 1459, 1967.
87. F.J. Hingston, A.M. Posner, and J.P. Quirk, *J. Soil Sci.*, **23**, 177, 1972.
88. H.J. Modi and D.W. Fuerstenau, " , " *J. Phys. Chem.*, **61**, 640, 1957.
89. F. Kulcsar, "A Microstructure Study of Barium Titanate Ceramics," *J. Am. Ceram. Soc.*, **39** (1) 13-17, 1956.
90. A. Beauger, J.C. Mutin, and J.C. Niepce, "Role and Behavior of Orthotitanate  $\text{Ba}_2\text{TiO}_4$  during the Processing of  $\text{BaTiO}_3$  Based Ferroelectric Ceramics," *J. Mat. Sci.*, **19**, 195-201, 1984.
91. D.F.K. Hennings, R. Janssen, and P.J.L. Reynen, "Control of Liquid-Phase-Enhanced Discontinuous Grain Growth in Barium Titanate," *J. Am. Ceram. Soc.*, **70** (1), 23-27, 1987.
92. L.A. Xue and R.J. Brook, "Promotion of Densification by Grain Growth," *J. Am. Ceram. Soc.*, **72** (2), 341-344, 1989.
93. L. Hanke and H. Schmelz, "The Significance of Barium Vacancies with Regard to the Doping Anomaly of Barium Titanates Ceramics," *Ber. Dtsch. Keram. Ges.*, **59** (4) 221-226, 1982.

94. K. Kinoshita and A Yamiji, "Grain Size Effects on Dielectric Properties in Barium Titanate Ceramics, " *J. Appl. Phys.*, **47** (1), 371-373, 1976.
95. Y. Matsuo and H. Sasaki, "Exaggerated Grain Growth in Liquid-Phase Sintering of BaTiO<sub>3</sub>," *J. Am. Ceram. Soc.*, **54** (9), 471, 1971.
96. T. Negas, R.S. Roth, H.S. Parker, and D. Minor, "Subsolidus Phase Relations in the BaTiO<sub>3</sub>-TiO<sub>2</sub> System," *J. Solid State Chem.*, **9**, 297-307, 1974.
97. H.M. O'Bryan and J. Thompson, Jr., "Phase Equilibria in the TiO<sub>2</sub>-Rich Region of the System BaO-TiO<sub>2</sub>," *J. Am. Ceram. Soc.*, **57**, 522-526, 1974.
98. G.H. Jonker, "Some Aspects of Semiconducting Barium Titanate," *Solid-State Electron.*, **7**, 895-903, 1964.
99. H. Kniepkamp and W. Heywang, "Depolarization Effects in Polycrystalline BaTiO<sub>3</sub>," *Z. Angew. Phys.*, **6** (9) 385-390, 1954.
100. A.S. Shaikh, R.W. Vest, and G.M. Vest, "Dielectric Properties of Ultrafine Grained BaTiO<sub>3</sub>," *IEEE Transactions on Ultrasonics, Ferroelectrics, and Frequency Control*, **36**, 407-412, 1989.
101. L. Egerton and S.E. Koonce, "Effect of Firing Cycle on Structure and Some Dielectric and Piezoelectric Properties of Barium Titanate Ceramics," *J. Am. Ceram. Soc.*, **38** (11), 412-418, 1955.
102. Materials Characterization, ASM Handbook, Volume 10, 9th edition, ASM International - The Materials Information Society, 1992.
103. S. Sugrue, T. Oja, and S. Bott, "Predicting and Controlling Colloid Suspension Stability Using Electrophoretic Mobility and Particle Size Measurements," *Am. Lab.*, **21** (2), 64-68, 1992.
104. R.W. O'Brien, D.W. Cannon, and W.N. Rowlands, "Electroacoustic Determination of Particle Size and Zeta Potential," *J. Colloid and Inter. Sci.*, **173** (1), 406-418, 1995.
105. Brookfield Engineering Laboratories, Inc., Wells-Brookfield Micro Viscometer Operating Instructions Manual, Stoughton, MA.
106. A.E. Martell and R.M. Smith, Critical Stability Constants, Plenum Press, New York, NY, 1974.
107. T.L. Brown and H.E. LeMay, Jr., "Chemistry - The Central Science," Appendix E3, p. 890, 3rd edition, 1985, Prentice-Hall, Inc., Englewood Cliffs, New Jersey.
108. R.E. Chodelka, S. Venigalla, A.A. Morrone, S.A. Costantino, and J.H. Adair, "The Aqueous Processing of BaTiO<sub>3</sub> for Multilayer Capacitor Fabrication: III Surface Chemical Passivation of BaTiO<sub>3</sub> via Oxalic Acid Additions," to be submitted to the *J. Am. Ceram. Soc.*
109. K. Uchino, E. Sadanaga, and T. Hirose, "Dependence of the Crystal Structure on Particle Size in Barium Titanate," *J. Am. Ceram. Soc.*, **72** (8), 1555-1558, 1989.

110. K.C. Thompson-Russell and J.W. Edington, Electron Microscope Specimen Preparation Techniques in Materials Science, Macmillan Press Ltd., 1977.
111. G.D. Parfitt, "Dispersion of Powders in Liquids," lecture presented to the Verfahrenstechnische Gesellschaft in Bad Durkheim, October 7, 1969.
112. P.M. Adler, "Spatially Periodic Suspensions," *J. Theoretical and Appl. Mech.*, Special Edition, 73-100, 1985.
113. D.C. Agrawal, R. Raj, and C. Cohen, "Nucleation of Flocs in Dilute Colloidal Suspensions," *J. Am. Ceram. Soc.*, **72** (11), 2148-2153, 1989.
114. G.D. Parfitt, "The Role of the Surface in the Dispersion of Powders in Liquids," **53**, 2233-2240, 1981.
115. N.L. Ackermann and H.T. Shen, "Rheological Characteristics of Solid-Liquid Mixtures," *AIChE Journal*, **25** (2), 327-331, 1979.
116. D. Horn, "Polyethyleneimine-Physicochemical Properties and Applications," in Polymeric Amines and Ammonium Salts, Edited by E.J. Goethals, pp 333-355, Pergamon Press, Elmsford, NY, 1980.
117. F.E. Bailey, Jr., and R.W. Callard, "Some Properties of Poly(ethylene oxide)<sup>1</sup> in Aqueous Solution," *J. Appl. Polymer Sci.*, **1** (1), 56-62, 1959.
118. V.K. LaMer, "Filtration of Colloidal Dispersions Flocculated by Anionic and Cationic Polyelectrolytes," *Disc. Faraday Soc.*, Colloid Stability in Aqueous and Non-Aqueous Media, **42**, 248-254, 1966.
119. L. Blecher, D.H. Lorenz, H.L. Lowd, A.S. Wood, and D.P. Wymar, Handbook of Water-Soluble Gums and Resins, R.L. Davidson, Eds., McGraw-Hill, Inc., 1980.
120. J.S. Reed, Introduction to the Principles of Ceramic Processing, John Wiley & Sons, NY, 1988.
121. R.E. Chodelka, S. Venigalla, S.A. Costantino, and J.H. Adair, "The Aqueous Processing of BaTiO<sub>3</sub> for Multilayer Capacitor Fabrication: IV Dispersion of the Oxalate-Treated BaTiO<sub>3</sub> via Polyethyleneimine Additions," to be submitted to the *J. Am. Ceram. Soc.*
122. W.K. Asbeck, "Fundamentals of the Rheology of Pigment Dispersions," (1), 65-83, 1961.
123. J.S. Chong, E.B. Christiansen, and A.D. Baer, "Rheology of Concentrated Suspensions," *J. Appl. Polymer Sci.*, **15**, 2007-2021, 1971.
124. F.M. Fowkes, "Dispersion of Ceramic Powders in Organic Media," *Advances in Ceramics*, **21**, 411-421, 1987.
125. F.T. Hesselink, "On the Theory of the Stabilization of Dispersions by Adsorbed Macromolecules. I. Statistics of the Change of Some Configurational Properties of the Adsorbed Macromolecules on the Approach of an Impenetrable Interface," *J. Phys. Chem.*, **75** (1), 65-71, 1971.

126. E.A. Boucher and P.M. Hines, "Effects of Inorganic Salts on the Properties of Aqueous Poly(ethylene Oxide) Solutions," *J. Polymer Sci.*, **14**, 2241-2251, 1976.
127. K. Esumi and M. Oyama, "Simultaneous Adsorption of Poly(vinylpyrrolidone) and Cationic Surfactant from Their Mixed Solutions on Silica," *Langmuir*, **9** (8), 2020-2023, 1993.
128. G.M. Kline, "Polyvinylpyrrolidone," *Modern Plastics*, **23** (3), 157-161, Nov., 1945.

## BIOGRAPHICAL SKETCH

Robert Edward Chodelka was born on a cold wintry morning, January 28, 1966, at 9:30 AM in Allegheny Valley Hospital, Natrona Heights. He entered the world with little hesitation, providing his mother with a brief, uncomplicated labor. Soon after his birth, he moved into his parents' house located at 786 Kennedy Avenue, New Kensington, Pennsylvania (a suburb of Pittsburgh, PA). He is the youngest sibling of Edward and Eleanor Chodelka with two older brothers and one older sister. Growing up outside of Pittsburgh, he was born a fan of the Steelers, Pirates, Penguins, and any other professional franchise to develop in the city, and will come to rest a die-hard Pittsburgher.

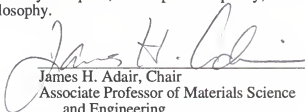
Interests in engineering as a profession were initiated throughout his childhood via his parental guidance. Robert's father continually challenged his ability to solve different household problems by asking the children for possible solutions. This forced the children to present solutions to everyday problems and support their ideas with respective pros and cons. Selling the Sunday newspaper at the age of twelve years exposed him to earning money and answering to a boss other than his parents. Selling the Sunday newspaper also provided him with the opportunity to accumulate a college savings fund. As an ambitious fourteen-year-old entrepreneur, Robert established his own lawn care service which taught him how to effectively communicate with a customer and reach agreeable terms for work rendered. While attending Valley High School in New Kensington, PA, he enrolled in college preparation classes, played the drums for the marching band, orchestra, stage band, and senior citizens choir. During his high school years, he also played basketball for one of the local Catholic Youth Organizations which lost two years in a row to the Western Pennsylvania State champions in the semi-final round. Delivering mail for the U.S. Postal

service was an unique opportunity to handle the pressure bestowed by residents eagerly awaiting the daily arrival of their mail.

Robert attended The Pennsylvania State University (New Kensington branch campus) in 1984 where he enrolled in the College of Engineering. Working at Shop 'N' Save grocery store while attending college forced him to budget his time successfully between work, school, and playing college basketball for the branch campus. In 1996 he transferred to the main campus where he enrolled in the Department of Ceramic Science and Engineering. He worked at the Materials Research Laboratory (MRL) the summer before his junior and senior year and then continued to work at this location for one year after graduating with a B.S. degree in Ceramic Science and Engineering. Working at MRL exposed him to the research environment: the delays associated with setting up experiments and waiting for ordered materials to arrive, downtime of pertinent machinery or instrumentation, and the professional planning of target dates using a Gant chart. More importantly, working at MRL allowed him to directly apply classroom knowledge to research projects within the ceramic field.

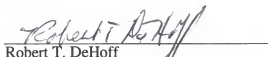
After working for one year after graduating with a B.S., Robert moved to Gainesville where he continued his education at the University of Florida. His Ph.D. study at the University of Florida provided him with the opportunity to improve his mind as well as his managerial skills. All of these jobs, along with his education and parental upbringing, have taught him how to communicate with people, manage time, and use his talents and knowledge to achieve a desired goal.

I certify that I have read this study and that in my opinion it conforms to acceptable standards of scholarly presentation and is fully adequate, in scope and quality, as a dissertation for the degree of Doctor of Philosophy.




James H. Adair, Chair  
Associate Professor of Materials Science  
and Engineering

I certify that I have read this study and that in my opinion it conforms to acceptable standards of scholarly presentation and is fully adequate, in scope and quality, as a dissertation for the degree of Doctor of Philosophy.



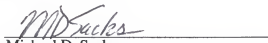
Robert T. DeHoff  
Professor of Materials Science and  
Engineering

I certify that I have read this study and that in my opinion it conforms to acceptable standards of scholarly presentation and is fully adequate, in scope and quality, as a dissertation for the degree of Doctor of Philosophy.




Brij M. Moudgil  
Professor of Materials Science and  
Engineering

I certify that I have read this study and that in my opinion it conforms to acceptable standards of scholarly presentation and is fully adequate, in scope and quality, as a dissertation for the degree of Doctor of Philosophy.



Michael D. Sacks  
Professor of Materials Science and  
Engineering

I certify that I have read this study and that in my opinion it conforms to acceptable standards of scholarly presentation and is fully adequate, in scope and quality, as a dissertation for the degree of Doctor of Philosophy.



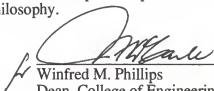
Russell S. Drago  
Graduate Research Professor of  
Chemistry

I certify that I have read this study and that in my opinion it conforms to acceptable standards of scholarly presentation and is fully adequate, in scope and quality, as a dissertation for the degree of Doctor of Philosophy.

  
Stephen A. Costantino  
Business Manager Barium Titanate  
Cabot Performance Materials

This dissertation was submitted to the Graduate Faculty of the College of Engineering and to the Graduate School and was accepted as partial fulfillment of the requirements for the degree of Doctor of Philosophy.

December, 1996

  
Winfred M. Phillips  
Dean, College of Engineering

\_\_\_\_\_  
Dean, Graduate School